Development of Affimer Reagents to Modulate the Enzyme Activity of NDM-1

Robert Samuel Cook

Submitted in accordance with the requirements for the degree of

Master of Science by Research.

The University of Leeds

Faculty of Biological Sciences

School of Molecular and Cellular Biology

August 2019

The candidate confirms that the work submitted is his own and that appropriate credit has been given where reference has been made to the work of others.

Acknowledgements

Firstly, I would like to express my thanks to Dr Darren Tomlinson. Thank you for the opportunity to carry out my MSc in your lab. Your guidance and knowledge have been invaluable over the past year. I would also like to thank Dr Christian Tiede for your patience, ideas and humour that have kept my project going. Also, to my co-supervisor, Dr Alex O'Neil for your advice and insights.

This project follows on from Dr Lia De Faveri PhD project, and I would like to thank her for her expertise, knowledge and words of encouragement. Additionally, I would like to thank Lewis Adams for his help and skills throughout this project.

I am extremely grateful to everyone in the Tomlinson Lab. Your encouragement, talent and good humour throughout this project has been wonderful. You have reminded me not to give up and have tolerated my attempts to be funny. Thank you for the memories and I wish you all the best of luck for your futures.

Finally, I would like to thank my friends and family for their support. Thank you for your encouragement, for patiently listening to my consistent ranting and for reminding me of life outside of the lab.

Abstract

Antimicrobial resistance is leading to the reduction of effective antibiotics and is a global crisis. Metallo-β-lactamases (MBLs) hydrolyse and inactivate a diverse range of β-lactam antibiotics. New Delhi metallo-β-lactamase 1 (NDM-1) can confer resistance to all available β-lactam antibiotics and the rapid, global dissemination of the bla_{NDM-1} gene has raised concern. Co-administration of β-lactamase inhibitors with currently available β-lactam antibiotics is a proven strategy to re-sensitise drug resistant bacteria. However, an effective and specific NDM-1 inhibitor remains elusive. Therefore, the development of highly specific Affimer reagents that inhibit NDM-1 activity may provide an alternative approach for targeting this protein.

Previous work has isolated Affimer 21 as an effective inhibitor of NDM-1 mediated hydrolysis of β-lactams. Affinity maturation of the Affimer 21 isolated a second candidate Affimer, CTL-18, as an effective inhibitor of NDM-1 activity. The isolation of CTL-18 by phage display informed potential changes to the methods to isolate even more effective binders. By increasing the stringency of the phage display strategy resulted in the isolation of a third candidate Affimer, CTL-C8.

Further characterisation of binding and investigations into the use of Affimers as an effective NDM-1 inhibitor is required. However, the isolated Affimers presented could provide a stepping stone in the fight against antimicrobial resistance.

Table of Contents

List of Figures and Tables

Abbreviations

MRSA - Methicillin-resistant Staphylococcus aureus

NDM-1 – New Delhi metallo-beta-lactamase 1

AMR – antimicrobial resistance

POCT – point of care test

CRP – C-reactive protein

ESBL – extended spectrum β-lactamases

WHO – World Health Organisation

PG – peptidoglycan (murein)

NAG - N-acetylglucosamine

NAM - N-acetylmuramic acid

PBP – penicillin binding proteins

LPS - lipopolysaccharide

MGE - mobile genetic elements

HGT - horizontal gene transfer

OM – outer membrane

MATE - multidrug and toxic compound extrusion transporters

SMR - small multidrug resistance transporters

ABC - ATP binding cassette transporters

MFS - major facilitator superfamily

RND - resistance-nodulation-cell-division family

LSBL - limited spectrum β-lactamases

MBL – metallo-β-lactamases

ES – enzyme substrate complex

EI – enzyme intermidate complex

EP – enzyme product complex

RF - replicated form

LB - Luria broth

2TY - 2x tryptone and yeast

SOC - Super Optimal broth with Catabolite repression

PBS - Phosphate-buffered saline

SDS-PAGE - sodium dodecyl sulfate–polyacrylamide gel electrophoresis

PCR - polymerase chain reaction

Chapter 1

Introduction

1.1 Background

Since the discovery of penicillin in 1929, antibiotics have revolutionised medicine (Fleming, 1929; Ventola, 2015). The successful use of antibiotics to prevent and treat infectious disease has not only saved countless lives, it has allowed for the progression of complex medical procedures. In 1943, penicillin was first introduced into wider public use and since then the average life expectancy in the US has increased from 47 years to 79 years thanks to a decrease in communicable diseases (Adedeji, 2016).

However, even before the introduction of penicillin, strains of *Staphylococcus* were found to be resistant to antimicrobials. In fact, shortly after the introduction of any newly discovered antibiotic, resistance would soon appear as described in figure 1.1. Furthermore, resistance to multiple classes of antimicrobials increase the complexity of the problem. Strains of Methicillin-resistant Staphylococcus aureus (MRSA) and, more recently, the rapid global dissemination of *Enterobacteriaceae* producing New Delhi Metallo β-lactamase 1 (NDM-1) have caused global concern and media interest. The resistance to antibiotics has become an impending global crisis with over 25 000 deaths per year already attributed to antimicrobial resistance (AMR) in Europe alone (World Health Organisation, 2017). Several factors have contributed to the rapid emergence AMR with the overuse and misuse of antibiotics for treatment in humans and the use of antibiotics in agriculture to improve livestock growth. Furthermore, the lack of novel antimicrobials in development amplifies the problem.

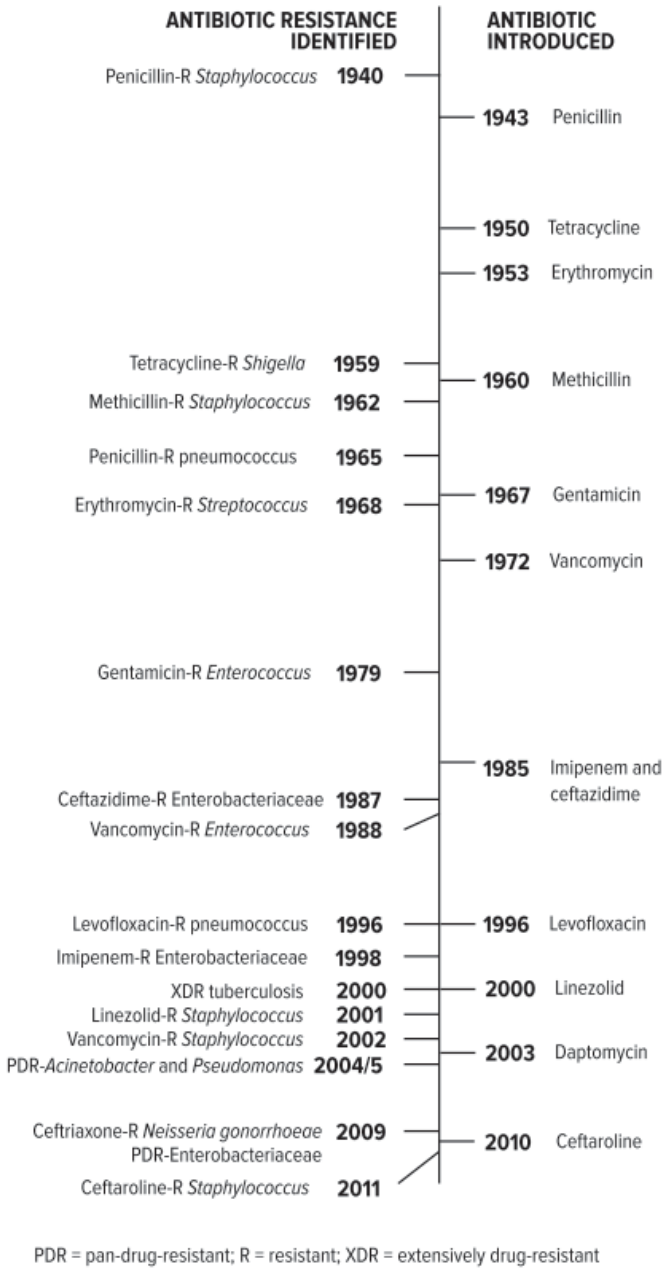

Figure 1.1.1 Timeline of the emergence of antimicrobial resistance following the introduction of antibiotic into widespread use. Shortly after the introduction of novel antimicrobials into clinical use, resistant strains of bacteria have been reported highlighting the rapid emergence of resistance (Ventola, 2015).

1.2. The Problem of Antimicrobial resistance

1.2.1. Clinical Overuse

Globally, antibiotics may be prescribed as a cure-all 'silver bullet' without proper investigation into the cause of the disease (such as expensive and lengthy laboratory analysis) (Michael et al., 2014). For example, in the UK, the Royal College of General Practitioners does not recommend the use of antimicrobials for the treatment of coughs or colds: the likely cause of such symptoms

being viral. However, a recent study found that in 2011, 51% of prescribed antibiotics were for coughs and colds in primary care setting (Hawker et al., 2014).

The inappropriate use of antimicrobials, such as finishing the antibiotic prior to completing the course, can lead to AMR due to bacterial adaptations to low levels of antibiotics (Viswanathan, 2014). It has been reported that bacterial stress response to subinhibitory doses of antibiotics can lead to changes in gene expression, increase in mutations and induce horizontal gene transfer: all potentially leading to the promotion of resistance. For example, the sigma factor RpoS regulates the stress response in *E.coli* and it has been shown that subinhibitory doses of β-lactam antibiotics can increase expression of RpoS (Gutierrez et al., 2013). It has been suggested that an increase in RpoS expression can lead to an increase in mutagenesis. In turn, this leads to a greater chance of the development of resistance. Additionally, subinhibitory doses of β-lactam antibiotics can change gene expression in biofilms of *Pseudomonas aeruginosa* (Bagge et al., 2004). In particular, the increased expression of *ampC*, a β-lactam resistance gene, was observed alongside increased biofilm volume. Subinhibitory levels of antibiotics can result in the promotion of resistance, therefore, use of antimicrobials should be carefully regulated.

To combat the misuse of antibiotics for viral infections, point of care tests (POCTs) in primary care settings could be used. Markers, such as C-reactive protein (CRP) titre, can help distinguish between viral or bacterial infections and could be used to inform treatment (Lubell et al., 2015). Trials of POCT of CRP in Vietnam has shown to reduce the inappropriate use of antibiotics and could be useful in tackling AMR (Do et al., 2016).

1.2.2. Agricultural Overuse

The widespread use of antimicrobials as growth promotors and disease prophylaxis has led to an exacerbation of AMR (Khachatourians, 1998). In particular, the use of low-level antibiotics in feed has allowed the growth of resistant strains of bacteria and the selection for resistance genes. One such example is resistance to ciprofloxacin in 104 strains of *Salmonella typhimurium* discovered in the mid 1990's (Threlfall et al., 1999). The increased use of subtherapeutic doses of ciprofloxacin in animal feed in the UK was associated with an increase in ciprofloxacin resistant *S.typhimurium* human infections.

Importantly, subtherapeutic use of antibiotics in agriculture can result in the spread of resistance genes to microbiota in the wider community including to human isolates (Khachatourians, 1998). The transfer of resistant genes, including intra-species transfer, can occur through several mechanisms as explained in section 1.4.2. A 2013 study identified resistance to β-lactam antibiotics may have transferred from poultry isolates of *E.coli* to human isolates (Voets et al., 2013). Genetically identical plasmids containing Extended-Spectrum β-Lactamase gene (ESBL)

encoding for AmpC, were found in *E.coli* isolates from poultry meat and human clinical samples. The authors suggest that this plasmid may have been transmitted by a foodborne route.

To combat the overuse of antimicrobials in agriculture, recent European Union legislation has curtailed the use of antimicrobials as prophylaxis in agriculture and has reserved some antibiotics for human use only (European Parliament, 2018). However, many countries do not have legislation or compliance mechanisms in place to combat and reduce the overuse of antimicrobials in agriculture (OIE, 2018).

1.2.3. Lack of development

In September 2017, the World Health Organisation (WHO) reiterated the serious lack of novel antibiotics in development (Kmietowicz, 2017). The pharmaceutical industry faces three major challenges when developing antibiotics (2018; Ventola, 2015). First, the recruitment of patients that are infected with resistant strains of bacteria on to clinical trials can be difficult. Clinicians will quickly attempt to resolve and contain the infection before the lengthy recruitment process can take place. Second, outbreaks of AMR strains of bacteria can be sporadic making it difficult to generate enough data to demonstrate the effectiveness of the novel drug against current treatments. And thirdly, antibiotics are curative therapies and therefore the volume of the drug sold after development will be small reducing profitability. Overall, the cost of developing a novel antibiotic outweighs the return.

To financially incentivise the development of novel antibiotics, both governmental and non-governmental programs are now in place (Simpkin et al., 2017). In particular, investment into early stage research has pushed forward innovation. However, there is still a lack of incentives to encourage clinical trials and commercialisation of novel drug products. Due to this lack of development, many antibiotics are based on derivatives of previously developed antibiotics such as the β-lactam family of antibiotics.

1.3. β-Lactam antibiotics

Along with penicillin, β-lactam antibiotics include cephalosporins and “last resort” carbapenems and represent the majority of available antibiotics (Poole, 2004). Whilst the central structure has remained the same, penicillin-based derivatives have been designed to overcome resistance. A 4-membered β-lactam ring forms the central structure as shown in figure1.3.1. These bactericidal antibiotics disrupt the formation of cell wall resulting in autolysin mediated lysis of the bacterial cell. B-lactam antibiotics are the oldest and most prevalently used antibiotics and as such, the mechanism of action is well understood (Kohanski et al., 2010).

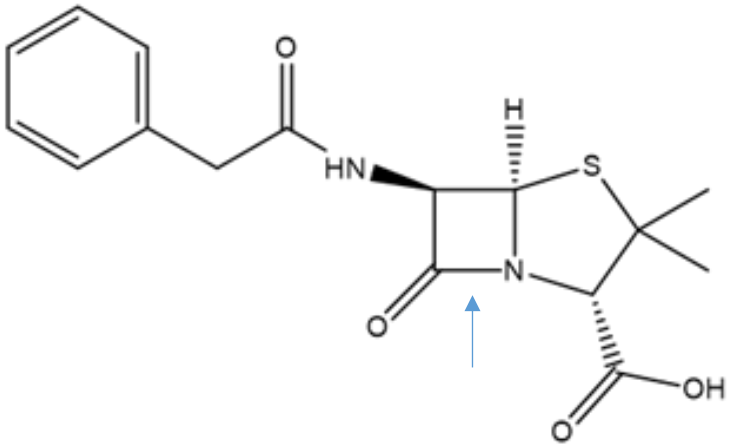

Figure 1.3.1 The 4 membered β-lactam ring as shown in penicillin. The central β-lactam ring is indicated by the arrow in the structure of penicillin. This ring forms the central structure of β-lactam antibiotics [ChemACX.com].

β-lactam antibiotics specifically interfere with the biosynthesis of peptidoglycan (PG), a 3D mesh-like structure that forms the cell wall of both gram-positive (20-80nm) and gram-negative (7-8nm) bacteria (Kohanski et al., 2010; Wise et al., 1965). PG, also known as murein, is a carbohydrate polymer that encapsulates bacterial cells and gives strength and elasticity to the cell to resist osmotic pressure (Höltje, 1998). This strength comes from the structure of PG: strands of alternating N-acetylglucosamine (NAG) and N-acetylmuramic acid (NAM). Glycans are covalently linked via peptide cross-links protruding from NAM. Cross-linked peptide side chains (in *E.*coli; $_{L}$-Ala, $_{D}$-Glu, $_{meso}$-Dap ,$_{D}$-Ala, $_{D}$-Ala) are formed first by (transpeptidase mediated) cleavage of the final $_{D}$-Ala $_{D}$-Ala link followed by the formation of a peptide bond (Park and Uehara, 2008). Membrane bound transpeptidase enzymes continually maintain the integrity of the PG cell wall and it is this family of enzyme, also known as penicillin binding proteins (PBP), that are targeted by β-lactams (Kohanski et al., 2010). A cyclic, 4-membered amide ring (figure1.3.1) forms the central structure of all β-lactam and whilst derivatives of the original penicillin molecule have been developed (primarily to overcome resistance), the bactericidal mechanism is consistent (Waxman et al., 1980). Similarities between the structure of the β-lactam ring and the $_{D}$-Ala $_{D}$-Ala provide a model for transpeptidase inhibition by β-lactam antibiotics (Tipper and Strominger, 1965).

Disruption of the formation of PG cross-linkage results in weakening of the structural integrity of the bacterial cell wall. Initially, it was thought that this weakening combined with internal pressure associated with cell growth resulted in cell lysis (Tomasz, 1979). However, it is now understood that hydrolysis of PG at multiple sites by Autolysins -normally involved with cell wall homeostasis – further contribute to the disruption of the cell wall (Foster et al., 2000). Interestingly, heterogeneity in cell wall degradation is observed dependent on the class of PBP

targeted by the β-lactam. This heterogeneity is due to different PBPs being involved in distinct processes such as defining cell shape, elongation and division (Spratt, 1975).

The cellular disruption caused by β-lactams have proven to be effective at treating a wide range of gram-negative bacterial infections. It is important to note that different classes of antibiotics, such as quinolones, rifamycins and aminoglycosides, have mechanisms of action distinct to that of β-lactams and are reviewed here (Kohanski et al., 2010). The extensive use of β-lactam antibiotics has, however, led to the natural development of resistance.

1.4. Antibiotic Resistance

1.4.1 Acquisition of resistance: Intrinsic resistance

Resistance to antimicrobial reagents pre-dates the use of antimicrobials in the clinic. Intrinsic resistance can protect bacterial species from naturally occurring antimicrobials (Cox and Wright, 2013). On the simplest level, the outer membrane of gram-negative bacteria prevents many small molecules, including antimicrobials, from entering the cell (Nikaido, 1994). Comprising mainly of lipopolysaccharide (LPS), the saturated fatty acid chains reduces permeability of the of the cell. The thick peptidoglycan cell wall of gram-positive bacteria, on the other hand, allows the diffusion of small molecules. In addition to preventing the influx of toxic material, mechanisms that control the efflux of toxins are intrinsic to some bacteria. With efflux pumps appearing on the chromosome of most bacteria, they are thought to expel toxic molecules including those produced by the host (Piddock, 2006a). Interestingly, even microbiomes isolated for 4 million years and protected from human antibiotic use have a diverse range of resistance genes (Bhullar et al., 2012). Soil microbiota also harbour diverse range of intrinsic, naturally occurring resistance genes providing a reservoir for dissemination to other bacterial strains (Forsberg et al., 2012).

1.4.2 Acquisition of resistance: Plasmids

The acquisition of resistance genes from one bacterial cell to another is often mediated by the transfer of a plasmid (Munita and Arias, 2016). Plasmids are circular strands of double-stranded DNA that collect mobile genetic elements (MGEs) and are distinct from the bacterial chromosomal DNA. MGEs such as transposons can be integrated into the plasmid providing a selective advantage such as genes resistant to antimicrobials. Plasmids can be disseminated throughout populations by three main strategies of horizontal gene transfer (HGT). 1) The transformation of ‘naked’ plasmids from the external environment 2) phage mediated transduction of plasmids; £3direct cell-to-cell conjugation. Through these methods, plasmids containing several resistance genes can be disseminated through populations of bacteria.

1.4.3. Mechanisms of Anti-Microbial Resistance

Bacteria have a diverse range of mechanisms to respond to the external environment. In addition to HGT, mutations to theses mechanisms can result in the acquisition of resistance to antimicrobials in the environment. The diverse range of antimicrobial mechanisms are highlighted in figure 1.4.3.1.

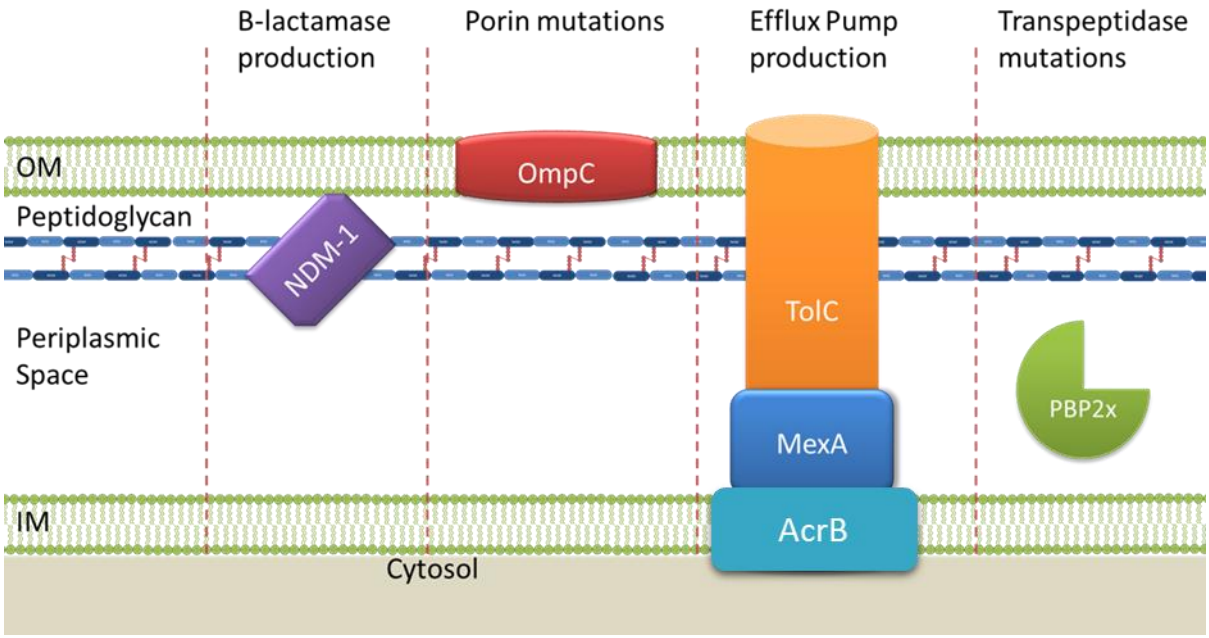

Figure 1.4.3.1 Schematics of mechanisms of resistance to β-lactam antibiotics in gram-negative bacteria. A diverse range of intrinsic and acquired mechanisms of resistance have been discovered. Destruction of the antibiotic molecule can be achieved by production of hydrolysing β-lactam enzymes, such as NDM-1, shown here anchored to the outer membrane (OM). Mutations to water filled porin molecules, such as OmpC can reduce the permeability of the cell to β-lactam antibiotics. Efflux pumps spanning the periplasmic space can eject β-lactam antibiotic from the cytosol. A protein complex of ArcB/MexA/TolC spans the periplasmic space from the IM (inner membrane) to the OM forming the efflux pump. Mutations to the target of β-lactams, Penecillin Binding Proteins such as PBP2x, can confer resistance in bacteria (Wilke et al., 2005)

1.4.3.1 Efflux pumps

Spanning the membrane of most bacterial cells, efflux pumps expel toxic compounds within the cytosol to outside of cellular membrane protecting the cell from damage (Piddock, 2006a). Efflux pumps use energy to pump molecules against a concentration gradient. These transmembrane transporters can limit the effect of antibiotics, by preventing the antibiotic molecule from reaching the target (Munita et al., 2016). Efflux pumps are found in both gram-negative and gram-positive and are categorised into 5 families: multidrug and toxic compound extrusion transporters (MATE); small multidrug resistance transporters (SMR); ATP binding cassette transporters (ABC); major facilitator superfamily (MFS); resistance-nodulation-cell-division

family (RND). AMR is conferred by efflux pumps in clinically relevant bacteria including *N. gonorrhoeae* and *S. aureus*.

An example of an RND efflux pump is the AcrB/TolC system expressed by the gram negative enterobacteria, *E.coli.* AcrB/TolC can efflux β-lactams and other antibiotics thereby conferring multidrug resistance (Piddock, 2006b). Spanning the inner membrane, AcrB is an efflux transporter formed from a homotrimer containing 12-transmembrane α-helices pore (Murakami et al., 2002). Substrates are actively transported through this pore into the connected TolC protein (Koronakis et al., 2000). TolC is formed from a α-helix barrel than spans the periplasmic space and a β-barrel that is integrated into the outer membrane providing a channel for effluxed substrates to translocate the periplasmic space. An adaptor protein, MexA, connects AcrB and TolC by forming a sheath around the proteins in the periplasmic space (Higgins et al., 2004).

1.4.3.2. Porins

In addition to the efflux of antimicrobials, further modifications to the bacterial membrane can reduce interactions between antimicrobial compounds and target site. Modifications that decrease the permeability of bacterial membrane can result in AMR and β-lactam resistance by reducing antimicrobial access to the target site (Munita et al., 2016). This is especially relevant for gram-negative bacteria where porins, β-barrel water-filled channels, located in the outer membrane allow rapid diffusion of soluble substrates. For hydrophilic antimicrobials, such as β-lactams, porins provide a diffusion channel for entry into the bacterial cell (Yoshimura and Nikaido, 1985). The OmpC family of porins, expressed by clinically relevant strains of *E.coli*, provide a channel of entry for the β-lactam carbapenems. It has been suggested that point mutations in the OmpC porin can dramatically alter the permeability of the outer membrane to carbapenems and by altering the electrophysiology of the porin (Bajaj et al., 2016). This reduction in permeability is correlated with the reduction in susceptibility to carbapenem.

1.4.3.3. Modification of the of Target

In addition to limiting access to the target site, mutations to the target protein can result in AMR. Point mutations can result in a change in structure of the drug target thereby preventing interaction (Munita and Arias, 2016).

For example, changes in the structure of penicillin binding proteins (PBPs) that lower the affinity of β-lactam binding (whilst still maintaining transpeptidase activity) can confer antibiotic resistance (Munita et al., 2016). Clinical isolates of β-lactam resistant, gram-positive *Streptococcus pneumoniae* have revealed mutant PBP2a genes that are highly resistant to β-

lactam antibiotics (Dessen et al., 2001). Crystallisation of PBP2a produced by the Sp328 strain of *S. pneumoniae* has revealed several mutations that disrupt β-lactam interaction. The T338A mutation, located within the active site, results in the loss of a water molecule thereby decreasing β-lactam acylation efficiency when compared to a β-lactam sensitive comparison. Additionally, S389L and N514H mutations further reduce β-lactam interactions by steric hindrance.

1.4.3.4 Inactivating Enzymes

Destruction of the antimicrobial molecule before it reaches the target site is an effective mechanism that confers AMR in many clinically relevant strains of bacteria (Munita et al., 2016). Several classes of β-lactamases have now been described and confer resistance to all currently available β-lactam antibiotics, including last resort carbapenams (Paterson and Bonomo, 2005). In general, β-lactamases hydrolyse the amide bond within the cyclic β-lactam ring rendering the antibiotic ineffective. Shortly after the limited introduction of penicillin use, *Staphylococcus aureus* were the first clinically relevant β-lactamase (penicillinase) producing bacteria in the 1940s and were resistant to antibiotic treatment (Abraham and Chain, 1940). To overcome this resistance, development of novel β-lactam containing antibiotics such as cephalosporins in 1948 and cabapenams in 1976 ensued and put into clinical use (Paterson and Bonomo, 2005). However, showing that antibiotic use can drive bacterial resistance, β-lactamases able to resist these novel antibiotics soon developed (Bush, 2013). This has led to a diverse range of β-lactamases that are able to resist multiple antibiotics.

1.5 β-lactamases

1.5.1 β-lactamases: Classification

In general, β-lactamases can be classified into 4 distinct (A, B, C and D) groups according to Ambler classification (Hall and Barlow, 2005). This classification system groups the β-lactamases based on amino acid sequence. Class A, C and D contain a serine within the active site of the enzyme and class B β-lactamases are metallo-proteases, with Zinc ion(s) (Zn) held within the active site. Whilst this classification system helps define different groups of β-lactamases based on amino acid sequence, it does not take into consideration structural or functional similarities between the enzymes (Hall and Barlow, 2003). The three classes of serine β-lactamases (A, C and D) may be distinct in amino acid sequence, however, structural homology between the classes suggest a common ancestor. Furthermore, the Ambler classification does not make the distinction between limited spectrum β-lactamases (LSBL) and extended spectrum β-lactamases (ESBL) (Paterson and Bonomo, 2005).

Class A serine β-lactamases include TEM-1 (Salverda et al., 2010). First described in penicillin resistant *Enterobacteriaceae* in 1965, over 170 alleles have now been identified. Substitution mutations are responsible for the development of many of these TEM-1 variants and can result in extending the spectrum of β-lactam resistance. For example, G238S mutation extended the resistance to include increased resistance to cephalosporins. This variant is found expressed in clinically relevant bacteria such as *E.coli* (Venkatachalam et al., 1994). In addition to TEM-1 variants, other class A ESBLs (such as CTX-M, and SHV) can be detected in many clinical isolates proving to be a significant factor in multi-drug AMR (Fang et al., 2008).

Class C and D serine β-lactamases can also confer extended resistance to β-lactam antibiotics. AmpC is a clinically relevant class C β-lactamase and the bla_{AmpC} gene is known to be expressed in many strains of *Enterobacteriaceae* (Jacoby, 2009). The wide dissemination of bla_{AmpC} is due to the plasmid location of the gene and association with insertion sequences such as IS*Ecp1* involved in mobilising the gene. Likewise, the OXA-type, class D β-lactamase, is associated with the insertion sequence IS*Aba1* (Evans and Amyes, 2014). Importantly this insertion sequence, upstream of bla_{OXA}, promotes increased gene expression and mobilisation

Class B β-lactamases are metallo-proteases and distinct from the other classes owing to Zinc ions within the active site as oppose to a serine residue (Mojica et al., 2016). Ion-chelating agents, such as EDTA (ethylenediaminetetraacetic acid) can, therefore, inactivate class B β-lactamases. Wide dissemination of clinically relevant metallo-β-lactamases (MBLs) has been reported. In particular, 4 families (IMP, VIM and NDM) are known to confer resistance to virtually all available β-lactam antibiotics (Mojica et al., 2016). The ability of class B β-lactamases to confer extended resistance and the dissemination of genes by horizontal gene transfer in both nosocomial and environmental settings result in a risk to public health.

1.5.2 β-lactamases: Global Dissemination

One of the biggest challenges to combating resistance to β-lactam antibiotics is the rapid, global dissemination of resistance genes. The global dissemination of MBL can be highlighted by resistance to carbapenems mediated by imipenemase or IMP family of MBLs. Predominantly reported in Japan and south-east Asia, isolates of *Serratia marcescent,* conferring IMP mediated resistance to β-lactams, were first isolated in 1991 in Japan (Osano et al., 1994). Since then, variants of the bla_{IMP} gene have been found worldwide and point mutations, including V67F, have conferred extended resistance to β-lactams (Mojica et al., 2016; Tada et al., 2013). Importantly, the rapid dissemination of bla_{IMP} has been attributed to the association of the gene within resistance cassettes in class 1 integrons (Zhao and Hu, 2011). Class 1 intergrons are considered to play an important role in the spread of multidrug resistance as they contain

several resistance genes and can transpose onto plasmids contributing to the global dissemination of β-lactam resistance.

In 2008, a novel MBL was described in an isolate of *Klebsiella pneumoniae* from a Swedish patient with a urinary tract infection who had recently travelled to India (Yong et al., 2009). The New Delhi metallo-β-lactamase-1 (NDM-1) has a wide global dissemination and is most prevalent in in the Indian subcontinent (Mojica et al., 2016). NDM-1 confers resistance to all available β-lactam antimicrobial. Clinical relevant strains of *E.coli, Vibrio cholerae* and *A.baumannii* have been reported to harbour the bla_{NDM} gene including strains that have caused epidemics. To date, 14 variants of NDM have been reported with NDM-1 being the most prevalent and therefore clinically relevant (Zou et al., 2015). The rapid global dissemination of bla_{NDM-1} is of concern to public health and this rapid spread of the gene is due to several factors including association with insertion sequence ISAba125 and IncL/M plasmids (Carattoli, 2013).

1.6 New Delhi Metallo-beta-lactamase-1

The rapid dissemination and the lack of effective antibiotics against bacteria producing NDM-1 means urgent action is needed. An understanding of the structure of NDM-1 and hydrolysis mechanism may help in the development of novel treatments.

1.6.1 Metallo-β-Lactamase: Common Structural Features

Despite the lack of amino acid sequence homology, several common features are observed within the MBL family (Mojica et al., 2016). As metalloproteins, MBLs have common structural features (Carfi et al., 1995). A common αβ/βα structural protein fold with external α-helices and an internal mixed β-sheet sandwich. In MBLs, the hydrophobic β-sheet internal fold creates a shallow groove containing one or two zinc ions that form the active site of the enzyme. These zinc ions are co-ordinated by the surrounding protein structure. The Zn1 metal ion is held within a tetrahedral formation, the second Zn2 ion forms a trigonal-pyramidal structure. Importantly, the zinc ions provide a site for a hydroxyl group to reside thereby providing a nucleophile for hydrolysis reactions. Furthermore, the shallow groove in which the active site is positioned extends in both directions (Meini et al., 2014). This allows a diverse range of substrates to be accommodated by the enzyme.

Despite low amino acid homology, further structural similarities that facilitate hydrolysis of the β-lactam ring are reported between MBLs (Mojica et al., 2016). Located 6 Å away from Zn2, a positively charged side chain, (Lys224 in NDM-1 and IMP-1, Arg228 in VIM-2) provides a counter-ion to the negatively charged carboxyl group found conserved in β-lactam antibiotics. Furthermore, active-site loop 10 (ASL10) contains a conserved asparagine (Asn233). This amidic

amino acid providing a site for hydrogen bonding with the carboxylate group formed following hydrolysis of the amide bond of a β-lactam ring. Additionally, a conserved flexible β-hairpin loop, active-site loop 3 (ASL3), provides a hydrophobic surface for β-lactam ring interaction. Importantly, limited conformation change within this loop upon ligand binding may contribute to β-lactamases activity (King and Strynadka, 2011a).

1.6.2 NDM-1 Structural Features

NDM-1 can hydrolyse the broadest range of β-lactam antibiotics. Therefore, unique structures within the enzyme may explain this promiscuity. First characterised in 2009 and then later crystallised by several groups in 2011, NDM-1 contains several unique characteristics to explain its efficacy (Green et al., 2011; Guo et al., 2011; King and Strynadka, 2011a; Yong et al., 2009).

NDM-1 proteins have a molecular mass of ~27kDa and have a general globular structure, with a pair of α-helixes (α1 – α4) either side of a wide groove formed by two anti-parallel β-sheets (β1-β7 and β8-β11) as shown in figure1.6.2.1 (Guo et al., 2011). The zinc ions are held within the active site with Zn1 in a tetrahedral formation with His120, His122, His189 and Asp124. And Zn2 in trigonal-pyramidal with Asp124, cys208 and His 250.

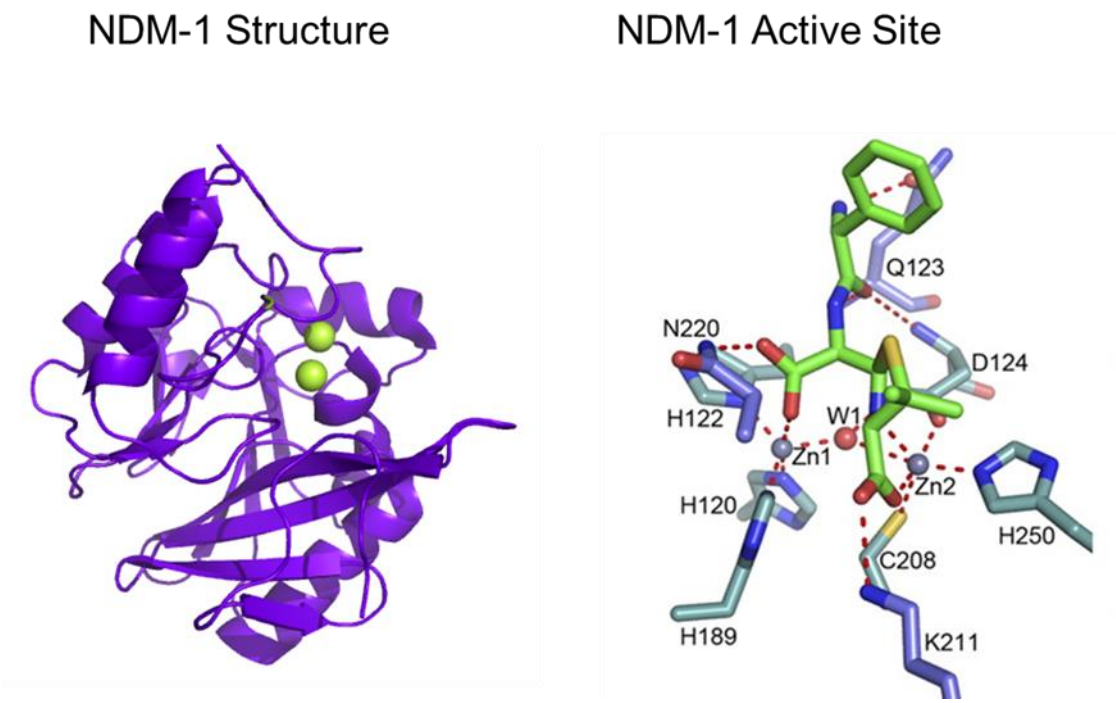

Figure 1.6.2.1 . NDM-1 structure and active site. The overall structure of NDM-1is shown in purple with the zinc core ions highlighted in green. The NDM-1 active site is shown interacting with ampicillin. The Zn1 ion is held in a tetrahedral formation with His120, His122, His189 and Asp124. A tetrahedral formation with ZN and His120, His122, His189 and Asp124 (Zhang and Hao, 2011) .

Unique motifs are observed within the NDM-1 structure (Yong et al., 2009). First, a HAHQD motif between residue 116 and 120 is involved in both Zn1 and Zn2 anchoring. This provides a precise site for enzyme activity. Away from the active site, a unique FAAN motif between residue 160 and 164 has been reported. It is suggested that the FAAN motif contributes to the formation of loop 8. It is loop 8 that is thought to mediate dimerization of NDM-1 proteins (King and Strynadka, 2011a). Furthermore, a type 1 N-terminal signalling sequence targets the protein to the periplasmic space of gram-negative bacteria. This sequence is thought to be cleaved following translocation to the periplasm. A lipobox (LSGC) motif downstream of the periplasmic signal forms a lipid anchor between NDM-1 and the bacterial outer membrane (González et al., 2016). This anchorage is thought to stabilise the enzyme and allow export of NDM-1 via outer-membrane vesicles.

The active site loops ASL3 and ASL10, contribute to the ability of NDM-1 to hydrolyse diverse range of β-lactams when compared to other MBLs (Carfi et al., 1995; King and Strynadka, 2011a; Meini et al., 2014; Nordmann and Poirel, 2002). Primarily, a wide active site groove and hydrophobic interactions with the β-lactam substrate allows this promiscuity. When compared to VIM-2, the wide active site of NDM-1 (520Å in NDM-1 compared to 450Å in VIM2) is because ASL3 and ASL10 are positioned further away from the zinc core. Furthermore, less bulky and hydrophobic amino acids within the NDM-1 active site, when compared to VIM-2, provides a site for stabilising interactions with the substrate. For example, VIM-2 contains phenylalanine at position 61 compared to the less bulky methionine in NDM-1. Moreover, in NDM-1 the hydrophobic proline in position 62 is found as oppose to the negatively charged aspartic acid fond in VIM-2. Additionally, the positively charged lysine residue in position 125 of NDM-1, adjacent to the Zn2 binding aspartic acid, is thought to help position the anionic β-lactam substrate for enzymatic action.

The structure of NDM-1 indicates that this enzyme has been naturally developed to be effective at multi-drug resistance (Mojica et al., 2016). An open active site with surrounding hydrophobic loops provides a structural surface for substrate stabilisation. This, combined with a dizinc active site core precisely held in place, provides the mechanism to hydrolyse the amide bond of a wide range of β-lactam derivatives.

1.6.3 NDM-1 Hydrolysis Mechanism

The mechanism of β-lactam hydrolysis is highly influenced by the structure of NDM-1 (Meini et al., 2015). X-ray crystallography of NDM-1 and substrate co-complexes have revealed a general mechanism for hydrolysis of the amide bond in the β-lactam ring.

In general, hydrolysis of the amide bond (C-N) is thought to be a two-step process (Guo et al., 2011). First, following the formation of an enzyme substrate complex (ES), a hydroxide molecule (held between Zn 1 and Zn2) acts as a nucleophile and attacks the carboxyl carbon (C7) of the β-lactam ring. This cleaves the amide bond (C-N) resulting in an open β-lactam ring (Kim et al., 2013). Both Zn ions are involved with the formation of anionic intermediate (EI): Zn1 binds with the newly formed C7 carboxylate group and Zn2 interacts with the with the amide nitrogen (N4) and a carboxylate group found on the ring fused to β-lactam. Protonation of the intermediate is the second step to form the enzyme product complex (EP) (Meini et al., 2015). It is thought that a water molecule originally bound to Zn2 provides a proton for this step of the reaction, however, alternatives have been suggested (Meini et al., 2015). Initially it was suggested that a conserved Asp-120 residue within the active site was the proton donor in this step. However, site directed mutagenesis of this residue in IMP-1, and subsequent kinetic assays, revealed this was not the case (Yamaguchi et al., 2005). Alternately, crystallography of NDM-1 in complex with ampicillin suggests that the proton is donated from the C7 carboxylate group formed by amide bond cleavage (Zhang and Hao, 2011).

NDM-1 is highly effective at hydrolysing a broad spectrum of β-lactam antibiotics leading to multi-drug resistance. One strategy to overcome this resistance is to inhibit the enzymic action of NDM-1 preventing the hydrolysis of the β-lactam ring. This would re-sensitise the resistant bacteria to β-lactam antibiotics.

1.7 Overcoming Resistance

1.7.1 Current β-lactamase inhibitors

The discovery of novel types of antibiotics may prove to be successful in tackling antimicrobial resistance. However, with a diverse range of β-lactam antibiotics already on the market, overcoming resistance mechanisms may also be beneficial (Docquier and Mangani, 2018). Co-administration of the β-lactamase inhibitor, clavulanic acid, with β-lactam antibiotics has proven to be a successful treatment. Clavulanic acid, discovered in 1977, contains a β-lactam ring and was isolated from *Streptomyces clavuligerus* (Reading and Cole, 1977). Whilst not directly acting as a β-lactam antibiotic, clavulanic acid will bind to serine based β-lactamases and inhibit activity. When co-administered with amoxicillin, these drugs are effective treatment against class A β-lactamase producing bacterial infections such as *E.coli,* and *K. pneumoniae* (NICE, 2019). In addition to clavulanic acid, sulbactam and tazobactam were developed in the 1980's and early 1990's as β-lactamase inhibitors and used successfully in conjunction with β-lactam antibiotics (Tehrani and Martin, 2018).

Despite the success of β-lactam/β-lactamase inhibitor combination at targeting AMR infections, further development is needed to overcome some limitations. First, resistance to β-lactamase inhibitors has been reported with the emergence TEM β-lactamases resistant to clavulanic acid, sulbactam and tazobactam (Chaïbi et al., 1999). Additionally, inhibitors against class B, Metallo-β-Lactamase have yet to be approved for clinical use (Rotondo and Wright, 2017).

1.7.2. Metallo-β-Lactamase Inhibitors

As shown with clavulanic acid, targeting the active site of β-lactamases may re-sensitise resistant bacteria to antimicrobials. EDTA has been shown to inhibit NDM-1 activity by chelating the Zn ions in the active core (Thomas et al., 2011). However, EDTA is not a viable treatment due to its unspecific nature. One category of metallo-β-lactames inhibitors that disrupt the Zn core contain thiol groups or compounds containing zinc-binding sulphur (Liénard et al., 2008). The sulphur atom, found within a thiol group, can form a bridge between the two zinc ions of the β-lactam core. This sulphur bridge results in the displacement of the hydroxyl group held within the active site thereby removing the nucleophile required for enzymatic action. Simple thiols, and other -SH containing compounds such as Homo-cysteinyl peptides have been shown to inhibit β-lactamase activity (Sun et al., 2006). A second group of β-lactamase inhibitors, including succinic acids, contain dicarboxylate groups that also disrupt the Zn active centre (Toney et al., 2001). Like thiols, the hydroxyl group held by the Zn ions is displaced by dicarboxylate inhibitors. The first carboxylate group forms a monodentate bridge between Zn1 and Zn2 displacing the hydroxyl group. The second carboxylate group further disrupts the Zn core of the enzyme by forming a bridge between the Zn2 ion and conserved Lysine residue. Aromatic rings linking the carboxylate groups can interact with ASL3 causing the loop to close over the active site (Toney et al., 2001). Several scaffolds have been successfully used to hold the two carboxylate group, such a pyridine ring, and have been shown to successfully inhibit β-lactamase activity (Tehrani and Martin, 2018). Naturally produced fragment compounds have also been reported to inhibit MBLs (Payne et al., 2002). Fungal extracts from *Chaetomium funicola* were shown to inhibit IMP-1 by carboxylate interaction with the zinc core, ASL3 interaction and hydrogen bonding with a conserved lysine residue (Payne et al., 2002).

1.7.3 Synthetic binding proteins as NDM-1 inhibitors

To increase the specificity of potential β-lactamase inhibitors, and in turn reduce the chance of off- target effects, synthetic binding proteins could be developed (Sha et al., 2017). In general, synthetic binding proteins (such as monobodies, nanobodies and Affimer reagents) have several properties that make them ideal candidates for therapeutics.

Monobodies are synthetic binding proteins, based on fibronectin type III (FN3) structure, and have been shown to modulate enzyme activity (Koide et al., 1998). The general structure of monobodies comprise of a β-sandwich fold (analogous to immunoglobulin domains) with three surface loops that form binding domains. These binding domains can be randomised to generate a library of synthetic binding proteins that can be screened against target proteins. Development of monobodies against the enzyme β-galatosidase has demonstrated that precise binding of the synthetic binding protein can be achieved (Tanaka et al., 2015).

Synthetic binding proteins known as nanobodies are single domain antibody fragments that are raised in dromedary camelids. In one study, nanobodies binding to the β-lactamase VIM-4 have been identified (Lauwereys et al., 1998). Lacking the light chain, these heavy chain antibodies contain a single binding domain (VHH) that is restricted to a monomer (as opposed to a dimer as on a full antibody). This binding domain contains 3 variable regions (CDR1, CDR2, CDR3) that can be modified to bind to target proteins. The VHH domain can be expressed as a 15KDa recombinant protein -independent of the heavy chain- known as nanobody fragments. Importantly, the protruding CDR3 loop can interact with the active site cleft of enzymes and therefore inhibit activity (Muyldermans et al., 1994). In 2013, a nanobody that was able to inhibit VIM-4, a clinically relevant MBL, was developed (Sohier et al., 2013). Interestingly, it was reported that this nanobody bound allosterically to loop 6 that is distant from the active site. The authors suggested that inhibition is due to the nanobody interfering with the conformation of active site loop 7.

The development of synthetic binding proteins to modulate enzyme activity, in particular the inhibition of MBLs, may prove to be clinically important tools in combating anti-microbial resistance. Therefore, the development of synthetic binding proteins that target and inhibit the promiscuous NDM-1 may prove to be clinically viable.

1.8 Affimer Reagents

Affimers are a class of non-antibody protein scaffold that have been developed as a molecular recognition reagent (Tiede et al., 2014). Previously termed Adhirons, there are two Affimer scaffolds and are based on similar molecular constructs. Type I are based on the human protease inhibitor stefin A (Woodman et al., 2005) with Type II based on a consensus sequence of 57 phytocystatin sequences (Tiede et al., 2014). The type II scaffold is used in this study. The consensus alignment resulted in a highly stable structure with a Tm of 101^{o}C. The Affimer scaffold consists of a single central α-helix and four anti-parallel β-sheets. Two variable regions consisting of 9 amino acids are positioned between the first and second β-sheets (VR1) and the third and fourth β-sheets (VR2) as shown in figure1.8.1. Several features of the Affimer scaffold

make it ideal as an artificial therapeutic protein. A small 12kDa size, monomeric, lack of disulphide bonds and is produced readily in *E.coli.* The variable regions have allowed diverse naïve libraries of 1.3 x 10^{10} unique constructs to be developed and a range of applications have been suggested (Tiede et al., 2017).

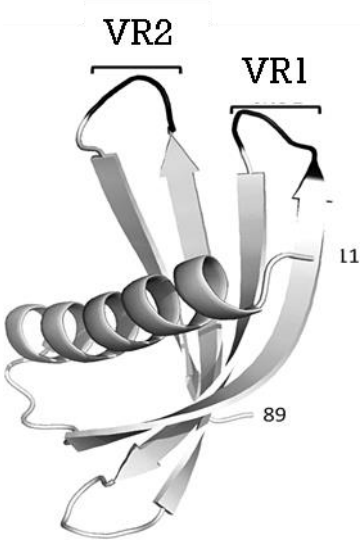

Figure 1.8.1 The structure of an Affimer scaffold. Based on the phytocystatin structure, 4 antiparallel β-sheets and a central α-helix form the main structure. Two variable regions (VR1, VR2) are located between two pairs of β-sheets. The VR contain 9 amino acid that can be engineered to conformationally recognise target molecules (Tiede et al., 2014).

An initial study, confirming the use of Affimers as synthetic binding proteins, was carried out to find binders against yeast SUMO protein (Tiede et al., 2014). In this study, phage display was used to screen the Affimer library against yeast SUMO and resulted in the isolation and subsequent characterisation of 4 unique Affimer binders. Furthermore, the Affimer library has been screen against a broad range of targets to be used for research and potential clinical applications (Tiede et al., 2017). This includes Affimers identified against Transient Receptor Potential Vanilloid 1 (TRPV1) ion channel that can modulate channel function; Affimers conjugated with eGFP that target Human epidermal growth factor receptor 4 (HER4) to be used in super-resolution microscopy; Affimers that target the intracellular signalling pathway such as the Src-homology 2 (SH2) domain.

The novel use of Affimers to inhibit enzyme activity, such as NDM-1 activity, has been shown to be promising. Several properties of Affimers make them ideal candidates as specific enzyme inhibitors. Affimers have been shown to be highly specific, therefore, reducing the risk of off target effects (Robinson et al., 2018). For example, Affimers have been identified that bind specifically to the FC receptor FcγRIIIa but not the analogue FcγRIIIb. The small 12kDa size and extended binding regions of Affimers make them ideal for binding to pockets, such as the active site of enzymes.

1.9 Phage Display

Phage display is a powerful method of high throughput screening of protein binders against target molecules (Rahbarnia et al., 2017). Large phage libraries of antibody fragments, peptides and artificial binding proteins have been generated and can be screened against target molecules to identify specific binders. A phage display strategy has been developed to screen Affimer libraries against target molecules to identify specific binders (Tang et al., 2017).

1.9.1 M13 Bacteriophage and Life Cycle

The phage display strategy developed for Affimer libraries uses M13 filamentous bacteriophage. Filamentous phage contains a circular single-stranded DNA (ssDNA) contained within a protein capsid. The cylindrical capsid consists of five different capsid proteins as shown in figure 1.9.1.1. The central column of the phage consists of around 2700 copies of pVIII protein. One end of the phage consists of five molecules each of pVII and pIX, at the other up to five molecules of pIII and pVI are found. The pIII protein interacts specifically with the F pilus of *E.coli* cells to mediate infection.

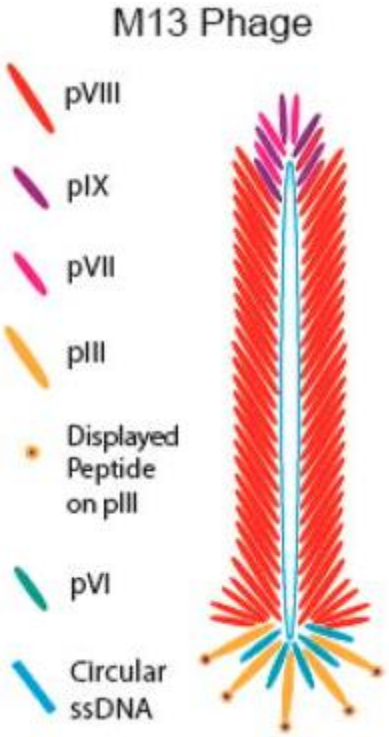

Figure 1.9.1.1 Schematic of M13 filamentous bacteriophage structure. The M13 phage has a cylindrical capsid. The central column is formed from pVIII protein. One end is capped with pVII and pIX protein with the other end capped with pIII and pVI. Circular ssDNA is found within the capsid. Up to 5 proteins of interest are displayed on pIII proteins (Yang et al., 2017)

The interaction between M13 and the F pilus of *E.coli* starts the infection cycle by triggering the retraction of the pilus as shown in figure 1.9.1.2 (Barbas, 2001). Uncoating of the phage is thought to be mediated by inner membrane bound proteins Tol Q, R and A resulting in

translocation of viral DNA into the cytoplasm. The ssDNA genome is then converted to a double stranded replicated form (RF) by host mechanisms. This provides a template for phage DNA replication and for transcription and translation of phage proteins. Regulation of RF DNA and biosynthesis of phage proteins is mediated by pII, pIV and pX. Dimers of pV bound to newly synthesised ssDNA prevent RF formation and allows viral assembly at the membrane. Progeny phage are released from the host cell without causing lysis allowing continual production of phage without disrupting growth of the *E.coli* culture.

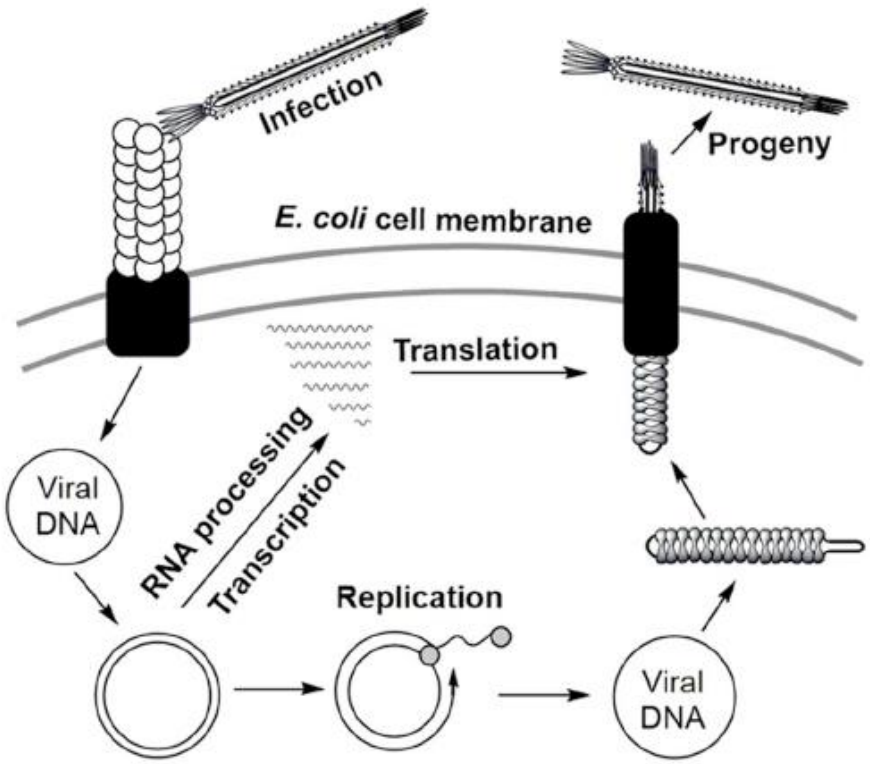

Figure 1.9.1.2 The life cycle of M13 bacteriophage. The M13 life cycle starts with pII mediated absorption of the phage via the F pilus and mediated by TolQ, TolR and TolA. Once uncoated, the phage genome, is replicated in the cytoplasm of the host *E.coli* and repackaged to generate new phage at the cell membrane. The host cell is not lysed in this process (Smeal et al., 2017).

Affimer proteins are fused to pIII coat proteins of M13 phage to allow phage display. Mulitple copies of the Affimer scaffolds are displayed on the phage surface without disrupting the life cycle of the phage (Tang et al., 2017). The Affimer coding region is inserted into the pDHis phagemid vector (also known as pBSTG1; GenBank KJ474865) between *NheI* and *NotI* restriction sites preceding the truncated pIII gene. A His tag has been introduced to the terminal end of the Affimer to allow nickel ion affinity purification. Following the His tag, a TAG amber stop codon has been introduced. This stop codon is supressed in ER2738 strains of *E.coli* that express tRNA

anti-codon which read the amber sequence as a glutamine allowing read-through. Strains such as BL-21 Star™ (DE3) read the stop codon as normal allowing production of the protein. A truncated c-terminal of pIII follows the Affimer sequence allowing insertion into the phage coat. M13K helper phage are used to provide structural proteins to bacterial cells containing the phagemid vector allowing the production of Affimer displaying phage. The helper phage DNA harbours a defective origin of replication and therefore the Affimer containing plasmid is favoured. An ampicillin resistance gene on the phagemid plasmid allows selection by antibiotic treatment.

1.9.2 Phage display Screening

Large libraries of M13 phage displaying peptides, such as Affimer, can be screened against target proteins to identify binding peptides (figure 1.9.2.1) (Tiede et al., 2017). The libraries are screened, or panned, against immobilised target protein allowing the capture of binding proteins by affinity. Non-binding proteins are removed by washing and results in the selection of protein-phage complex that display Affimer binders. Target bound phage can then be eluted and amplified by infecting *E.coli* resulting in an enriched phage library containing target binding Affimers. Individual clones can be selected from the enriched library and tested by phage ELISA to confirm target binding and negatively select non-specific binders. DNA sequencing can allow the identification of any consensus amino acids in the variable regions and subsequent subcloning of the Affimer insert can allow production of the protein binders.

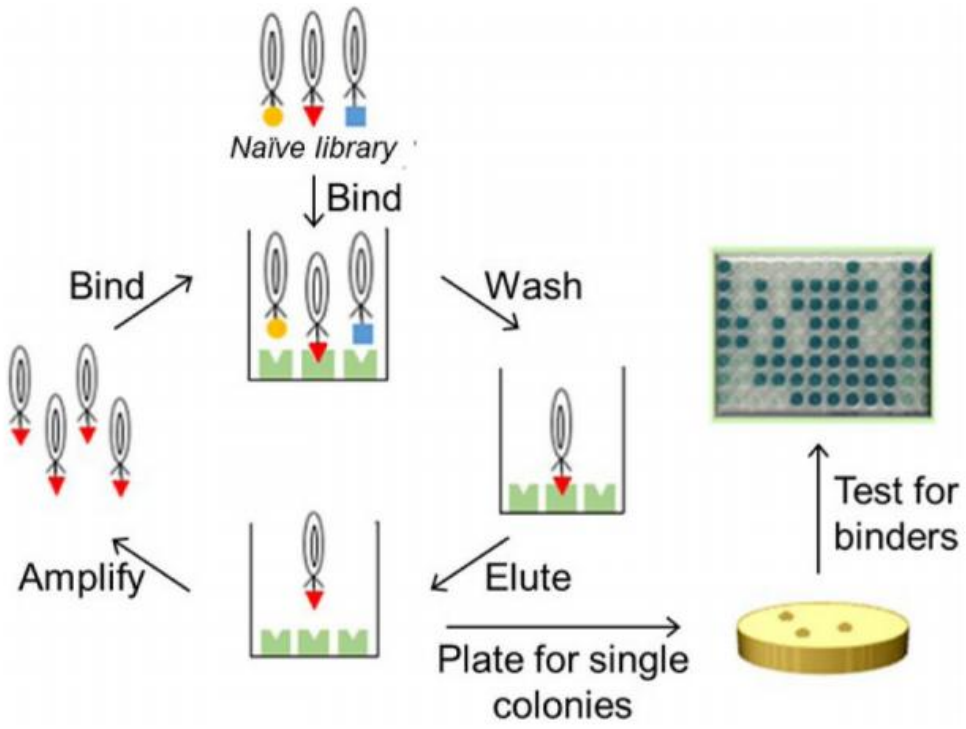

Figure 1.9.2.1 Schematic of phage display protocol. Phage display is used to screen naive libraries of Affimers against an immobilised target. Binders with low affinity are removed by washing. The strongest binders are eluted and used to identify unique binding Affimers by phage ELISA and generate enriched libraries (Gorman et al., 2018)

1.10 Identification of NDM-1 Binding Affimer

Using phage display, Affimer reagents have been identified against a diverse range of targets (Tiede et al., 2017). This has included the identification of an Affimers that bind to NDM-1. Several Affimer reagents were identified by L De Faveri as binding to NDM-1. This was achieved by screening naïve Affimer phage libraries against the NDM-1 target by phage display. From this naïve library screen, several Affimer binders were identified. The inhibition of NDM-1 activity by the Affimer binders was determined by β-lactamase activity assay as described in 2.2.9. This process identified one Affimer, Aff 21, as binding and effectively inhibiting NDM-1 activity. Despite attempts to improve the inhibition of NDM-1 by improved binding affinity (including identification of essential binding proteins by alanine scanning and screening of enriched phage libraries) Aff 21 remained the candidate Affimer. This project builds on the work carried out by L De Faveri, with Aff 21 as the initial candidate binder. This novel use of Affimers to inhibit enzyme activity may be promising and further development and characterisation of Aff 21 is required.

1.11 Objectives

Previously an Affimer, Aff 21, has been identified as inhibiting NDM-1 activity. The aim of this project is to develop on this work and, through a process of affinity maturation, identify Affimer reagents that inhibit NDM-1 activity to a greater extend.

Chapter 2

Materials and Methods

2.1 Materials

2.1.1 Broths Culture

LB broth (Lennox)

10g/l Tryptone; 5g/l Yeast Extract; 5g/l NaCl

LB (Lennox) broth powder (Invitrogen; 20g/l) was dissolved in deionised water before sterilisation in an autoclave at 121°C, 15 psi for 20 min.

2TY

16g/l Tryptone (Oxoid); 10g/l Yeast extract (Oxoid); 5/l NaCl (Fisher Scientific)

The above reagents were dissolved in deionised water before sterilisation in an autoclave at 121°C, 15 psi for 20 min.

LB agar (Lenox)

15g/l Agar; 10g/l Tryptone; 5g/l Yeast Extract; 5g/l NaCl

LB (Lennox) agar powder (Invitrogen; 32g/l) was dissolved in deionised water before sterilisation in an autoclave at 121°C, 15 psi for 20 min. Agar solution was then cooled to ~50^{o}C before addition of appropriate antibiotic at required working concentration. Following aseptic techniques, ~25ml of agar was poured into petri dishes and allowed to fully set before use.

SOC (Super Optimal broth with Catabolite repression)

20 g/l Tryptone (Oxoid); 5 g/l Yeast Extract (Oxoid); 4.8 g/l $MgSO_4$ (Fisher Scientific); 3.603 g/l dextrose(Fisher Scientific); 0.5g/l NaCl(Fisher Scientific); 0.186 g/l KCl (Acros Organics)

The above reagents were dissolved in deionised water before sterilisation in an autoclave at 121°C, 15 psi for 20 min.

2.1.2 Antibiotics

Antibiotic	Manufacturer	Stock Concentration	Working Concentration
Kanamycin	Merk	25mg/ml	50µg/ml
Tetracycline	Merk	12mg/ml	12µg/ml
Carbenicillin	Fisher Scientific	50mg/ml	100µg/ml

Table 2.1.2.1 List of antibiotics used with manufacture, stock concentration and working concentration.

2.1.3 Induction Media

Media	Manufacturer	Stock Concentration	Working Concentration
L-rhamanose	Sigma aldrich	20%w/v	0.2%w/v
IPTG (Isopropyl β-D-1-thiogalactopyranoside)	Generon	1M	0.1mM

Table 2.1.3.1 List of induction media used with manufacture, stock concentration and working concentration.

2.1.4 Buffers

β-lactamase activity assay buffer 50mM HEPES buffer (4-(2-Hydroxyethyl)piperazine-1-ethanesulfonic acid(Sigma) pH7; 20µM $ZnSO_4$ (VWR Chemicals); 10µg/ml bovine serum albumin (Sigma)

Periplasmic lysis buffer 100mM Tris (Bio Basic); 20%w/v sucrose (Fisher Scientific); 1mM EDTA (VWR Chemicals); pH8

Lysis Buffer 50mM NaH_2PO_4 (Sigma); 300mM NaCl (Fisher Scientific); 30mM Imidazole (VWR Chemicals); 10%v/v glycerol (Fisher Scientific); pH7.4

Wash buffer 50mM NaH_2PO_4 (Sigma); 500nM NaCl (Fisher Scientific); 20mM Imidazole (VWR Chemicals); pH7.4

Elution Buffer 50mM NaH_2PO_4 (Sigma); 500nM NaCl (Fisher Scientific); 300mM Imidazole (VWR Chemicals); 10%v/v glycerol (Fisher Scientific); pH7.4

PBS (Phosphate-buffered saline) 137mM NaCl (Fisher Scientific); 4.3mM Na_2HPO_4 (Fisher Scientific); 1.47mM KH_2PO_4 (Fisher Scientific); 2.7mM KCl (Fisher Scientific); pH7.4

PBST PBS with 1% v/v Tween-20 (Chem Cruz)

PEG-NaCl 20%w/v PEG 8000 (Sigma), 2.5M NaCl (Fisher Scientific)

2X Blocking Buffer 10 x blocking buffer (Sigma) diluted 1:5 in PBS-T

Orange G loading dye 30%v/v glycerol (Fisher Scientific); 0.2%v/v Orange G; H_2O

SDS-PAGE running buffer 25mM Tris (Bio Basic); 200mM glycine (Fisher Scientific); 0.1% w/v SDS (Fisher Scientific); pH8.3

Sample Buffer 200mM Tris-HCl (pH 6.8); 20% v/v glycerol (Fisher Scientific); 8% w/v SDS (Fisher Scientific); 0.4%w/v bromophenol blue; 20% v/v β-mercaptoethanol

Coomassie Blue stain 45%v/v (Fisher Scientific); 7% v/v acetic acid (Fisher Scientific); 0.25%w/v Coomassie Brilliant Blue R-250 (Fluka)

TE Buffer 10mM Tris, 1mM EDTA, pH8

Destain 50% v/v H_2O; 40% v/v methanol (Fisher Scientific); 10% v/v acetic acid

TAE running buffer 40mM Tris-acetate; 1mM EDTA (VWR Chemicals); pH8.3

2.1.5 Equipment and Kits

Equipment / Kit	Manufacturer
Thermomixer Heatblock	Eppendorf
Multitron Incubator	Infors HT
Heraeus Multifuge X3R centrifuge	ThermoScientific
Tube Roller	StarLab
NanoDrop Lite Spectrophotometer	ThermoFisher Scientific
F96 Maxisorp Nunc-Immuno Plate	Thermo Scientific
Hydrospeed Plate Washer	Tecan
QIAprep Spin Miniprep	Qiagen
Amersham Imager 600	GE Healthcare
Centrifuge tabletop GenFuge 24D	Progen
Nunc™ MicroWell™ 96-Well Microplates	ThermoFisher Scientific
Spark ® 10M microplate reader	Tecan
Incubator 1000 microplate shaker	Heidolph
QIAGEN Plasmid Maxi Kit	Qiagen
Streptavidin Coated (HBC) 8-well strips	Thermo Scientific
NeutrAvidin Coated (HBC) 8-well strips	Thermo Scientific
Corning™ Centrifuge Tubes 14ml/50ml	Fisher Scientific
Genova Spectrophotometer	Jenway
NucleoSpin® Gel and PCR Clean-up	Macherey-nagel
G-Storm GS2 thermal cycler	Gene Technologies
Multiskan Ascent Plate Reader	Thermo

Table 2.1.5.1 List of equipment and kits used with manufacture information.

2.1.6 Bacterial Cells

BL21 Star™ (DE3) *E. coli* expression strain chemically competent cells (Invitrogen) genotype: F- ompT hdSB (rB-, mB-) galdcmrne131 (DE3)

XL1-Blue Supercompetent *E.coli* cells (Agilent Technologies) genotype: recA1 endA1 gyrA96 thi-1 hdR17 supE44 relA1 lac [F´ proAB lacIq ZΔM15 Tn10 (Tetr)]

ER2738 *E. coli* cells (Lucigen) genotype: [F'proA+B+ lacIq Δ(lacZ)M15 zzf::Tn10 (tetr)] fhuA2 glnVΔ(lac-proAB) thi-1Δ(hdS-mcrB)5

2.1.7 Vectors

pET11a (Novagen) T7 promoter; lac repressor gene; ampicillin resistance.

pD861-pelB (Atum) rhaBAD promoter; pelB signal sequence; kanamycin resistance.

pDHis (Tiede *et al*., 2014) Affimer coding sequence; dsbA secretion signal; domains 2 and 3 from gene III of bacteriophage M13; ampicillin resistance.

2.1.8 Biological agent

***NheI* and *NotI* Restriction Enzymes** (New England Biolabs)

M13K07 helper phage (New England Biolabs)

anti-Fd-Bacteriophage-HRP antibody (Seramun Diagnostica GmbH)

2.1.9 Sequence Primers

Plasmid	Primer Name	Primer Position	Sequence	Manufacturer
pET11a	T7F	Forward	5'TAATACGACTCACTATAGGG 3'	Genewiz
pDHis	M13R	Reverse	5' CAGGAAACAGCTATGAC 3'	Genewiz
pD861-pelB	pD861-NDM-1	Forward	5' GACTGGTCGTAGAGACCATG 3'	Genewiz

Table 2.1.9.1 List of sequence primers used including sequence and manufacture information.

2.1.10 PCR primers

Primer Name	Sequence
pDHisIID-final-for	5' TTCTGGCGTTTTCTGCGTCTGC 3'
pDHisIID-final-rev	5' TACCCTAGTGGTGATGATGGTGATGC 3'

Table 2.1.10.1 List of PCR primers used including sequence information. 6Xhis tag is underlined.

2.2 Methods

2.2.1 Transformation of vector into *E.coli* bacterial cells

Vectors were transformed into XL-1 Blue supercompetent cells for vector amplification; BL21 star™ (DE3) cell for protein production or ER2738 cells for phage production. 10µl of thawed component cells were incubated with 1µl of vector at 10ng/µl on ice for 30mins. Cells were heat shocked in a heat block (Eppendorf) at 42°C for 45sec followed by a 2min incubation on ice. SOC (20 g/l Tryptone; 5 g/l Yeast Extract; 4.8 g/l MgSO4; 3.603 g/l dextrose; 0.5g/l NaCl; 0.186 g/l KCl) media, 190µl, was added to the cells and incubated for 1hour at 37°C, 250rpm. The transformed cells were plated onto LB (Lennox) agar (15g/l Agar; 10g/l Tryptone; 5g/l Yeast Extract; 5g/l NaCl) plates with appropriate antibiotic and grown overnight at 37°C.

2.2.2 Miniprep purification of DNA from *E.coli*

DNA plasmids were extracted and purified from 5ml *E.coli* cultures that had been incubated overnight at 37°C, 230rpm. Cells were harvested by a 15min centrifugation at 4 816xg (Heraeus Multifuge X3R centrifuge; ThermoScientific). Following the manufacturer's instructions, a QIAprep Spin Miniprep kits (Qiagen) was used to extract and purify DNA. DNA was eluted into 50µl of nuclease free H_2O and stored at -20 °C.

2.2.3 Nanodrop Readings (DNA and Protein)

To determine the concentration of DNA and soluble protein in solution, NanoDrop Lite Spectrophotometer (ThermoFisher Scientific) reading were taken. The sample buffer, without DNA or protein, was used to blank the spectrophotometer before measurement. A 1µl DNA sample or 2µl protein sample was loaded onto the Nanodrop stage. For DNA samples, an absorbance reading at A_{260} was taken and concentration was determined. using the Beer-Lamberts equation $C = A / \varepsilon.l$. When C is concentration, A is absorbance value, ε is extinction coefficient (50ng-cm/µl for DNA) and I is the light path length in cm (1cm). For protein samples, an A_{280} reading is taken and concentration is determined using the Beer-Lamberts equation $C = A / \varepsilon.l$. The extinction coefficient for each protein was calculated by ExPASy ProtParam analysis (https://web.expasy.org/protparam/) of the amino acid sequence.

2.2.4 NDM-1 Production and Purification

BL-21 Star™ (DE3) cells (Life Technologies) were transformed with pD861 vector containing the truncated NDM-1 sequence as described in methods 2.2.1. A transformed cell colony was selected for a 10ml, 2TY (16g/l Tryptone; 10g/l Yeast extract; 5/l NaCl) with 1%w/v glucose (Fisher Scientific) starter culture and incubated overnight at 37°C, 230rpm. A 400ml LB (lennox), kanamycin (50µg/ml) broth was seeded with 8ml of starter culture and incubated at 37°C,

230rpm to an OD_{600} ~0.8 before 0.2 %w/v L-rhamnose induction. Following an overnight incubation at 25°C and 230rpm, the culture is centrifuged (Heraeus Multifuge X3R centrifuge; ThermoScientific) at 4 816xg for 15mins. The subsequent pellet is gently resuspended in 40ml periplasmic lysis buffer (100 mM Tris, 20%w/v sucrose, 1 mM EDTA, pH 8) and incubated at 4°C, on a tube roller (StarLabs) for 30mins. Resuspended cells were centrifuged 4 816xg for 20mins, the supernatant was discarded, and the pellet was resuspended in 20ml $MgSO_4$ (5mM) and incubated at 4°C, on a tube roller for 30mins. The sample was then centrifuged at 10 000xg (Heraeus Multifuge X3R centrifuge; ThermoScientific) for 20mins and the supernatant, containing soluble 6*His tagged NDM-1, was subsequently incubated with 500µl of washed Amintra Ni-NTA resin (Expedeon) for 1hour at 4°C on a tube roller (StarLabs). Ni- NTA resin bound with NDM-1 was repeatedly washed with 3ml of wash buffer (50mM NaH2PO4; 500mM NaCl; 20mM Imidazole; pH7.4) through a disposable polypropylene column containing a polyethylene disc filter (Thermo Scientific) until a run-through reading of A_{280} <0.09 was measured by NanoDrop Lite Spectrophotometer (methods2.2.3). Bound NDM-1 was eluted from the resin by several 10min incubations with 500µl of elution buffer (50mM NaH2PO4, 500mM NaCl; 300mM Imidazole; 10%v/v Glycerol; pH7.4). Collected elution was dialysed overnight using BioDesign Dialysis Tubing (8000MWCO ThermoFisher Scientific) into 1XPBS (Phosphate Buffered Saline; 137mM NaCl; 10mM Phosphate; 2.7mM KCl; pH7.4) with 10% v/v glycerol (Fisher Chemical), two changes of the 5l buffer were made. Following dialysis, samples were centrifuged (Progen) at 16 000xg for 10mins to remove precipitate and soluble NDM-1 protein was snap frozen by briefly immersing the aliquoted samples in a dry ice/ethanol bath and stored at -80°C. An SDS PAGE (sodium dodecyl sulfate–polyacrylamide gel electrophoresis) gel with Coomassie staining was run to show each stage of the purification process (methods2.2.8).

2.2.5 Subcloning

The DNA coding sequence of each Affimer were subcloned out of pDHis vector into pET11a for protein production. pET11a vector was purified (Maxiprep; Qiagen) from an overnight culture of transformed XL-1 cells (Agilent Technologies) in a 250ml LB (lennox) broth with 100µg/ml carbenicillin. The purified vector (~10µg in 89µl) was digested for 3h at 37°C with 20 U NotI-HF™ and 20 U NheI-HF™ restriction enzymes (New England BioLabs) supplemented with 12µl CutSmart™ Buffer (New England BioLabs) and 14ul of H_2O. Antartic Phosphatase in 1x reaction buffer (New England BioLabs) was added for the final 1h. Digested products were cleaned using gel electrophoresis (method2.2.6) in a 0.7%w/v agarose gel. Subsequently, the digested vector was extracted from the gel by NucleoSpin® Gel and PCR Clean-up kit (Macherey-Nagel) following the manufacturer's instructions eluting into 25µl nuclease free H_2O stored at -20°C. Affimer

coding regions were amplified by PCR from pDHIs. A master mix of 1X Phusion HF buffer (Thermo Scientific), 25mM each dNTP Mix (MP Biomedicals), 3%v/v DMSO (ThermoScientific). 0.8µM forward primer Affimer short; 5' – ATGGCTAGCGGTAACGAAAACTCCCTG), 0.8µM reverse primer (pDHisIID-final-rev 5' – TACCCTAGTGGTGATGATGGTGATGC) and Invitrogen™ UltraPure Water (Thermo Scientific) to a total of 24µl per reaction was made up. 1µl of purified pDHis template DNA containing Affimer construct sequence was mixed with 24µl master mix per reaction and transferred to G-Storm GS2 thermal cycler for PCR:

Cycle Step	Temperature	Time	Cycles
Initial Denaturation	98°C	30 seconds	1
Denaturation Annealing Extension	98°C 54°C 72°C	20 seconds 20 seconds 20 seconds	30
Final Extension Hold	72°C 4°C	10 minutes Hold	1

Table 2.2.5.1 PCR cycle steps including temperature, time and cycle numbers.

Following PCR, the dam methylated template was digested with 0.5µl *DpnI* (New England BioLabs) for 1hour at 37°C and the PCR product was cleaned using NucleoSpin® Gel and PCR Clean-up kit (Macherey-Nagel). The Affimer sequence inserts were then digested with *NheI* and *NotI* restriction enzymes as previously described for the pET11a vector. The purified digested inserts were ligated into the pET11a vector. An overnight incubation of 7ng of digested Affimer insert with 45ng of digested pET11a at 4°C mixed with 1µl T4 DNA Ligase (Roche) and 0.5µl T4 DNA Ligase Buffer (Roche) made up to a total volume of 4µl with H_2O was carried out. A negative control where nuclease free water replaced the insert was performed. Ligation products (1µl) were transformed into 10µl of XL-1 (Agilent Technologies) and plated on to LB (lennox) agar plates overnight at 37°C.

2.2.6 Agarose Gel Electrophoresis and DNA clean-up

A 14ml, 0.7% or 2% (w/v) agarose gel matrix at was made using 1X TAE buffer (1mM EDTA; 20mM glacial acetic acid; 40mM Tris base) with the addition of 1x SYBRsafe DNA gel stain (Invitrogen). DNA samples were prepared by mixing with 10X Orange G loading dye (30%v/v glycerol; 0.25% w/v Orange G] before 10µl of each sample was loaded into sample wells set into the gel. In one well, 4µl MassRuler DNA Ladder Mix (ThermoFisher) was loaded. Gels were run at 50V for around 40mins in a RunOne Electrophoresis Cell (EmbiTec) bathed in 1X TAE running buffer. Images were taken under UV using the Amersham Imager 600 (GE Healthcare).

2.2.7 Affimer Reagent Protein Production and Purification

Individual colonies of BL21 star™ (DE3) cells transformed with pET11a vectors (method2.2.1) containing Affimer inserts were selected from LB (lennox) agar (15g/l Agar; 10g/l Tryptone; 5g/l Yeast Extract; 5g/l NaCl) plates. Starter cultures were propagated in 2ml of 2TY (16g/l Tryptone; 10g/l Yeast extract; 5g/l NaCl) broth with 1%w/v glucose (Fisher Scientific) and carbenicillin (100µg/ml) overnight at 37°C, 230rpm. Subsequently, a larger 50ml 2TY culture was seeded with 1ml of starter culture and allowed to grow to OD_{600} ~0.8 before induction by 0.1mM IPTG (Isopropyl β-D-1-thiogalactopyranoside; Generon). Cells were harvested following an overnight incubation at 25°C, 230rpm. Lysis buffer (50mM NaH2PO4; 300mM NaCl; 20mM Imidazole; 10%v/v Glycerol; pH7.4) supplemented with Benzonase® Nuclease, Purity > 99% (Novagen®), Halt Protease Inhibitor Cocktail EDTA-Free (100X; Thermo Scientific) and Triton X – 100 (Sigma-Aldrich) to a total volume of 1ml was used to lyse cells. Lysates were heat denatured at 50°C for 20min (heat block; eppendorf) and soluble protein was isolated by centrifugation at 12 000 xg for 10 mins (Table-top centrifuge; Progen). Supernatant was incubated with 150µl of Amintra Ni-NTA resin (Expedeon) for 1hour at room temperature. Using a disposable polypropylene column containing a polyethylene disc filter (Thermo Scientific), the resin was repeatedly washed with 3ml wash buffer (50mM NaH2PO4; 500mM NaCl; 20mM Imidazole; pH7.4) until a NanoDrop Lite Spectrophotometer reading (method 2.2.3) of A280 <0.09 was measured from the run-through. His-tagged Affimer reagent was eluted from the Ni-NTA resin by 10min incubation with 250µl elution buffer (50mM NaH2PO4, 500mM NaCl; 300mM Imidazole; 10%v/v Glycerol; pH7.4). Eluted protein was dialysed overnight using Pur-A Lyzer Mini 6000 (Sigma) into 5L of 1XPBS (Phosphate Buffered Saline; 137mM NaCl; 10mM Phosphate; 2.7mM KCl; pH7.4) with 10%v/v glycerol (Fisher Chemical) with two changes. Dialysed samples were centrifuged (Progen) at 16 000xg for 10mins to remove precipitated protein before being stored at -20°C. Samples were taken at each stage for SDS PAGE (sodium dodecyl sulfate–polyacrylamide gel electrophoresis) and stained with Coomassie as described in methods 2.2.8.

2.2.8 SDS-PAGE and coomassie blue staining

SDS-PAGE and coomassie blue staining was used to separate (based on motility through an SDS polyacrylamide Gel matrix) and visualise proteins within a sample. Around 5ml of SDS-agarose separating gel (15% v/v acrylamide (Severn Biotech Ltd); 375mM Tris (pH 8.8); 0.1%w/v SD; 0.15%w/v ammonium persulfate (APS); 0.04%v/v N N N’ N’ tetramethylethylenediamine (TEMED)) was decanted between casting plates and allowed to set for 1hour at room temperature using a Bio-Rad mini-PROTEAN casting system. Isopropanol was also decanted between the casting plates before the incubation to ensure a level interface. Following incubation, isopropanol was removed and around 1ml of stacking gel (5%v/v acrylamide;

125mM Tris (pH 6.8); 0.1% w/v SDS; 0.1% w/v APS; 0.1% v/v TEMED) was poured with the addition of a 15 well comb to create the sample wells. Samples were prepared by incubating 1µl of collected sample with 9µl of deionised H_2O and 3.3µl of 4X sample buffer (200 mM Tris-HCl, pH 6.8, 20 %v/v glycerol, 8 %w/v SDS, 0.4 %w/v bromophenol blue, 20%v/v β-mercaptoethanol) at 95^{o}C for 5mins. In one well, 4µl of PageRuler™ Prestained Protein Ladder (ThermoFisher Scientific) was added as a size standard and 13.3µl of sample was added to the other wells as indicated in the results section. Loaded gels underwent electrophoresis in a Mini-PROTEAN® Tetra Vertical Electrophoresis Cell at 130V in SDS-PAGE running buffer (25mM Tris; 200mM glycine; 0.1%w/v SDS; pH 8.3) for around 90mins. SDS-PAGE gels were stained with Coomassie Blue stain (45%v/v methanol; 7%v/v acetic acid; 0.25%w/v Coomassie Brilliant Blue R-250 (Fluka)) for at least 1hour. Gels were incubated with destain (25 %v/v) methanol, 7.5 %v/v acetic acid) overnight and imaged using an Amersham Imager 600 (GE Healthcare).

2.2.9 β-lactamase activity assay

Quantification of NDM-1 activity, and inhibition in the presence of Affimer reagent, was carried out by spectrophotometric measurement of nitrocefin. On hydrolysis of the β-lactam ring, nitrocefin undergoes a yellow to red colour change that was measured at 482nm using a Tecan Spark ® 10M microplate reader at a constant temperature of 25^{o}C. Assay buffer (50mM HEPES pH7.0; 20µl $ZnSO_4$; 10mg/ml Bovine Serum Albumin) was used to dilute reagents to a final volume of 150µl in a Nunc™ MicroWell™ 96-Well Microplates (Thermo Fisher Scientific). Unique Affimer reagents (500nM) were incubated with NDM-1 (100nM) in individual wells before the addition of nitrocefin (65mM; Merck,) immediately before spectrophotometric reading. Readings were taken every 12sec over 15mins for each condition. Control conditions were included on each plate including zinc chelating EDTA (10mM) minus NDM-1 target; minus Affimer Reagent; non-binding Affimer reagent (500mM). The candidate Affimer reagent (Aff21 or CTL-18) was also performed on each 96-well plate for comparison. Triplicates of each condition were performed on each plate and repeated to n=3.

To determine initial rate of reaction, first, absorbance values were converted into concentration using followed by linear regression analysis performed ($y = mx + c$ where y is concentration, x is time, m is the gradient of the slope and indicates rate with c is the intercept) for the first 250sec of the assay to determine initial rate (µM/s).

2.2.10 Phage ELISA

96-deep well plates (Greiner Bio-One) were used to grow individual colonies of ER2738 cells, in 200µl of 2TY (16g/l Tryptone; 10g/l Yeast extract; 5/l NaCl) media with Carbenicillin (100µg/ml) overnight at 30°C, 1050rpm (microplate shaker, Heidolph Incubator 1000). From the overnight starter cultures, a 25µl sample was used to seed 200µl of 2TY Carbenicillin and incubated for 1hour at 37°C, 1050rpm. M13K07 helper phage (titre ca. 10^{14}/ml) were added at 1:1000 dilution and incubated for 1hour at 25°C, 450rpm. Kanamycin was added to a final concentration of 50µg/ml and incubated overnight at 25°C, 750rpm. Phage cultures were centrifuged at 3 500xg (Heraeus Multifuge X3R centrifuge; ThermoScientific) for 10mins to result in phage containing supernatant. In the meantime, Streptavidin coated 96- well plates were prepared by incubating 50µl of 5mg/ml streptavidin (Life Technologies) in F96 Maxisorp Nunc-Immuno Plate (Thermo Scientific) at 4°C overnight. The streptavidin-coated plates were blocked with 2x casein blocking buffer (Sigma) overnight at 37°C. Biotinylated NDM-1, at concentrations described in the results, was immobilised in the wells of the 96-well streptavidin coated plate for 1hour at 25°C, 450rpm. Corresponding wells on the same plate were left without immobilised target as a negative control. Phage containing supernatant (40µl + 10µl 10X casein blocking buffer) was incubated with the target and the negative control wells for 1hour at 25°C, 450rpm. Plates were washed 1 time with 300µl PBST (137mM NaCl; 10mM Phosphate; 2.7mM KCl; pH7.4; 0.1%v/v Tween-20) using a hydrospeed plate reader (Tecan). Following washing, test and control wells were incubated with a 1:1000 dilution of anti-Fd-Bacteriophage-HRP antibody (Seramun Diagnostica GmbH) at 25°C, 450rpm for 1hour. A final 10X wash with 300µl of PBST using a Hydrospeed plate reader (Tecan) removed unbound antibody. The addition of 50µl of 3,3',5,5'-Tetramethylbenzidine (SeramunBlau® fast TMB/substrate solution; Seramun) detection solution was allowed to develop for a either 3mis of 12mins as described in the results section. Absorbance was measured using a Multiskan Ascent Plate reader (Thermo) at 620nm. For the ELISA pre-trail, as described in results section, 50µl stop solution of 0.16M Sulphuric acid (H_2SO_4) was added to the wells after allowing TMB to develop for 3min and absorbance reading were taken at 460nm.

2.2.11 Phage Display

Affimer reagent constructs that bind to NDM-1 were isolated from a phage library (generated by Christian Teide) by phage display as described in the introduction. A stringent strategy over three rounds was used to select for binders with high affinity as summarized in figure 2.2.11.1.

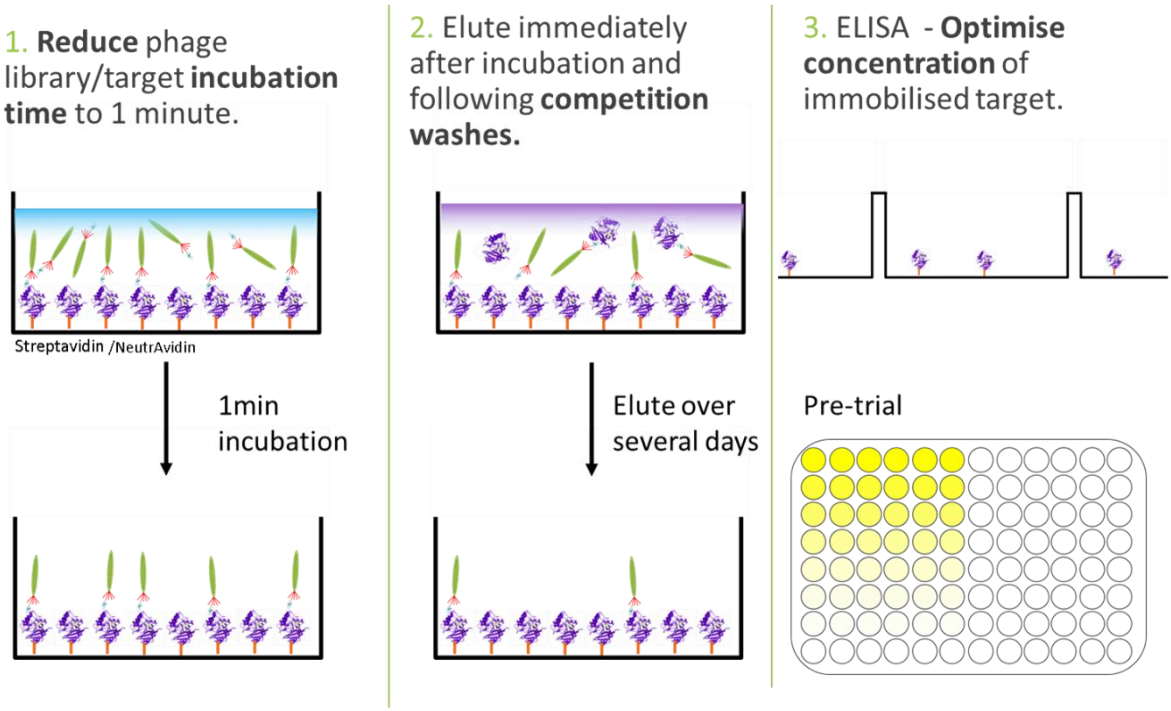

Figure 2.2.11.1 Schematic of stringent phage display strategy. A stringent phage display strategy was devised to identify binders with a higher affinity to NDM-1 than CTL-18.

2.2.11.1 Panning Round 1

Streptavidin Coated (HBC) 8-well strips (Thermo Scientific) were blocked overnight with 2x casein blocking buffer (Sigma) at 37°C. To remove non-specific binders, pre-pan of 5µl of purified phage library in 200µl of 2x blocking buffer was performed three times. In the meantime, 200µl biotinylated NDM-1, at a concentration described in the results, was immobilised in one well of the strip (1hour, 450rpm, room temp) for each elution day as indicated in figure 2.2.11.1.1. Pre-panned phage library was incubated with immobilised target (and control well without target) for 1min before being washed with PBST (137mM NaCl; 10mM Phosphate; 2.7mM KCl; pH7.4; 0.1%v/v Tween-20) for 27 times using a plate washer (TECAN HydroSpeed). Bound phage were eluted from the target and control well by a 10min incubation with 0.2M Glycine (Fisher Scientific), pH 2.2 and neutralisation by 15 µl of 1M Tris-HCl (Bio Basic) pH9.1. A further elution was performed using 100µl of 100mM Triethylamine (Sigma-Aldrich) for 6mins then neutralised by 50 µl of 1M Tris-HCl(Bio Basic), pH7. Eluted phage were allowed to infect 8ml of ER2738 (OD_{600}~ 0.6) and incubated at 37°C, 90rpm for 1hour before being plated onto LB (lennox) agar plates at a range of volumes and incubated overnight. The remaining culture was centrifuged at 3,000 xg for 5 mins, re-suspended in 100µl of broth and plated to create a pool plate for the generation of an enriched page library. Wells containing bound Affimer regent to be eluted of preceding days underwent competition washing, as described in Tang *et.al* 2017, by incubating the wells with 300µl of PBS with 2X Blocking Buffer 16%v/v Glycerol 1x Halt Protease Inhibitor Cocktail (100X) and 2.5 µg Non-biotinylated NDM-1 at room temperature, 450rpm. The wells

were sealed, and the wash was changed twice every 24hours, then eluted as above on the appropriate days. Individual colonies were picked from the overnight plates to be analysed by phage ELISA.

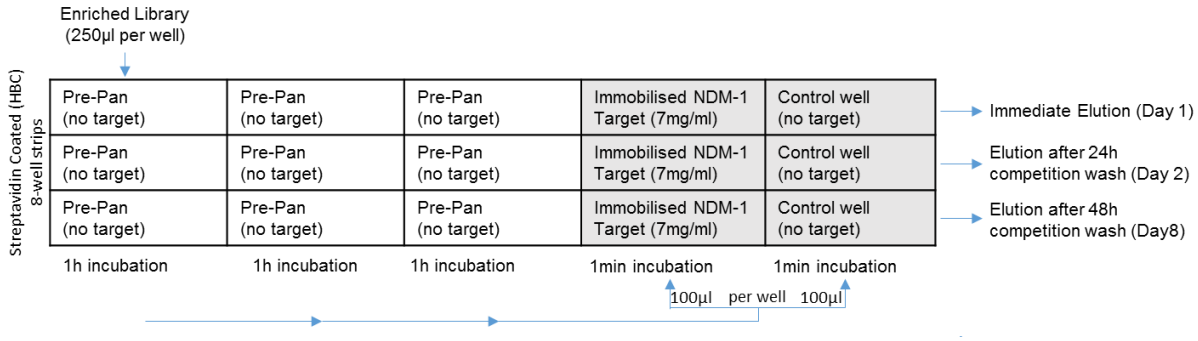

Figure 2.2.11.1.1. Phage display round one well plan.

2.2.11.2 Phage library amplification and purification

To generate phage libraries following phage display panning round, pooled LB (lennox) agar plates are generated as describe in the phage display method. The pooled plate was scraped then diluted in 8ml of 2TY with 100µg/ml Carbenicillin and incubated at 37°C to an OD_{600} ~ 0.8. M13K07 helper phage (titre ca. 10^{14}/ml) was added to the ER2738 cell culture for 30mins at 37°C, 90 rpm before the addition of 16 µl of 25mg/ml kanamycin. The phage-infected culture was incubated overnight at 25°C, 170rpm and harvested by centrifugation at 3,500 *xg* for 10 mins. Phage was precipitated from the supernatant by the addition of PEG-Nacl (20%w/v PEG 8000, 2.5M NaCl) and overnight incubation at 4°C. The precipitated phage was centrifuge at 4,816 *xg* for 30 mins and the resulting pellet was resuspended in 320µl TE (10 mM Tris; 1 mM EDTA; pH 8.0). The phage containing TE buffer was centrifuge at 16,000 *xg* for 10 mins to remove any debris then stored at 4°C.

2.2.11.3 Panning Round 2

The phage library for round 2 was an enriched library generated from the previous phage display round. The second round of phage display followed the same protocol as round 1 and figure 2.2.11.3.1 indicates the wells used in this round.

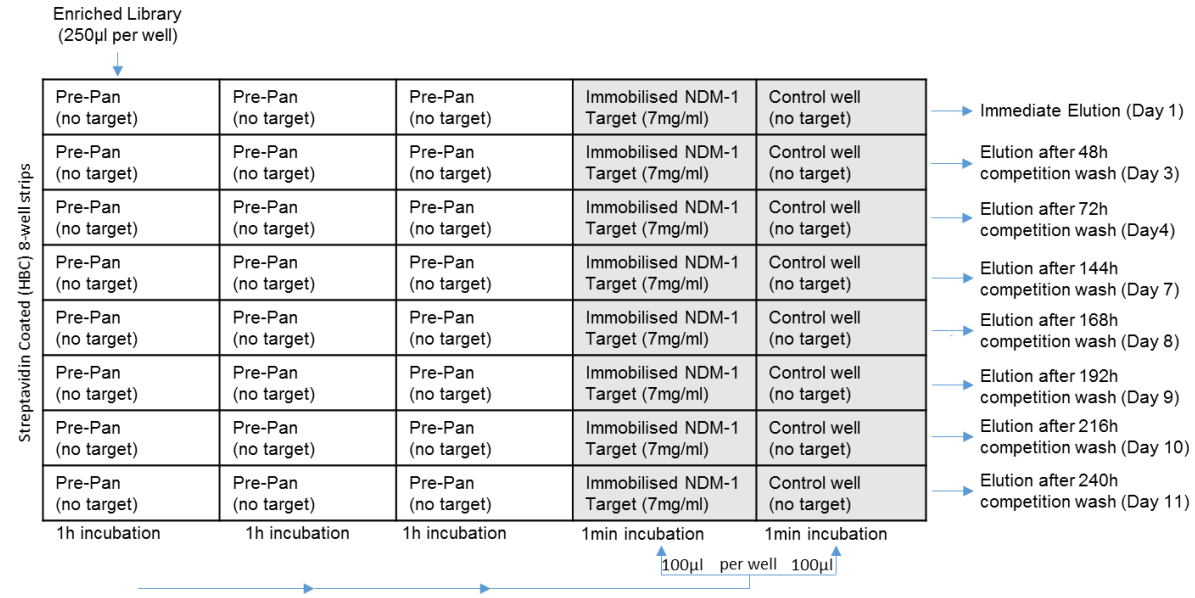

Figure 2.2.11.3.1 Phage display round two well plan.

2.2.11.4 Panning Round 3

The final round of phage display took forward an enriched phage library from the second panning round. For round 3, the protocol from round 1 was followed, however, two changes were made. First, NeutrAvidin Coated (HBC) 8-well strips (Thermo Scientific) were used instead of streptavidin coated strips and a 5ml ER2738 culture was infected as opposed to an 8ml culture.

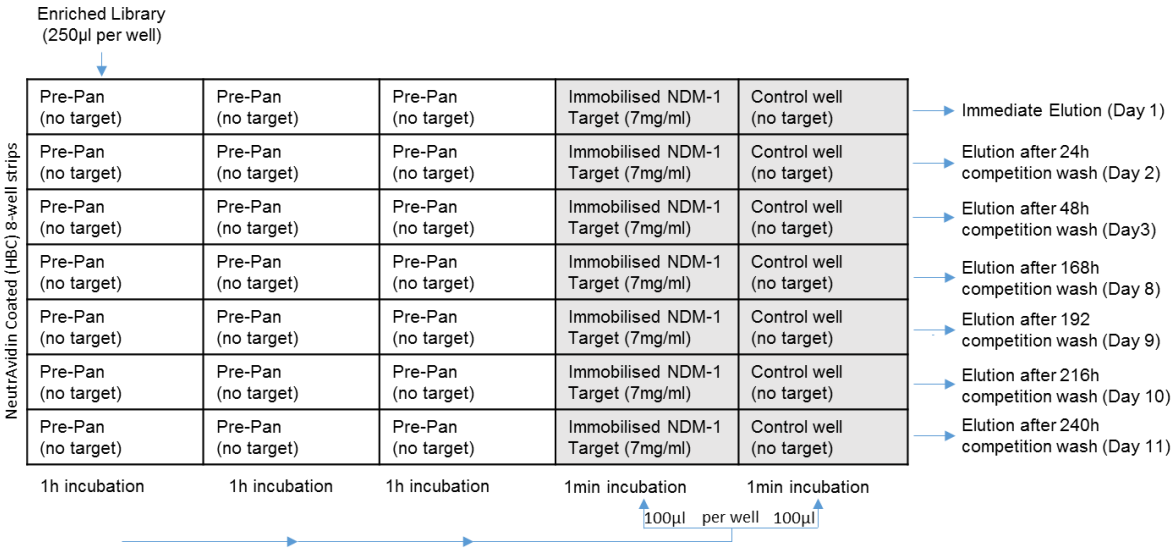

Figure 2.2.11.4.1 Phage display round two well plan.

2.3 Statistical Analysis

Statistical analysis was carried out using Prism 8 (Graphpad) and Excel (Microsoft) software. All data was tested for normality using Shapiro-Wilks test. Data presented in this report is mean with +/- standard deviation. The parametric one-way ANOVA test for significance was carried out followed by Dunnett's multiple comparison test where appropriate.

Chapter 3

Results

Results

3.1 NDM-1 production and purification

In order to identify Affimer constructs that are able to inhibit NDM-1 activity, truncated NDM-1 was initially produced. To produce NDM-1 protein, pD861-pelB-NDM-1 vector was transformed into BL21 Star™ (DE3) cells (methods2.2.1).

The pD861 vector contained a rhaBAD promoter sequence to allow Rhamnose-Inducible NDM-1 protein production. The vector contains a kanamycin resistance gene to allow for antibiotic (non β-lactam) mediated selection. A pelB leader sequence at the N-terminal of the NDM-1 gene directs the protein to the periplasm following protein production to ensure appropriate cellular localisation. The N-terminus of the NDM-1 sequence has been truncated to remove the lipobox motif (LSGC) to prevent lipid anchoring of the protein to the outer membrane as described in section 1.6.2. At the C-terminus of the NDM-1 gene there is an 8X His Tag to allow NiNTA purification. Preceding the His tag, a Human Rhinovirus (HRV) 3C protease site allows protease mediated removal of the His tag if required.

Samples were taken throughout the production and purification of NDM-1 protein (methods 2.2.4) and analysed by SDS-PAGE (methods 2.2.5) to confirm size (expected ~25kDa) and purity of produced protein.

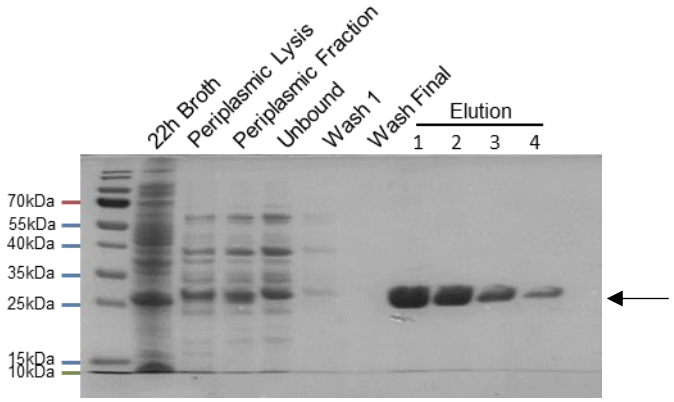

Figure 3.1.1 NDM-1 production and purification as analysed by SDS-PAGE. 1µl samples of NDM-1 protein production and purification were loaded onto 15%w/v SDS-polyacrylamide followed by electrophoresis and Coomassie staining. A two-step bacterial lysis method followed by Ni-NTA purification resulted in purified NDM-1 protein as shown in the elution fraction at ~25kDa as indicted by the arrow. The Ni-NTA resin was fully saturated at indicated by the NDM-1 band in the unbound fraction.

A two-step, periplasmic lysis protocol resulted in the extraction of NDM-1 that was then incubated and bound to nickel resin by use of 8x His tag. Several wash steps successfully reduced background proteins, and imidazole (300mM) mediated efficient elution of bound protein from the resin. The gel shows that NDM-1 (~25kDa) was produced in sufficient quantities and purity for further work as shown in figure 3.1.1 Following elution, NDM-1 protein was dialysed overnight in PBS + 10%v/v glycerol resulting in soluble NDM-1 at a concentration of 4.1mg/ml (146.7µM) as measured by nanodrop. This gave a total yield of 11.07mg of NDM-1 protein from a 400ml culture. To maintain enzyme integrity, soluble NDM-1 was snap-frozen and stored at -80^{o}C. Protein was thawed on ice before use. Previously, L De Faveri had demonstrated that freeze thawing of NDM-1 did not have a detrimental effect on NDM-1 activity.

3.2 Affimer Subcloning

Previously, NDM-1 Affimer binders were identified by Dr C. Tiede and L. De Faveri. This was accomplished by screening three separate phage libraries, as summarised in figure 4.2.1, against NDM-1. The LP1/2 library was generated by keeping variable region 2 (VR2) the same as Aff 21 and randomising the non-essential amino acids (as identified by alanine scanning). The CTL library was generated by maintaining variable region 1 (VR1) the same as Aff 21 and randomising VR2. The CTS library was generated by, first, generating two separate libraries were either VR1 or VR2 was maintained and the other VL was randomised. From each of the two libraries, NDM-1 binders were identified by phage display. From this, the randomised regions of the Affimers that bound to NDM-1 were shuffled and joined together to generate the CTL library.

From the screening of these three libraries, 24 Affimers were identified as NDM-1 binders and were subcloned (methods 3.3.5) from a phagemid into an expression vector (pET11a) to allow protein production. Gel electrophoresis (methods 2.2.6) was carried to confirm the PCR amplification of Affimer inserts and digestion of the pET11a recipient vector.

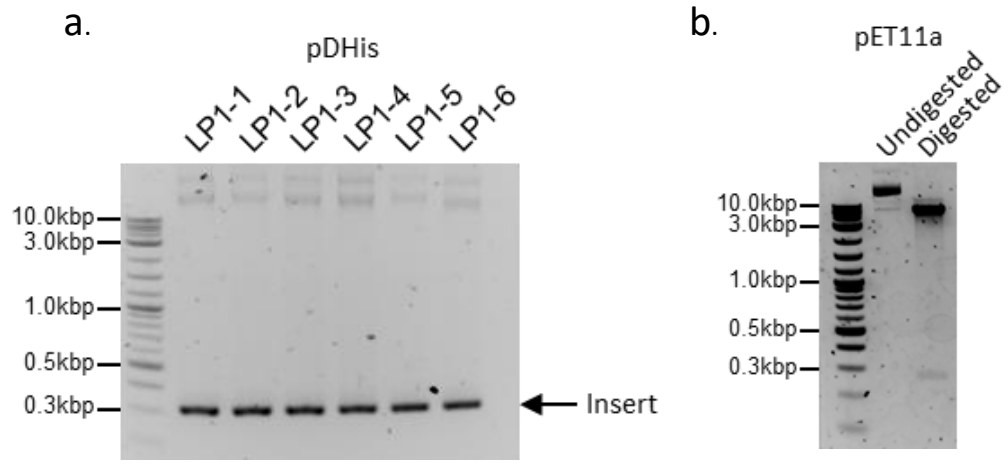

Figure 3.2.1 Agarose gel electrophoresis analysis of Affimer subcloning. a) PCR product following amplification of Affimer insert from pDHis phagmid vector. Inserts are identified at 0.3kbp for 6 Affimers previously identified as NDM-1 binders. b) pET11a vector pre and post double digestion with *NotI*-HF™ and *NheI*-HF™ restriction enzymes. The digested pET11a vector is shown in a band at around 7.0kbp and excised insert at 0.3kbp.

In figure 3.2.1a, the agarose gel electrophoresis of amplified Affimers inserts of LP1-1 to LP1-6 are shown at ~0.3kbp. Amplified Affimer inserts and were ligated into digested pET11a, figure 3.2.1b, vector in order to produce Affimer protein. The remaining 18 Affimer binders were subcloned by L. Adams.

3.3 Affimer Reagent Sequencing

To ensure successful cloning, ligated pET11a containing Affimer insert were sequenced (Genewiz, T7 forward primer) and translated to amino acid sequence. Additionally, a non-binding negative control Affimer (Aff-Bla) and a known NDM-1 activity inhibiting Affimer (Aff-21) was sequenced.

	Variable Region 1									Variable Region 2								
Aff - Bla	V	V	A	G	*	*	*	*	*	P	W	E	*	*	*	*	*	*
Aff- 21	**G**	**Y**	**K**	**V**	**W**	**T**	**P**	**Y**	**G**	**T**	**H**	**W**	**D**	**N**	**G**	**G**	**L**	**R**
LP1 - 1	P	Y	K	I	W	T	P	Y	F	T	H	W	D	N	G	G	L	R
LP1 - 2	N	Y	K	V	W	T	P	L	F	T	H	W	D	N	G	G	L	R
LP1 - 3	V	Y	K	V	W	T	P	H	F	T	H	W	D	N	G	G	L	R
LP1 - 4	T	Y	K	I	W	T	P	M	G	T	H	W	D	N	G	G	L	R
LP1 - 5	G	Y	K	H	W	T	P	Y	G	T	H	W	D	N	G	G	L	R
LP1 - 6	W	Y	K	I	W	T	P	D	F	T	H	W	D	N	G	G	L	R
LP2 - 7	G	Y	K	I	W	T	P	F	G	T	H	W	D	N	G	G	L	R
LP2 - 8	G	Y	K	V	W	T	P	M	G	T	H	W	D	N	G	G	L	R
LP2 - 9	G	Y	K	T	W	T	P	F	G	T	H	W	D	N	G	G	L	R
LP2 - 10	G	Y	K	V	W	T	P	F	Y	T	H	W	D	N	G	G	L	R
LP2 - 11	G	Y	K	T	W	T	P	M	G	T	H	W	D	N	G	G	L	R
LP2 - 12	G	Y	K	V	W	T	P	L	Y	T	H	W	D	N	G	G	L	R
LP2 - 13	G	Y	K	I	W	T	P	Y	G	T	H	W	D	N	G	G	L	R
LP2 - 14	G	Y	K	V	W	T	P	F	F	T	H	W	D	N	G	G	L	R
LP2 - 15	G	Y	K	V	W	T	P	E	F	T	H	W	D	N	G	G	L	R
CTL - 17	G	Y	K	V	W	T	P	Y	G	K	F	M	Q	D	M	T	I	Q
CTL - 18	G	Y	K	V	W	T	P	Y	G	K	F	F	Q	G	G	K	I	Q
CTL - 19	G	Y	K	V	W	T	P	Y	G	F	E	F	T	N	N	A	F	Y
CTL - 20	G	Y	K	V	W	T	P	Y	G	L	E	F	I	Q	N	A	F	W
CTS - 21	G	Y	K	V	W	T	P	Y	G	K	E	F	L	R	N	Q	I	Y
CTS - 22	G	Y	K	V	W	T	P	Y	G	L	T	F	E	Y	N	K	F	Q
CTS - 23	Q	H	V	E	G	W	S	Q	V	A	H	V	F	K	K	S	P	K
CTS - 24	G	Y	K	V	W	T	P	Y	G	V	E	F	H	N	Q	M	F	H
CTS - 25	G	Y	K	V	W	T	P	Y	G	K	E	F	V	A	N	H	Y	V

Basic	K H R
Acidic	D E
Polar	S T C Y N Q
Non - Polar	G A V L I M F W P

Figure 3.3.1 Amino acid sequence showing variable loop regions (VL1/VL2) of NDM-1 binding Affimers. The variable loop regions of NDM-1 binding Affimers as sequenced from pET11a vectors. The loop sequences of non-binding Affimer (Aff-Bla) and NDM-1 inhibiting Affimer (Aff-21) are shown. Amino acid characteristics are colour-coded as indicated.

The sequence data, as indicated in table 3.3.1, confirms subcloning of Affimer inserts into pET11a vectors.

3.4 Affimer Reagent production and purification

Following sequence confirmation of pET11a vectors containing Affimer inserts, DNA was transformed into BL21 star^{TM} (DE3) cells (methods 2.2.1). Affimers were produced, purified and dialysed (method2.2.7) with samples collected for analysis by SDS-PAGE (methods3.3.8) for confirmation of size and purity as shown in figure 3.4.1.

Aff 21

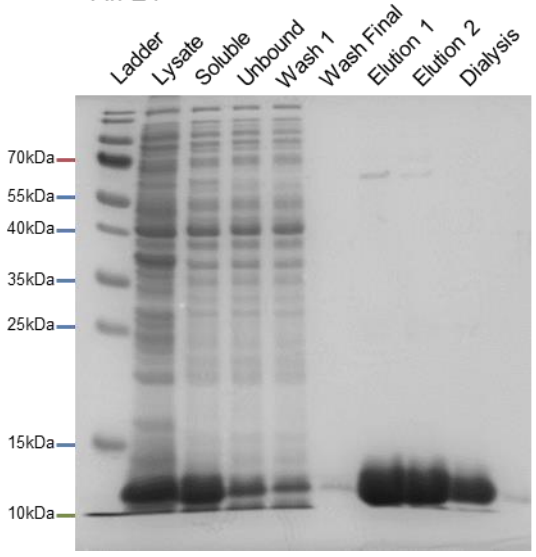

Aff Bla

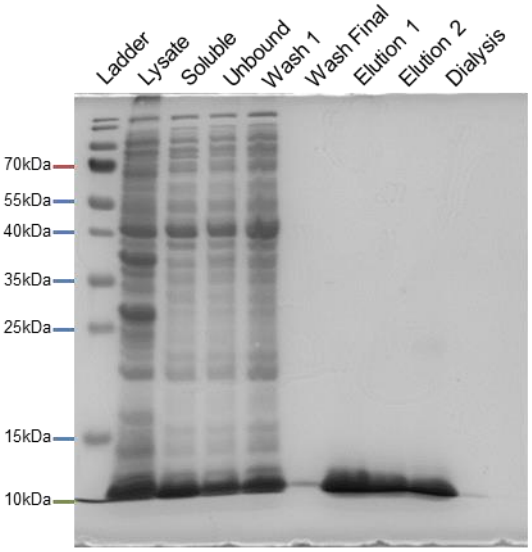

LP1-1

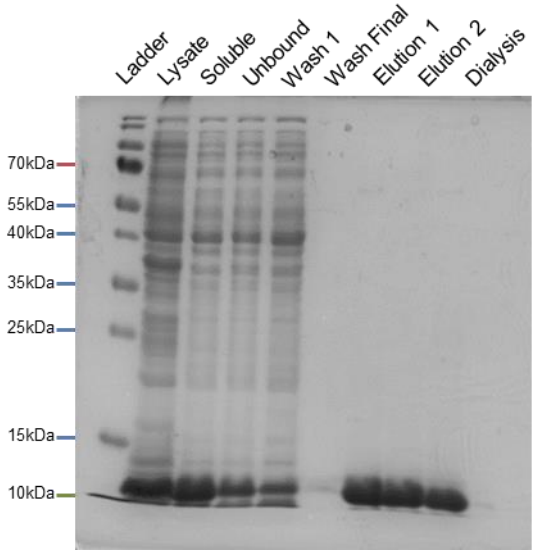

LP1-2

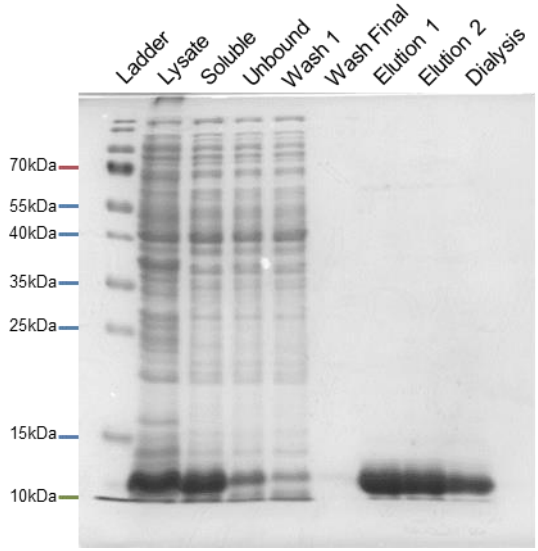

LP1-3

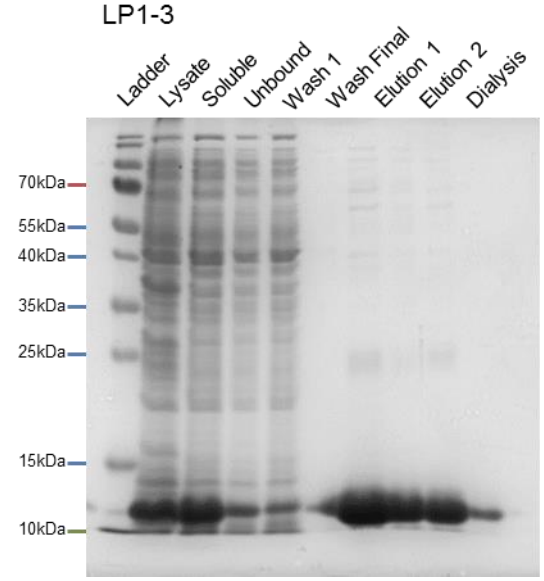

LP1-4

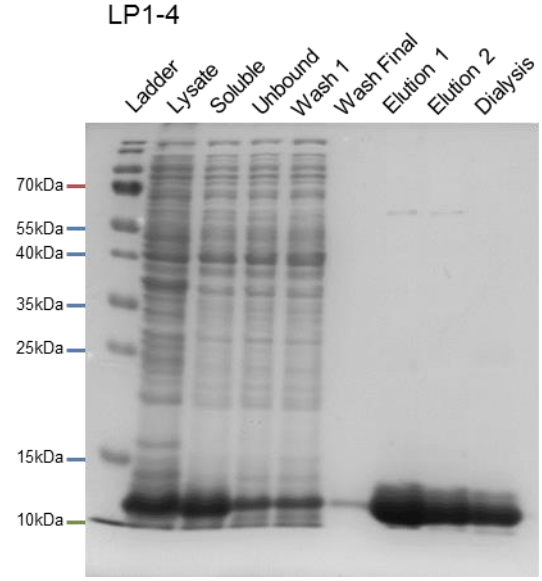

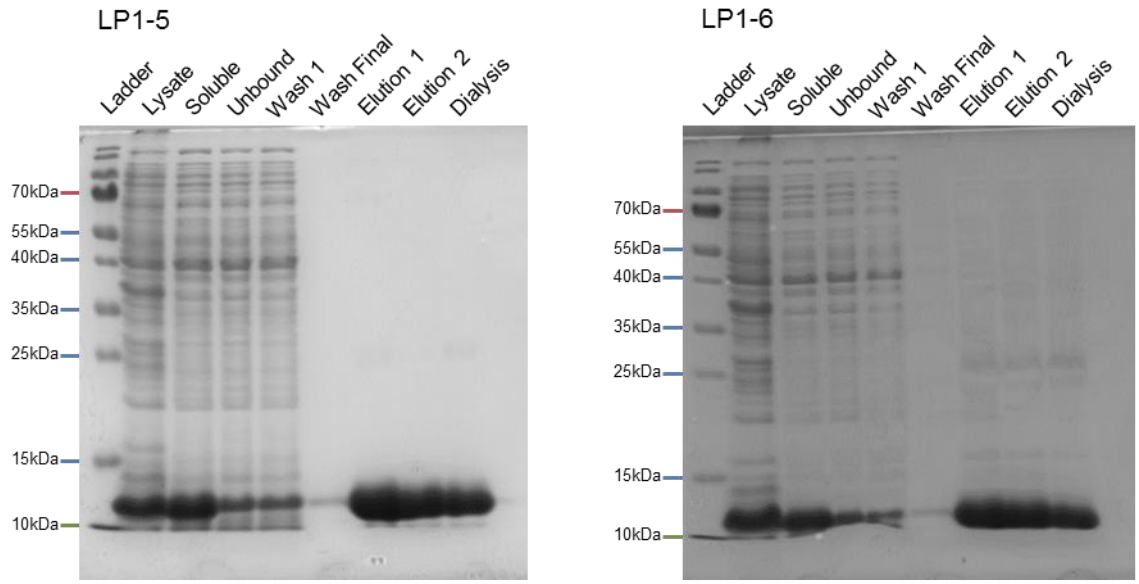

Figure 3.4.1 SDS-PAGE analysis of Affimer production and purification. Samples (1µl) were taken throughout the production and purification of Affimers and analysed by SDS-PAGE followed by coomassie staining. SDS-PAGE gels for a batch of 6 NDM-1 binding Affimers (LP1-1 to LP1-6) are shown with the non-binding Affimer (Aff-Bla) and known NDM-1 inhibitor Affimer (Aff-21). Affimers were purified from the lysate of transformed BL21 star™ (DE3) cells using nickel ion affinity. Affimers are shown by the band at ~12kDa

Figure 3.4.1 shows SDS-PAGE analysis indicated that purified Affimer protein (~12kDa) was present in the elution and dialysed fractions. Soluble Affimer protein was stored at -20°C until required.

3.5 Confirmation of Affimer concentration

The concentration of soluble Affimer protein was determined as described in method 2.2.3. Affimer physical and chemical parameters, including extinction coefficients, were determined by sequence analysis using ExPASy ProtParam online software as shown in table 3.5.1.

Affimer	Molecular Weight	Extinction Coefficient	Absorbance 0.1%	Theoretical pI	Dialysed Sample Concentration (mg/ml)
Aff - Bla	10985.5	15470	1.408	6.75	2.075
Aff - 21	**12335.96**	**23950**	**1.941**	**8.01**	**1.601**
LP1 - 1	12480.18	23950	1.919	8.01	0.707
LP1 - 2	12433.12	22460	1.806	8.03	0.737
LP1 - 3	12442.13	22460	1.805	8.04	1.460
LP1 - 4	12362.06	22460	1.817	8.03	1.951
LP1 - 5	12373.97	23950	1.936	8.02	1.379
LP1 - 6	12521.19	27960	2.233	7.17	1.280
LP2 - 7	12426.09	23950	1.927	8.01	1.332
LP2 - 8	12303.98	22460	1.825	8.03	1.738
LP2 - 9	12321.94	22460	1.823	8.03	1.697
LP2 - 10	12426.09	23950	1.927	8.01	1.057
LP2 - 11	12305.95	22460	1.825	8.03	2.130
LP2 - 12	12392.07	23950	1.933	8.01	0.946
LP2 - 13	12349.99	23950	1.939	8.01	1.717
LP2 - 14	12410.09	22460	1.81	8.03	1.560
LP2 - 15	12392.03	22460	1.812	7.18	1.966
CTL - 17	12422.21	18450	1.485	7.99	2.226
CTL - 18	12333.09	18450	1.496	9.05	2.211
CTL - 19	12433.07	19940	1.604	7.14	1.590
CTL - 20	12448.18	23950	1.924	7.14	0.852
CTS - 21	12491.24	19940	1.596	8.74	1.890
CTS - 22	12470.18	19940	1.599	7.98	1.042
CTS - 23	12321.04	15470	1.256	8.78	1.995
CTS - 24	12469.17	18450	1.48	7.2	1.822
CTS - 25	12387.09	19940	1.61	7.99	2.327

Table 3.5.1 Physical and chemical properties of purified Affimer Reagents. Amino acid Sequence analysis was performed by ExPASy ProtParam software to determine chemical and physical properties of Affimers. 24 NDM-1 binding Affimers were analysed along with the non-binding Aff-Bla control and known NDM-1 inhibitor, Aff-21.

To confirm nanodrop readings, SDS-PAGE analysis was performed by loading 1ug of each Affimer and comparing intensity of resulting 12kDa band as shown in figure 3.5.1

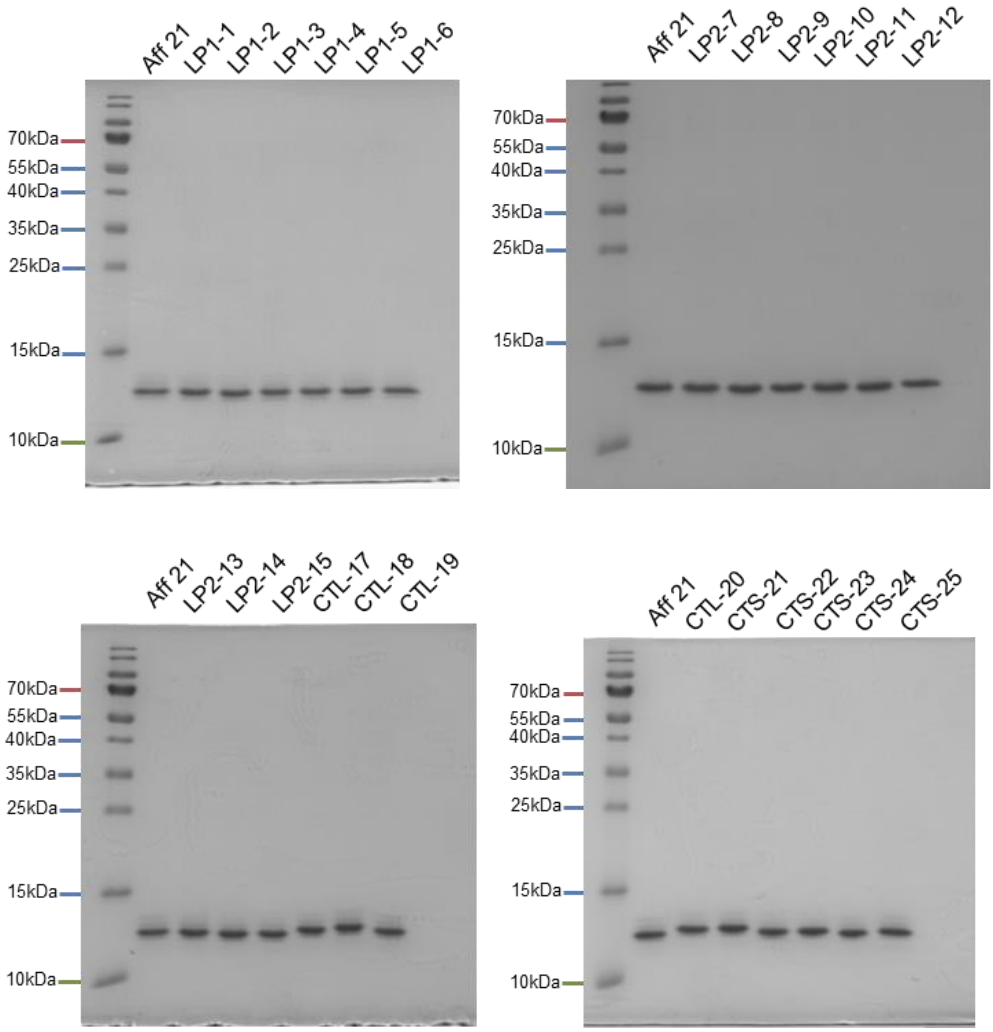

Figure 3.5.1 SDS-PAGE analysis of 1µg of Affimer sample. Nanodrop reading were used to determine the concentration of Affimer samples (LP1-1 to CTS-25). To confirm accurate nanodrop readings, 1µg of each Affimer was analysed by SDS-PAGE gel. The intensities of the ~12kDa Affimer binds are comparable in each batch.

Comparable intensities of Affimer bands (~12kDa) on SDS-PAGE gels, as shown in figure 3.5.1, confirms the amount of Affimer loaded on to the gel to be approximately the same. This, therefore, confirms the concentrations as measured by nanodrop. Once accurate concentrations of Affimer was determined, the potential inhibitory effect of Affimers that bind to NDM-1 could be assessed.

3.6 β-lactamase activity assay

To determine the effectiveness NDM-1 activity inhibition by the Affimers, β-lactamese activity assays were carried out (method 2.2.9). Nitrocefin contains a β-lactam ring and undergoes a colour change on hydrolysis and can therefore by used to analyse NDM-1 activity and any Affimer-mediated inhibition. Aff-21 is a known inhibitor of NDM-1 and, therefore, all NDM-1 binding Affimers were compared to Aff-21 in each batch. Controls included an EDTA negative control (chelating Zn^{2+} from NDM-1 active site resulting in enzyme inactivity). An NDM-1 only positive control demonstrated maximal NDM-1 activity. Additionally, control conditions containing a non-binding Affimer (Aff-Bla) was used. Each condition was performed in triplicate per run and three technical repeats were performed.

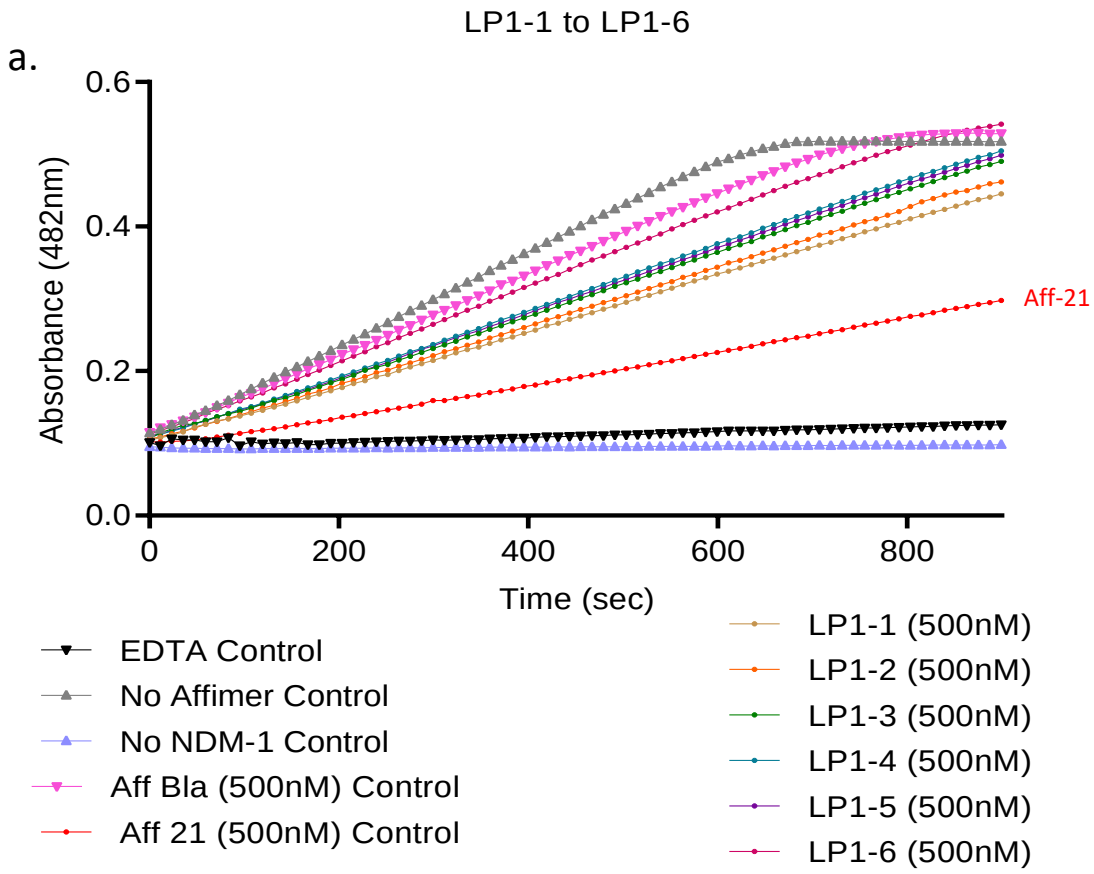

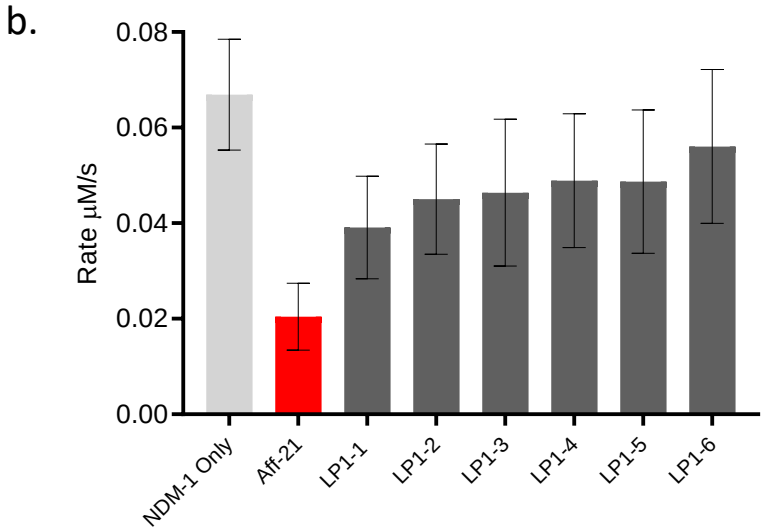

Figure 3.6.1 Quantification of the Affimer mediated inhibition of NDM-1 hydrolysis activity (LP1-1 to LP1-6). Quantification of NDM-1 (100nM) activity was measured by incubating NDM-1 with nitrocefin (65mM) at 25^{o}C and measuring absorbance 482 nm every 12sec for 15mins.a) 6 Affimers (LP1-1 to LP1-6) were incubated with NDM-1 in triplicate to analyse inhibitory effect and absorbance measurements are taken. Control conditions are indicated. b) Absorbance values were normalised to EDTA control and Initial rate of nitrocefin hydrolysis activity recorded as mean µM/s (n=3 technical repeats). Aff 21 significantly (p=0.0027) inhibits the rate of NDM-1 activity to a mean of 0.020µM/s (SD± 0.007) when compared to NDM-1 only mean rate of 0.067 µM/s (SD± 0.011).

The β-lactamase activity assay sown in figure 3.6.1, confirmed that Aff-21 inhibited β-lactam hydrolysis by NDM-1 to a mean rate of 0.020µM/s (SD± 0.007) when compared to a mean rate of 0.067 µM/s (SD± 0.011) for NDM-1 only. The Affimers LP1-1 to LP1-6 showed no improvement on the inhibitory effects of Aff-21. Each condition was performed in triplicate per run and three technical repeats were performed.

a.

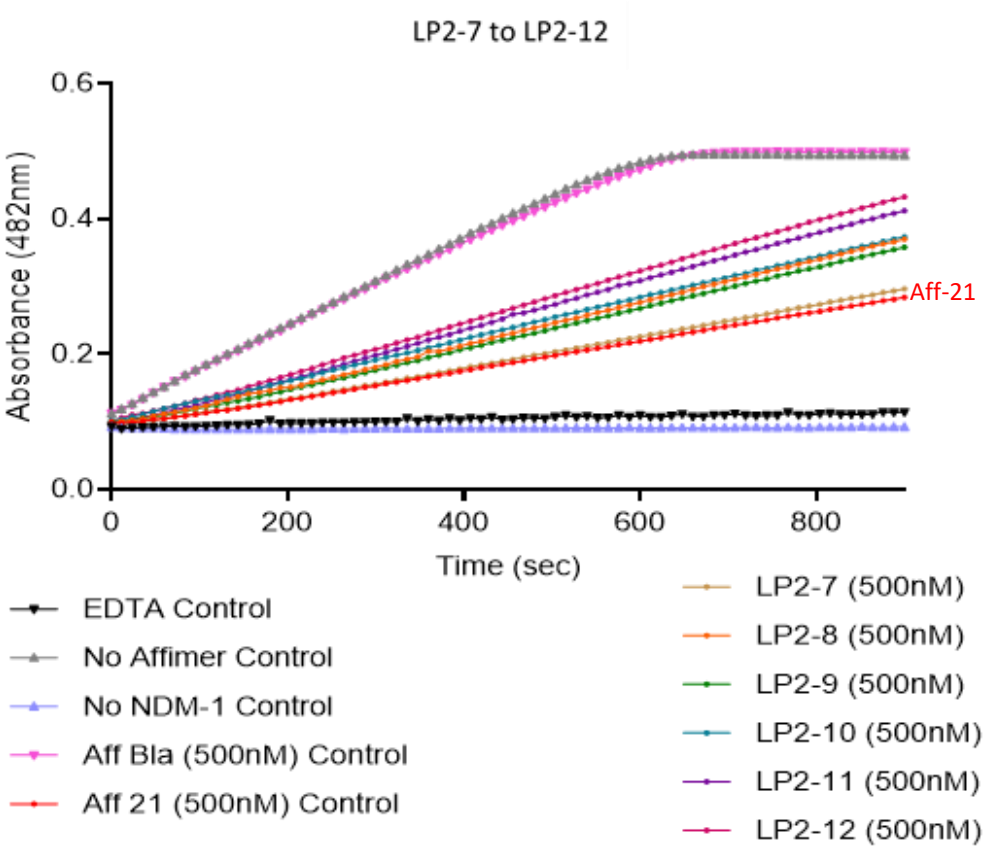

b.

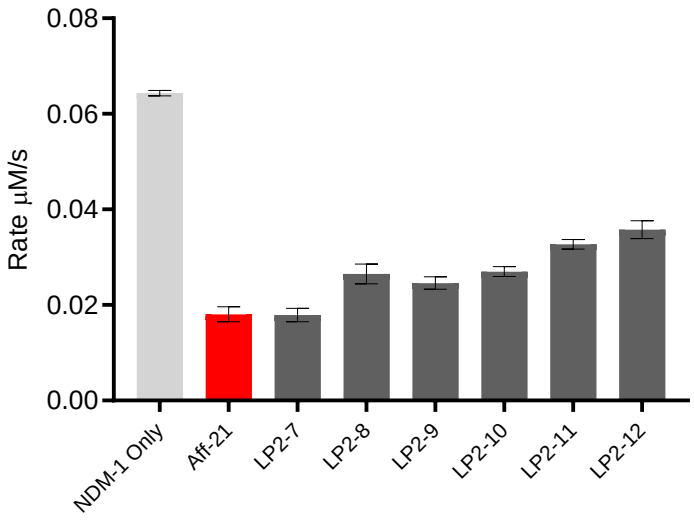

Figure 3.6.2 Quantification of the Affimer mediated inhibition of NDM-1 hydrolysis activity (LP2-7 to LP2-8). The activity of NDM-1 (100nM) was quantified by the hydrolysis of nitrocefin (65mM) at 25°C and measuring absorbance 482 nm every 12sec for 15mins.a) Absorbance values measured when 6 Affimers (LP2-7 to LP2-8; 500nM) were incubated with NDM-1 in triplicate to analyse inhibitory effect. Positive and negative controls were included as indicated. b) Each condition was normalised to the EDTA control and initial rates (µM/s) were determined by linear regression for the first 250sec. (n=3 technical repeats).

The β-lactamase activity assay, as shown in figure 3.6.2a, suggested that Affimers LP2-7 to LP2-12 inhibited NDM-1 mediated hydrolysis of the β-lactam ring in nitrocefin as measured by absorbance change at 482nm. The initial rate of hydrolysis, as shown in figure 3.6.2b, indicated that Aff 21 inhibited NDM-1 activity to a mean rate of 0.01805µM/s (SD±0.002704) compared to a mean rate of 0.06435µM/s (SD± 0.0009762) for NDM-1 only. The Affimer LP2-7 inhibited NDM-1 activity to a slightly greater extent than Aff 21 to a mean initial rate of 0.01790µM/s (SD±0.002477). Each condition was performed in triplicate per run and three technical repeats were performed.

a.

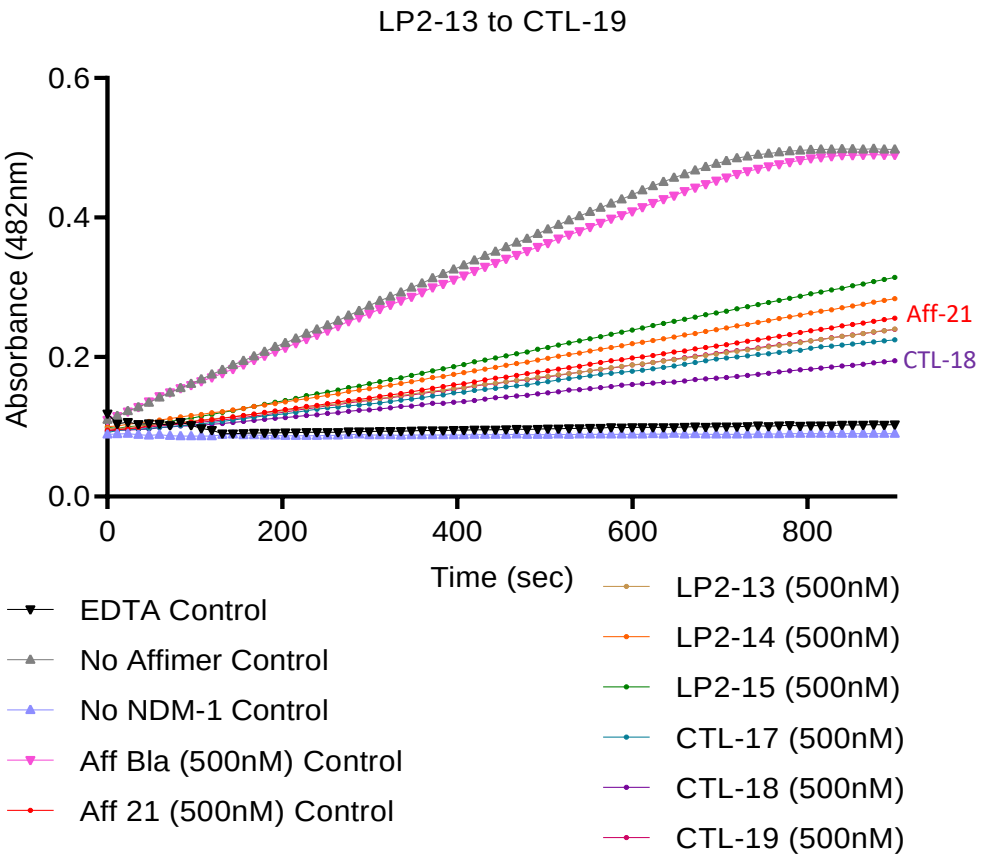

b.

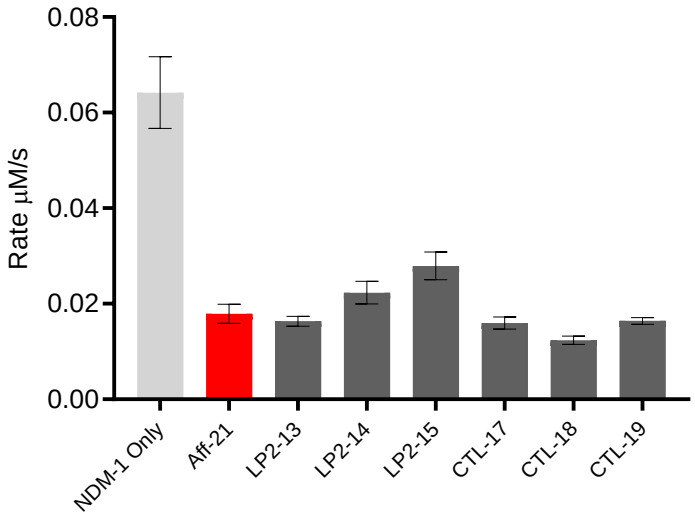

Figure 3.6.3 Quantification of the Affimer mediated inhibition of NDM-1 hydrolysis activity (LP2-13 to CTL-19). NDM-1 (100nM) was incubated with nitrocefin (65mM) to quantify β-lactam hydrolysis by measuring absorbance at 482nM every 12sec for 15mins. a) The Affimers LP2-13 to CTL-19 (500nM) were incubated in triplicate with NDM-1 to determine inhibitory effect as measured by absorbance. b) Initial rate was determined for each condition by normalising absorbance to the EDTA control and converting absorbance to concentration. Rate was determined by liner recreation for the initial 250sec. (n=3 technical repeats)

The β-lactamase activity assay, as shown in figure 3.6.3, suggested that Affimers LP2-13 to LP2-19 inhibited NDM-1 mediated hydrolysis of the β-lactam ring in nitrocefin as measured by absorbance change at 482nm. The mean initial rate of hydrolysis of NDM-1 only is 0.064µM/s (SD±0.0074) is inhibited by Aff 21 to 0.018 µM/s (SD±0.0020). Affimers that showed improved inhibition than Aff21 are LP2-13 (0.016µM/s SD±0.0010), CTL-17 (0.016µM/s SD±0.0013), CTL-19 (0.016µM/s SD±). The Affimer CTL-18 inhibited NDM-1 hydrolysis to the greatest extent to a mean rate of 0.012µM/s (SD±0.0009). Each condition was performed in triplicate per run and three technical repeats were performed.

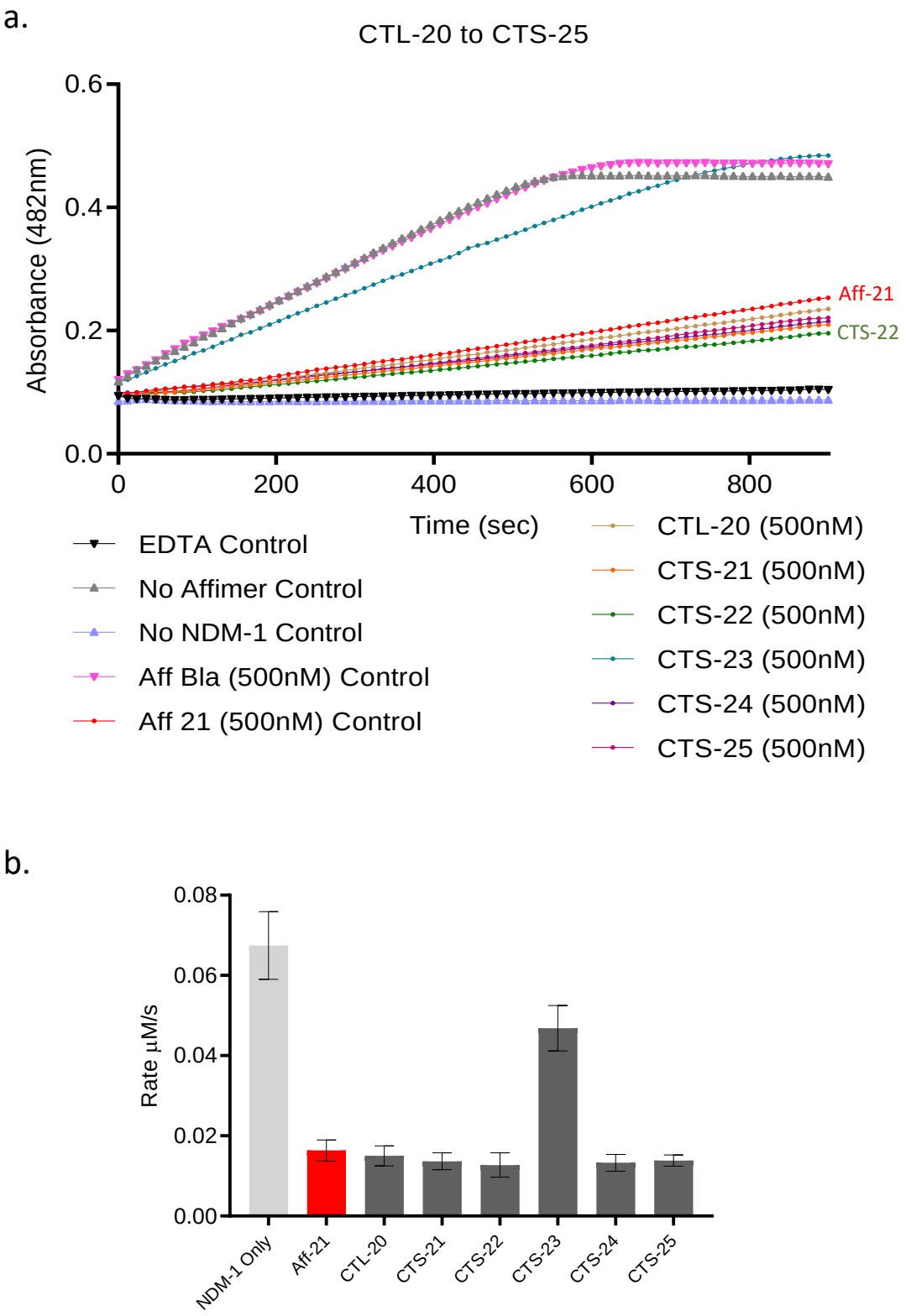

Figure 3.6.4 Quantification of the Affimer mediated inhibition of NDM-1 hydrolysis activity (CTL-20 to CTS-25). To quantify the hydrolysis of β-lactam ring, NDM-1 (100nM) was incubated with nitrocefin (65mM) and absorbance was measured at 482nm every 12sec for 15mins. a) Affimers CTL-20 to CTS-25 (500nM) were incubated with NDM-1 to determine inhibitory effect as measured by nitrocefin absorbance change. b) Rate of NDM-1 activity was determined by normalising absorbance values to EDTA control before converting to concentration (n=3 technical repeats). The initial rate was determined by linear regression for the first 250sec.

The β-lactamase activity assay, as shown in figure 3.6.4, suggested that Affimers CTL-20 to CTS-25 inhibit NDM-1 hydrolysis activity. hydrolysis of the β-lactam ring in nitrocefin as measured by absorbance change at 482nm. The mean initial rate of hydrolysis of NDM-1 only is 0.067 µM/s (SD±0.0084) is inhibited to 0.016µM/s (SD± 0.0026) by Aff 21. Affimers that showed improved inhibition than Aff 21 are CTL-20 (0.015 µM/s SD±0.0025), CTS-21 (0.014 µM/s SD±0.0021), CTS-24 (0,013 µM/s SD±0.0021), CTS 25 (0.014 µM/s SD±0.0014). The Affimer CTS-22 showed the greatest inhibition of NDM-1 to a mean rate of 0.0127µM/s (SD±0.0031).

3.7 CTL-18, CTS-22 and Aff-21 Comparison β-lactamase activity assay

CTL-18 and CTS-22 were identified as Affimers that inhibit NDM-1 activity to a greater extent than Aff 21. To confirm previous results, CTL-18 and CTS-22 were produced and purified alongside Aff Bla non-binding control and Aff 21 known inhibitor. β-lactamase activity assays were performed (figure 3.9) to directly analyse inhibition of NDM-1 activity by Aff-21, CTL-18 and CTS-22. The initial rate was determined using the beer-lambert law and liner regression analysis for the first 250sec. Each condition was performed in triplicate per run and three biological repeats were performed.

a.

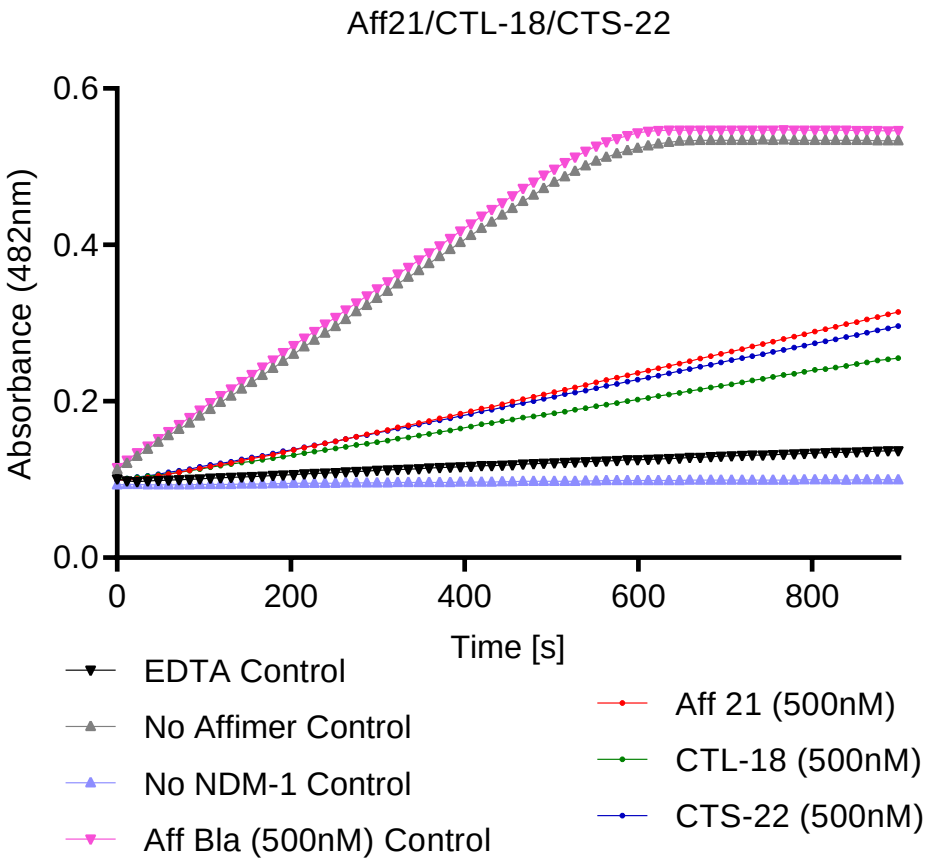

b.

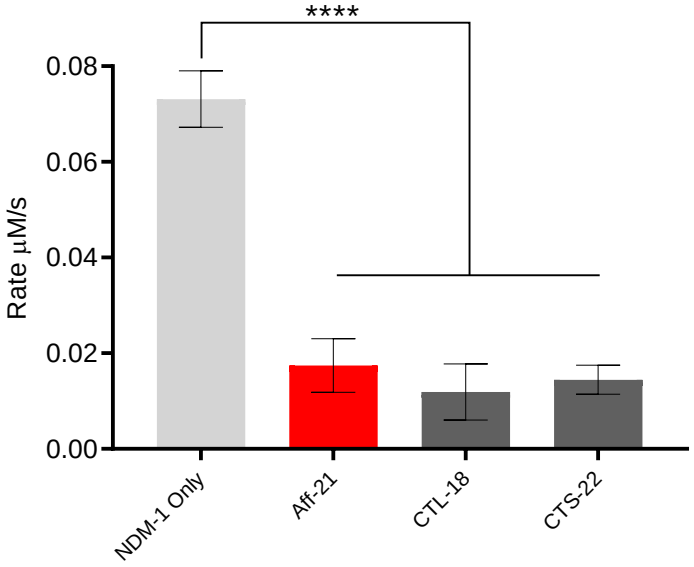

Figure 3.7.1 Direct comparison of β-lactam (nitrocefin) hydrolysis by NDM-1 when inhibited by Aff-21, CTL-18 and CTS-22. Quantification of NDM-1mediated hydrolysis of β-lactam was measured by incubating 100nM of NDM-1 with nitrocefin (65mM) and measuring absorbance at 482nm every 12sec for 15mins.a) The Affimers Aff21, CTL-18 and CTS-22 25 (500nM) were incubated with NDM-1 to determine inhibitory effect (n=3)**.** . b) Rate of NDM-1 activity was determined by normalising absorbance values to EDTA control before converting to concentration (n=3 biological repeats). The initial rate was determined by linear regression for the first 250sec. p<0.0001

The β-lactamase activity assay, as shown in figure 3.7.1, confirmed that Aff 21, CTL-18 and CTS-22 significantly (p<0.0001) inhibit NDM-1 hydrolysis activity. The mean initial rate of hydrolysis of NDM-1 only is 0.073µM/s (SD±0.0059) and is inhibited to 0.017 µM/s (SD±0.0056) by Aff 21. The Affimer CTS-22 inhibits NDM-1 activity to a greater extent to 0.014µM/s (SD±0.0030). CTL-18 inhibits NDM-1 activity further to 0.012µM/s (SD±0.0059).

3.8 NDM-1 phage ELISA optimisation

Following the identification of CTL-18 as the candidate Affimer, phage display (methods 2.2.11) was carried out using the enriched CTL library (Figure 4.2.1) to identify binders with a higher affinity. Three modifications were made to the standard phage display to increase stringency (figure 2.2.2.11.1). 1) Incubate enriched phage library with the target for a reduced period of 1 minute. 2) Bound phage was washed with solution containing non-biotinylated NDM-1 and eluted over several days. 3) The concentration of immobilised target NDM-1 used in the phage ELISA step was reduced. To optimise the concentration of NDM-1 used in phage ELISA, a pre-trial was carried out. The pre-trail involved immobilising increasing concentrations of biotinylated-NDM-1 in a Maxisorp 96-Well Microplates then incubating with CTL-18 displaying M13 phage. The ELISA signal generated were analysed to determine the optimised concentration to use in future phage ELISA assays. Stop solution (sulphuric acid) was used to stop the TMB reaction after 2 mins and absorbance was measured at 450nm using Multiskan Ascent Plate Reader

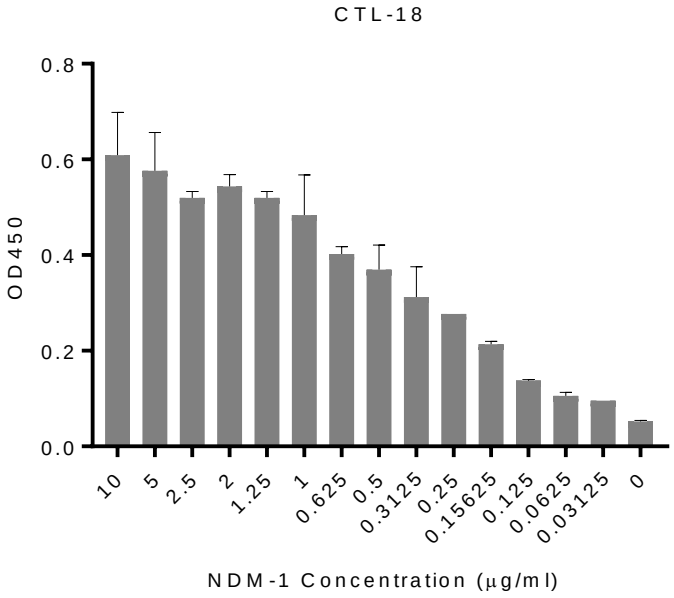

OD_{Max}	0.6284 Au
OD_{50}	0.325 µg/ml

Figure 3.8.1 Phage ELISA absorbance values of CTL-18 phage against increasing concentrations of immobilised NDM-1. Phage ELISAs (n=3) were performed using increasing concentrations of immobilised NDM-1 (0.0mg/ml to 0.325mg/ml)

The ELISA results from the pre-trial, as shown in figure 3.8.1, indicate that from a maximum absorbance reading of OD_{450} 0.6384, the ELISA signal decreases as the concentration of immobilised NDM-1 target decreases. At a concentration of 0.325mg/ml of immobilised target, half of the maximal signal is achieved (OD_{50}). Therefore, a concentration of 0.325mg/ml was used as the optimised concentration for phage ELISA analysis of binders identified by phage display.

3.9 Phage Display Round 1

Phage display was used to identify Affimers that bound with high affinity to NDM-1 (method 2.2.11.1) using the CTL library (figure4.2.1). To increase stringency, a reduced incubation time was used and, additionally, bound phage were eluted after rt (Day 1) and following a competition wash for 24h (Day 2) and 48h (Day3) (figure 2.2.11.2.1). The library was panned against a saturated NDM-1 (7mg/ml) target well and a negative control well (with no immobilised target to monitor for non-specific binding Affimers).

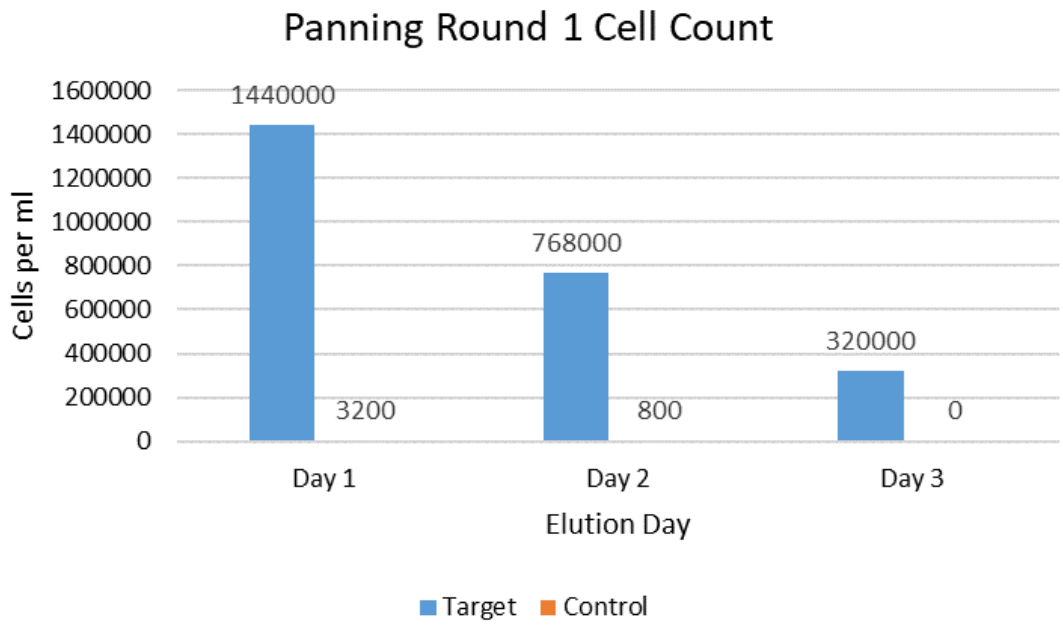

Figure 3.9.1 Number of phage infected cells per ml after panning enriched CTL phage library against immobilised NDM-1 target. Following the first panning round, eluted phage from the target and control wells were incubated with ER2738 cells and plated onto LB agar plates. Colonies were counted the following day to determine the number of phage infected cells. Elutions were taken immediately after incubation (Day 1) and after competition wash for 24h (Day 2) and 48h (Day 3).

On Day 1, as shown in figure 3.9.1, the colony count indicated that 1440000 ER2738 cells per ml were infected with phage compared to control cultures, which were only 3200 cells per ml on Day 1. Following 24 hours of competition wash (wash solution containing free NDM-1 protein) a reduction in NDM-1 bound phage was observed to 768000 infected ER2738 cells per ml compared to Day 1. A further reduction in Day 3 was observed. Following on, 32 colonies from each elution were picked at random to be used in phage ELISA (methods 2.2.10) using the optimised concentration of target. CTL-18 was included to identify Affimer reagents with increased ELISA signal. All Affimers were screened against an empty ELISA plate well as a control to identify non-specific binders.

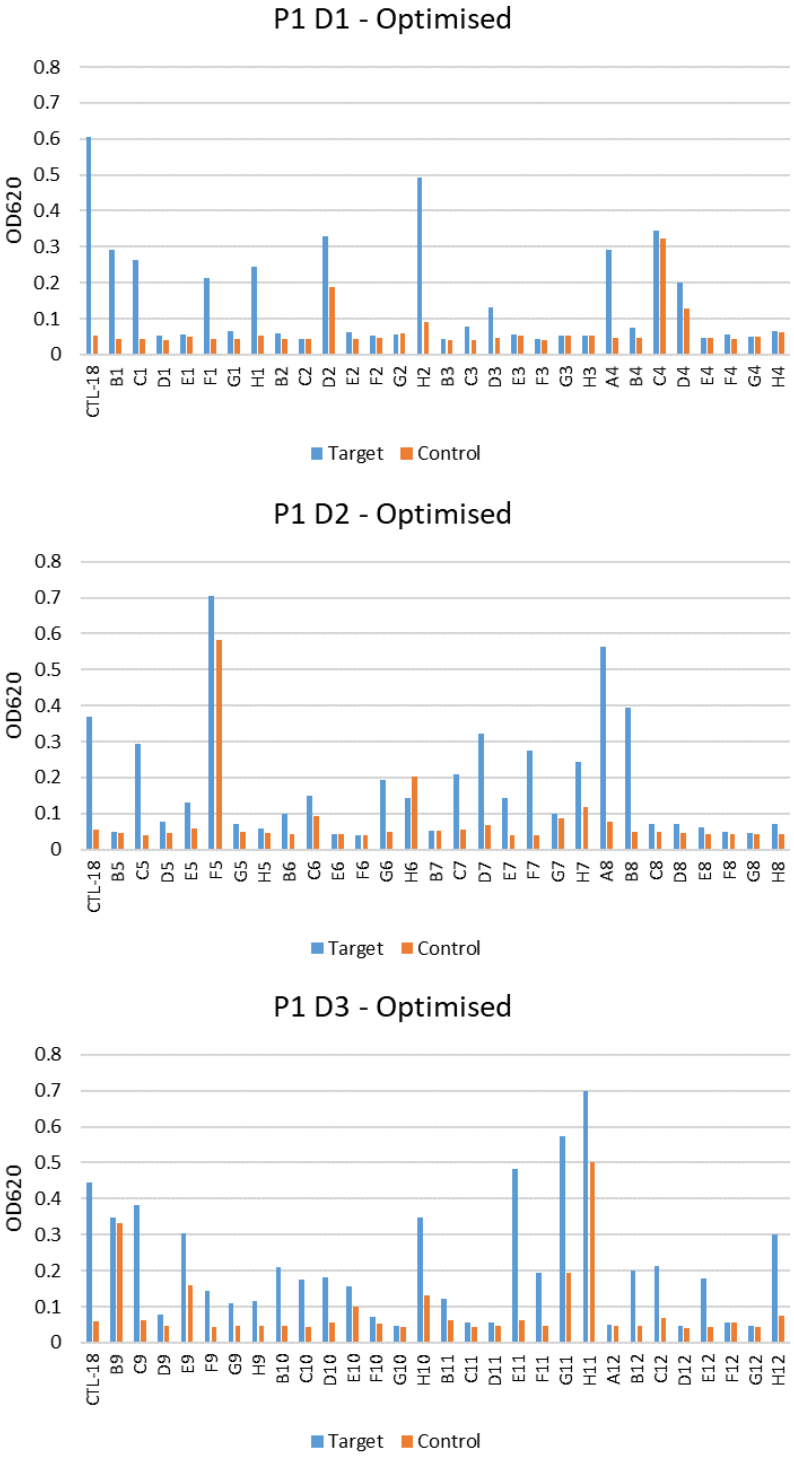

Figure 3.9.2 Phage ELISA results for Affimer reagents selected during panning round 1 from the CTL library against NDM-1 target. Following the first panning round, single colonies (containing one Affimer reagent) were selected at random and tested in an optimised (0.325mg/ml immobilised NDM-1 target) phage ELISA. Empty control wells were included to identify non-specific binders. Bound phage was identified with anti-Fd bacteriophage-HRP antibody followed by the addition of TMB which was allowed to develop for 10 -13mins. Absorbance was measured at 620nm.

After pan 1, several Affimer hits were identified in the optimised phage ELISA to have a higher signal than CTL-18 as shown in figure 3.9.2. Any Affimer that showed a high signal in the control well (such as P1D2 F5, P1D3 H11 and P1D3 G11) was screened out as this would suggest non-specific binding. From this round, Affimers CTL-B8, CTL-A8 and CTL-E11 were selected, and sequenced.

	Variable Region 1									Variable Region 2									
Aff 21	G	Y	K	V	W	T	P	Y	G	T	H	W	D	N	G	G	L	R	
CTL-18	**G**	**Y**	**K**	**V**	**W**	**T**	**P**	**Y**	**G**	**K**	**F**	**F**	**Q**	**G**	**G**	**K**	**I**	**Q**	
CTL-B8	G	Y	K	V	W	T	P	Y	G	I	W	Q	H	T	H	N	I	M	P1D2
CTL-A8	G	Y	K	V	W	T	P	Y	G	R	L	G	N	Y	G	N	F	M	P1D2
CTL-E11	G	Y	K	V	W	T	P	Y	G	K	L	L	T	G	P	H	I	K	P1D3

Basic	K H R
Acidic	D E
Polar	S T C Y N Q
Non - Polar	G A V L I M F W P

Figure 3.9.3 Amino acid sequence showing the variable regions of ELISA hits from round 1 of phage display. The variable loop regions of NDM-1 binding Affimers as sequenced from pDHis vectors. Amino acid characteristics are colour-coded as indicated.

The sequences in figure 3.9.3 show, as expected variable region 1 of the Affimer hits are the same as the templates, Aff21 and CTL-18. Since only three Affimer hits were identified further panning rounds were carried out to identify more Affimer binders. New amplified and enriched phage libraries were generated from each elution day following (methods2.2.11.2). The library generated from Pan 1 Day 3 will have low numbers of non-specific binders (as shown by the lack of colonies on the colonies on the control plate in figure 3.9.1) additionally, this library is expected to be enriched with binders of high affinity due to the stringent phage display strategy and reduced number of cell counts observed from the target wells at Day 3.

3.10 Phage Display Round 2

For pan 2 (methods2.2.11.3), the enriched library form Pan 1 Day 3 was used. Again, a stringent phage display strategy was used to select for NDM-1 binding Affimers with a high affinity. The Library was incubated with immobilised NDM-1 (7mg/ml) for one minute followed by immediate elution and elutions on several days following competition washes as sown in figure 2.2.11.3.1.

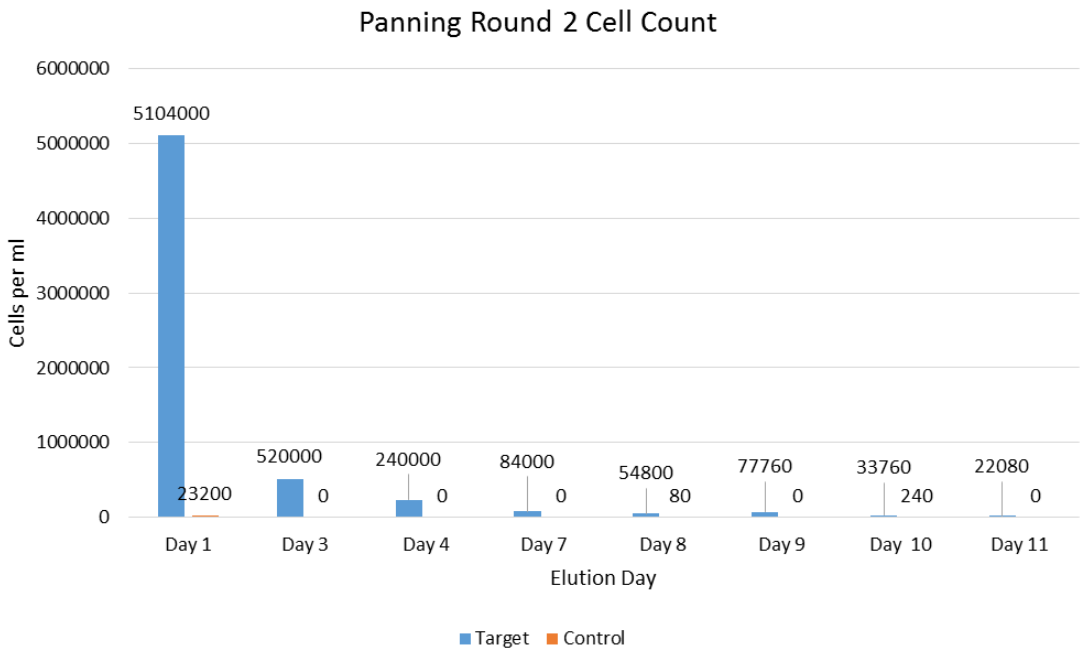

Figure 3.10.1 Number of phage infected ER2738 cells per ml following panning round 2. The enriched P1D3 phage library was panned against biotinylated NDM-1 target and empty control well. From separate wells, several elutions were made. First, immediately after the incubation of the library with the target (Day 1) then on several day after competition washes. Eluted phage was allowed to infect an 8ml culture of ER2738 cells and then grown overnight on agar plates. The number of infected cells on each elution day are an indication of the number of bound phage eluted from the target and control wells.

In panning round 2, the number of ER2738 cells infected by eluted phage decreases following competition wash as shown in figure 3.10.1. On the first elution, Day 1 immediately following phage library and target panning, 5 104 000 ER2783 cells per ml of culture were infected. After 24h of competition washing (Day 2) this had decreased to 520 000 cells per ml. Further days of competition washing saw a further decrease in infected ER2738 cells to 22 080 per ml following 24h of competition washing on Day 11. Throughout the second panning round, the number of non-specific binders remain low with the smallest difference being on Day 10 when 240 cells per ml of non-specific binders were observed compared to 33 760 (a factor of 140.6 greater).Individual colonies were selected from each elution day to be tested in an optimised phage ELISA (methods 2.2.10) to identify Affimer hits with a higher ELISA signal that CTL-18 (figure 3.10.2)

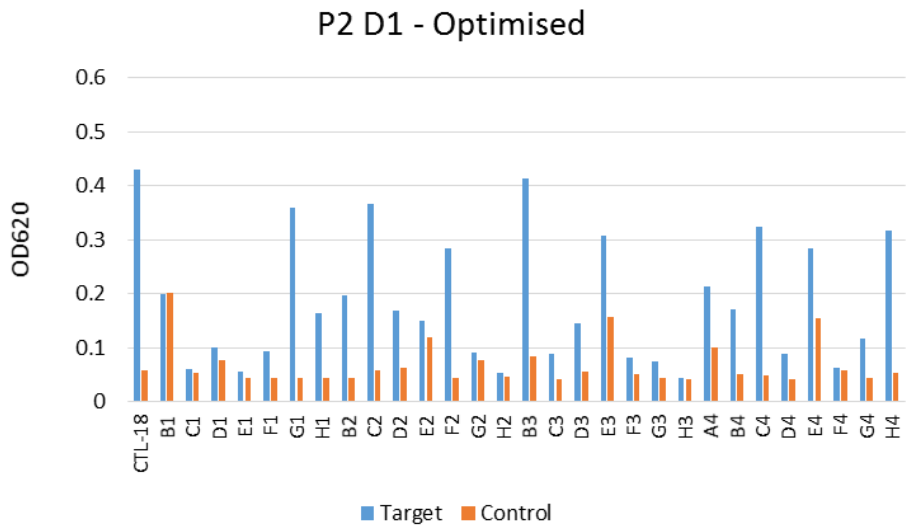
P2 D1 - Optimised
OD620
0.6
0.5
0.4
0.3
0.2
0.1
0
CTL-18 B1 C1 D1 E1 F1 G1 H1 B2 C2 D2 E2 F2 G2 H2 B3 C3 D3 E3 F3 G3 H3 A4 B4 C4 D4 E4 F4 G4 H4
Target
Control

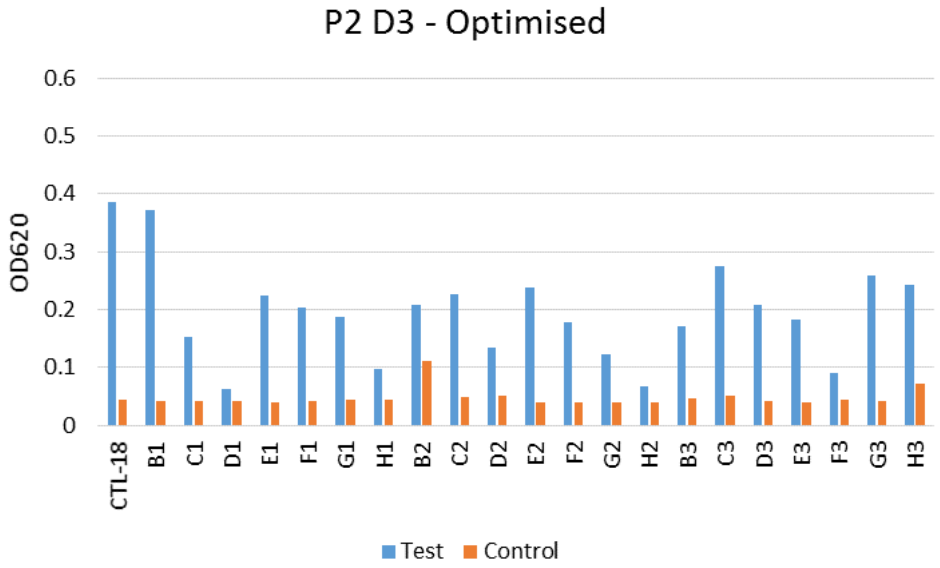
P2 D3 - Optimised
OD620
0.6
0.5
0.4
0.3
0.2
0.1
0
CTL-18 B1 C1 D1 E1 F1 G1 H1 B2 C2 D2 E2 F2 G2 H2 B3 C3 D3 E3 F3 G3 H3
Test
Control

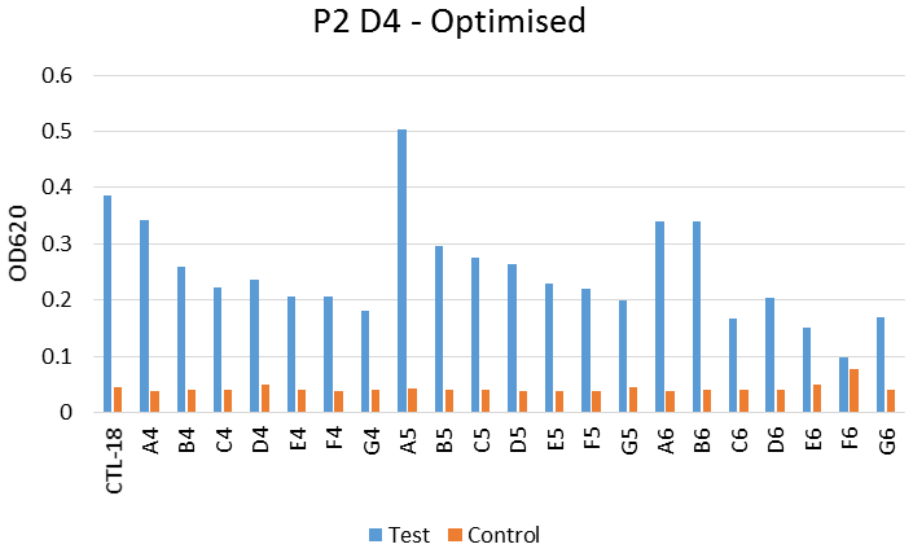
P2 D4 - Optimised
OD620
0.6
0.5
0.4
0.3
0.2
0.1
0
CTL-18 A4 B4 C4 D4 E4 F4 G4 A5 B5 C5 D5 E5 F5 G5 A6 B6 C6 D6 E6 F6 G6
Test
Control

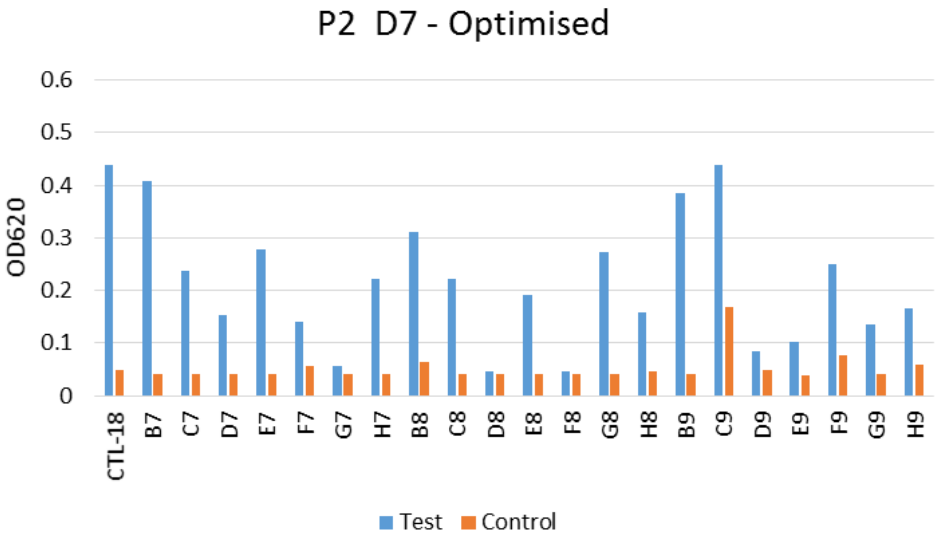
P2 D7 - Optimised
OD620
0.6
0.5
0.4
0.3
0.2
0.1
0
CTL-18 B7 C7 D7 E7 F7 G7 H7 B8 C8 D8 E8 F8 G8 H8 B9 C9 D9 E9 F9 G9 H9
Test
Control

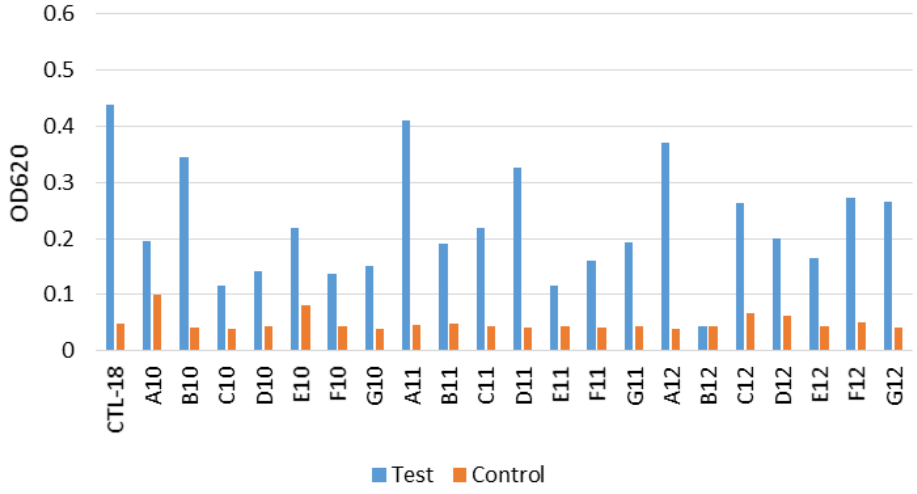
P2 D8 - Optimised
OD620
0.6
0.5
0.4
0.3
0.2
0.1
0
CTL-18 A10 B10 C10 D10 E10 F10 G10 A11 B11 C11 D11 E11 F11 G11 A12 B12 C12 D12 E12 F12 G12
Test
Control

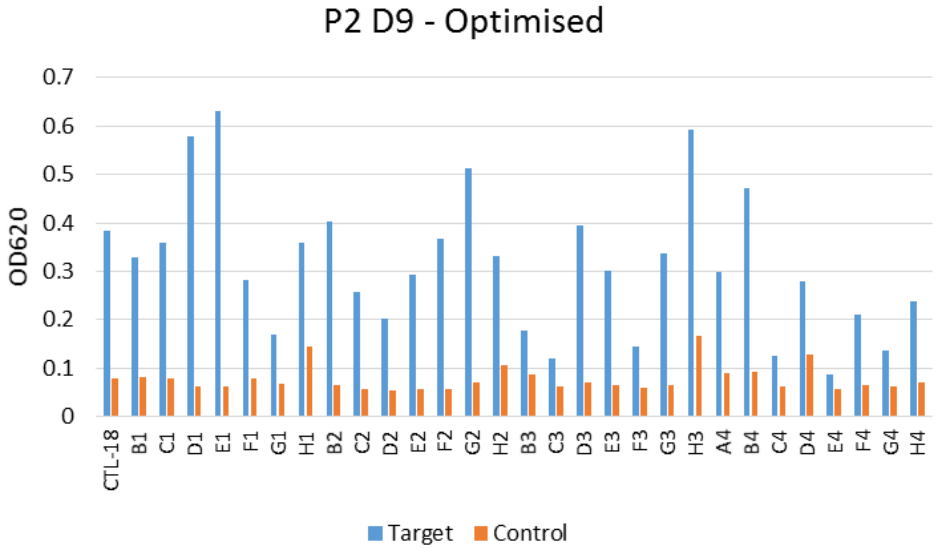
P2 D9 - Optimised
OD620
0.7
0.6
0.5
0.4
0.3
0.2
0.1
0
CTL-18 B1 C1 D1 E1 F1 G1 H1 B2 C2 D2 E2 F2 G2 H2 B3 C3 D3 E3 F3 G3 H3 A4 B4 C4 D4 E4 F4 G4 H4
Target
Control

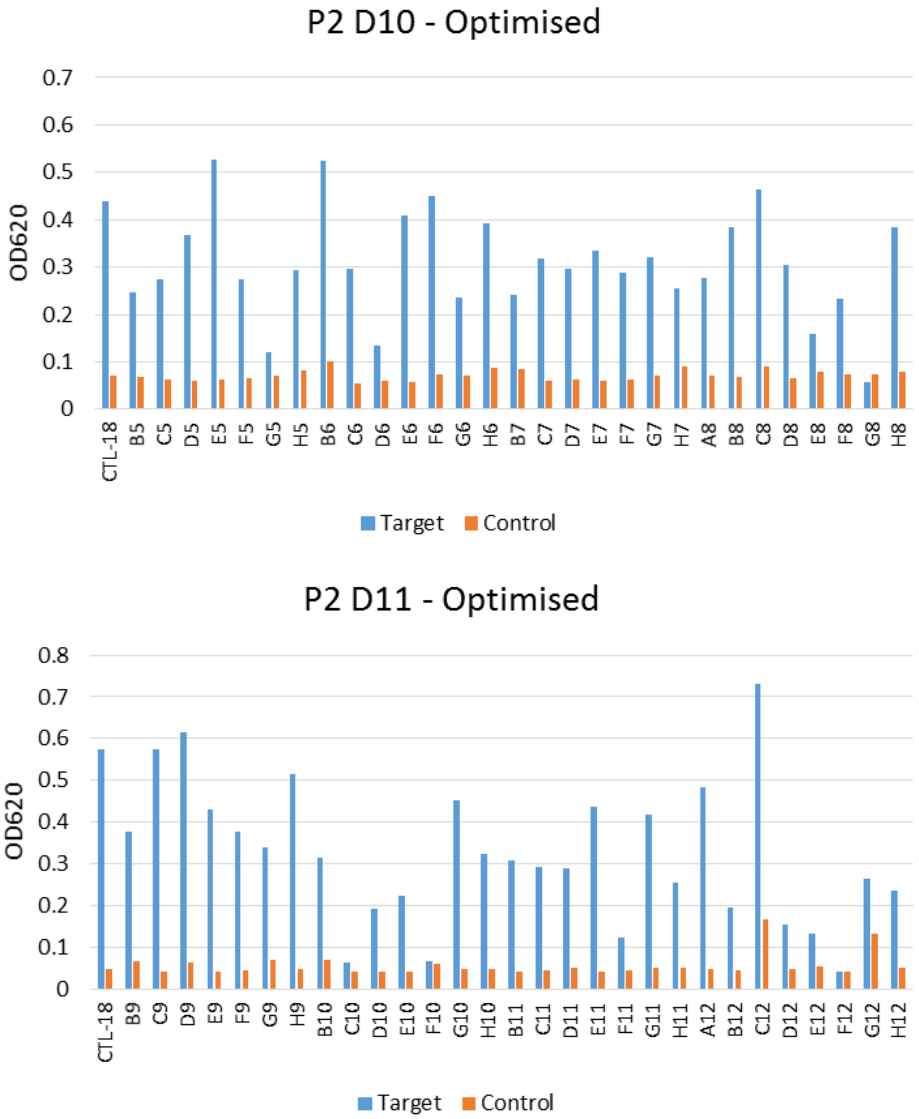

Figure 3.10.2 Phage ELISA analysis of Affimers selected after 8 separate elutions following panning of enriched phage library (P1D3) against NDM-1. Optimised phage ELISA (0.325µg/ml immobilised NDM-1) was performed following each elution day of the second panning round. Individual colonies of ER2783 cell, representing one Affimer, were selected at random following overnight culture on LB (lennox) agar plate. For each elution day, the CTL-18 candidate Affimer was included and empty control wells were also included to identify non-specific binders. Bound phage was identified with anti-Fd bacteriophage-HRP antibody followed by the addition of TMB. Following a 10 -13mins incubation, absorbance was measured at 620nm.

The phage ELISA results, shown in figure 3.10.2, identify several Affimers that bind to NDM-1 and produce an ELISA signal greater than the signal produced by CTL-18. Again, Affimers with a high control signal, such as H3 in P2 D9 were screened out. Affimers with a higher ELISA signal than CTL-18 in each plate were selected, pDHis vectors purified (methods 2.2.2) and sequenced as shown in figure 3.16.

a.

	Variable Region 1									Variable Region 2									
Aff 21	G	Y	K	V	W	T	P	Y	G	T	H	W	D	N	G	G	L	R	
CTL-18	**G**	**Y**	**K**	**V**	**W**	**T**	**P**	**Y**	**G**	**K**	**F**	**F**	**Q**	**G**	**G**	**K**	**I**	**Q**	
CTL-B8	G	Y	K	V	W	T	P	Y	G	I	W	Q	H	T	H	N	I	M	P1D2
CTL-A8	G	Y	K	V	W	T	P	Y	G	R	L	G	N	Y	G	N	F	M	P1D2
CTL-E11	G	Y	K	V	W	T	P	Y	G	K	L	L	T	G	P	H	I	K	P1D3
CTL-A5	G	Y	K	V	W	T	P	Y	G	K	V	F	K	A	N	M	F	H	P2D4
CTL-E1	G	Y	K	V	W	T	P	Y	G	K	M	H	H	K	G	T	I	V	P2D9
CTL-D3	G	Y	K	V	W	T	P	Y	G	K	S	Y	N	N	N	R	I	L	P2D9
CTL-B2	G	Y	K	V	W	T	P	Y	G	L	I	M	L	D	K	N	F	I	P2D9
CTL-B4	G	Y	K	V	W	T	P	Y	G	T	E	Y	K	N	L	H	Y	S	P2D9
CTL-G2	G	Y	K	V	W	T	P	Y	G	T	E	L	I	Y	H	K	I	Y	P2D9
CTL-D1	G	Y	K	V	W	T	P	Y	G	I	L	Q	I	H	G	T	V	R	P2D9
CTL-E5	G	Y	K	V	W	T	P	Y	G	K	V	F	K	Q	G	L	M	L	P2D10
CTL-C8	G	Y	K	V	W	T	P	Y	G	K	F	F	R	Q	N	M	I	R	P2D10
CTL-B6	G	Y	K	V	W	T	P	Y	G	T	Y	M	R	S	G	R	I	W	P2D10
CTL-F6	G	Y	K	V	W	T	P	Y	G	W	V	Q	H	M	S	L	V	R	P2D10
CTL-D9	G	Y	K	V	W	T	P	Y	G	K	E	G	F	Y	G	K	F	W	P2D11
CTL-C9	G	Y	K	V	W	T	P	Y	G	S	F	Y	E	S	G	Y	L	A	P2D11
CTL-C12	G	Y	K	V	W	T	P	Y	G	S	L	L	K	L	G	R	V	F	P2D11

Basic	K H R
Acidic	D E
Polar	S T C Y N Q
Non - Polar	G A V L I M F W P

b.

		Variable Region 2							
	CTL-18	K	F	F	Q	G	G	K	I	Q
Basic	K	7	0	0	4	1	1	2	0	1
	H	0	0	1	3	1	2	2	0	1
	R	1	0	0	2	0	0	3	0	3
Acidic	D	0	0	0	0	1	0	0	0	0
	E	0	3	0	1	0	0	0	0	0
Polar	S	2	1	0	0	2	1	0	0	1
	T	3	0	0	1	1	0	2	0	0
	Y	0	1	3	0	3	0	1	1	1
	N	0	0	0	2	2	3	3	0	0
	Q	0	0	3	0	2	0	0	0	0
Non-Polar	G	0	0	2	0	1	8	0	0	0
	A	0	0	0	0	1	0	0	0	1
	V	0	3	0	0	0	0	0	3	1
	L	1	4	3	1	1	1	2	1	2
	I	2	1	0	2	0	0	0	7	1
	M	0	1	2	0	1	0	2	1	2
	F	0	2	3	1	0	0	0	4	1
	W	1	1	0	0	0	0	0	0	2
	P	0	0	0	0	0	1	0	0	0

c.

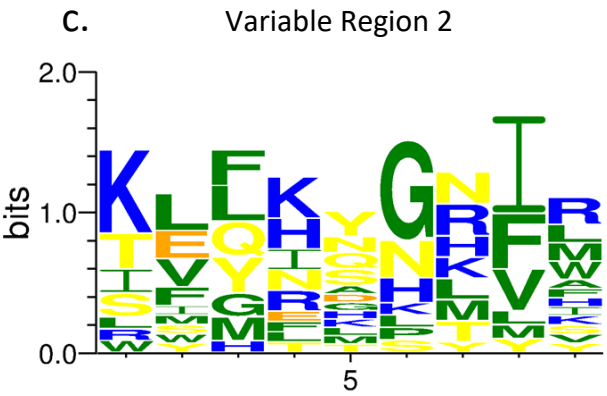

Figure 3.10.3 Amino acid sequence showing the variable regions of the Affimer hits as identified in the first two panning rounds of an enriched phage library against NDM-1. a) The variable loop regions of NDM-1 binding Affimers as sequenced from pDHis vectors. b) Heat map of variable region 2 showing frequency of amino acid found in each position. c) Protein logo of variable region 2 showing frequency of amino acid found in each position. Amino acid characteristics are colour-coded as indicated.

The sequencing results from the Affimer hits identified in the first two panning rounds are shown in figure 3.10.3.a. As expected, the enriched CRL library only contains Affimers with loop 1 being the same sequence as the candidate Affimers Aff-21 and CTL-18. A heat map of the second variable loop, figure 3.10.3.b, and the sequence logo, figure 3.10.3.c, identifies common amino acids found in loop two of the hits. In position 2.1, a lysine residue is present in 7 of the 17 hits and a glycine residue is present in 8 out of 17 hits in position 2.6. In position 2.8, a non-polar residue is present in 16 out of 17 hits with isoleucine in this position in 7 of the hits.

3.11 Phage Display Round 3

Following on from the second panning round, the enriched library (methods 2.2.11.2) from P2 D9 was used in the third panning round. This library was panned against immobilised NDM-1 at 7µg/ml and an empty control well. This library was selected due to the greatest number of hits being identified in the phage ELISA step. Panning round 3 was carried out as described in methods2.2.11.4. The P2 D9 enriched library was incubated for 1min against immobilised NDM-1 and empty control wells (NeutrAvidin Coated (HBC) 8-well strips). Following a wash step, Day 1 phage were eluted immediately and the subsequent elutions were made following competition washing. Eluted phage was incubated with ER2738 cells, plated on to LB (Lennox) agar plates and colonies were counted the following day to indicate the number of phage infected bacterial cells as shown in figure 3.11.1.

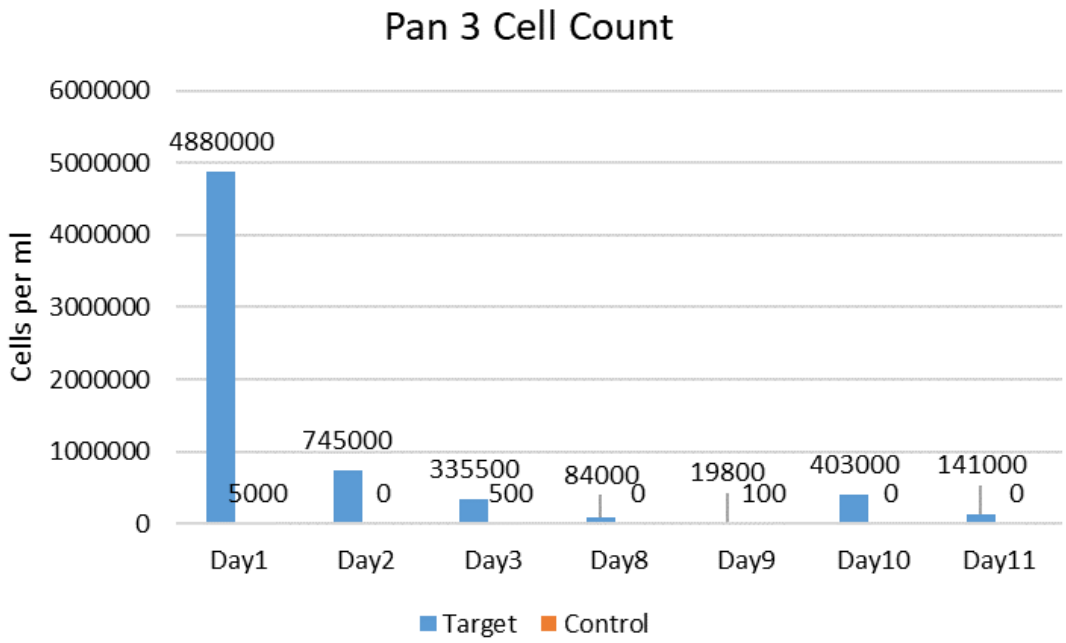

Figure 3.11.1 Number of ER2738 cells per ml infected with phage after incubating following panning round 3. The enriched P2 D9 library was incubated for 1min with immobilised NDM-1 (7mg/ml) and empty control well. Several elutions were made from separate well. The first Day 1 elution was made immediately after library incubation. The following days elutions were performed following competition washing to increase stringency. A 5ml culture of ER2738 cells was infected with eluted M13 phage and then grown overnight on agar plates.

In panning round three, the number of ER2738 cell infected by eluted phage decreases following competition wash as shown in figure 3.11.1. On Day 1, phage were eluted immediately after panning the enriched P2 D9 library with NDM-1 for 1min. The Day 1 cell count indicated that 4 880 000 ER2783 cell per ml were infected with phage. On Day 2, the number of infected cells decreased to 745 000 cells per ml. After 11 days of competition washes, 141 000 infected cells

per ml were indicated. The control wells indicated that the number of non-specific binding Affimers remains low in each elution.

From each elution day, colonies representing individual Affimers were selected for phage ELISA analysis as described in methods 2.2.10 (figure 3.11.2).

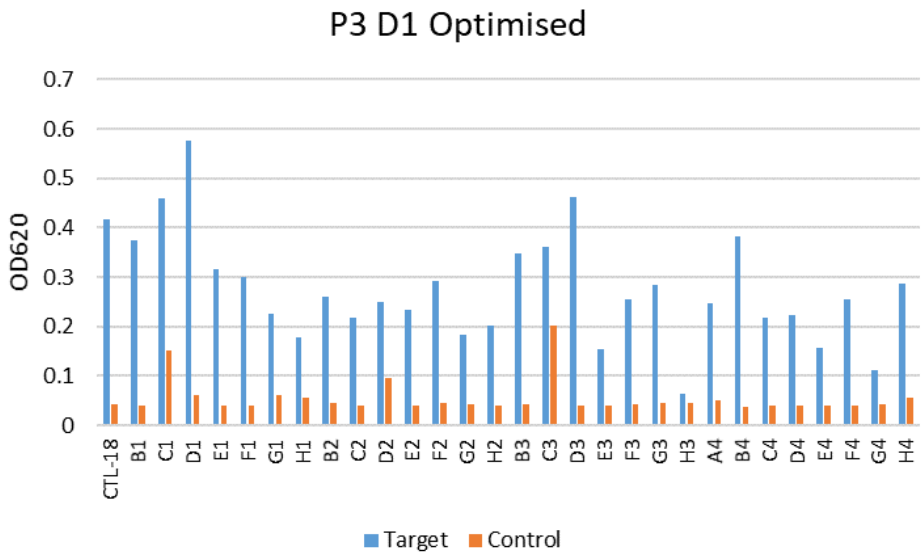

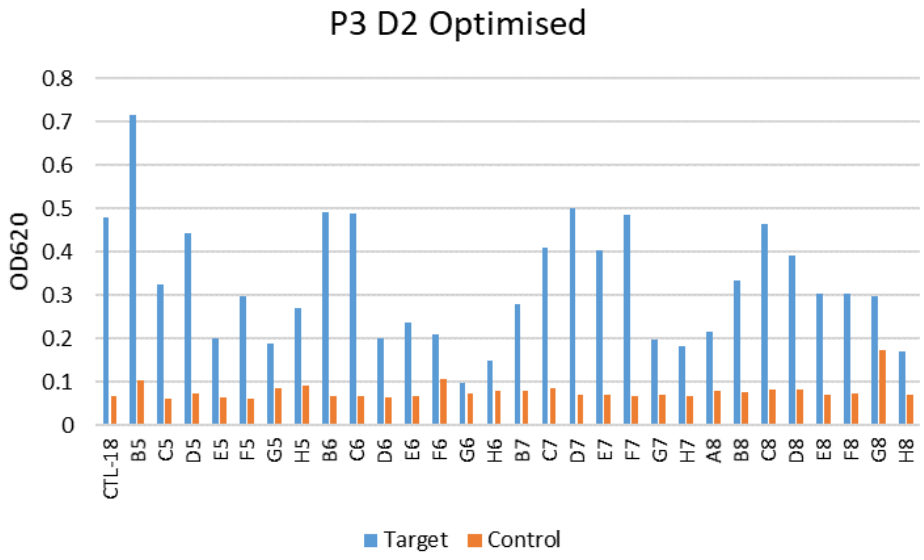

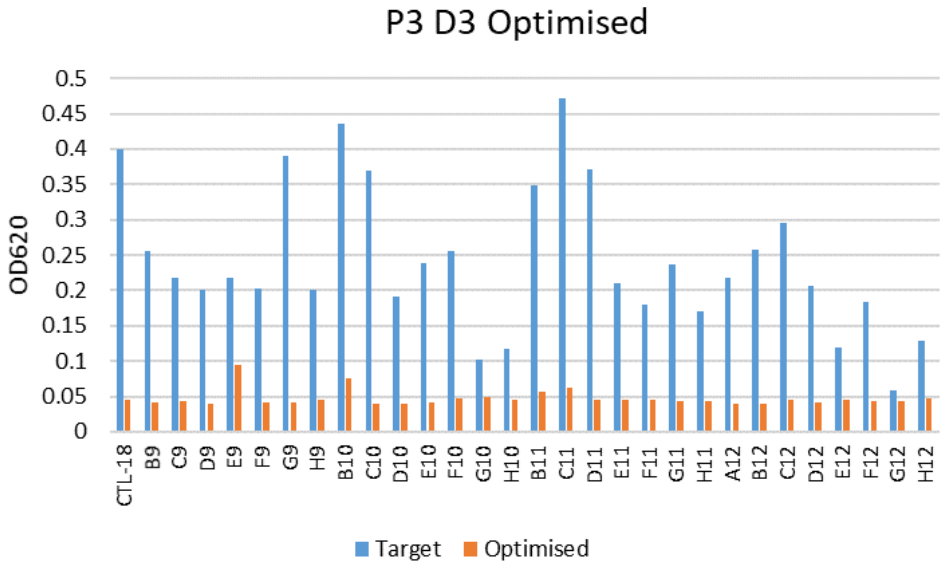
P3 D3 Optimised
OD620
0.5
0.45
0.4
0.35
0.3
0.25
0.2
0.15
0.1
0.05
0
CTL-18 B9 C9 D9 E9 F9 G9 H9 B10 C10 D10 E10 F10 G10 H10 B11 C11 D11 E11 F11 G11 H11 A12 B12 C12 D12 E12 F12 G12 H12
Target
Optimised

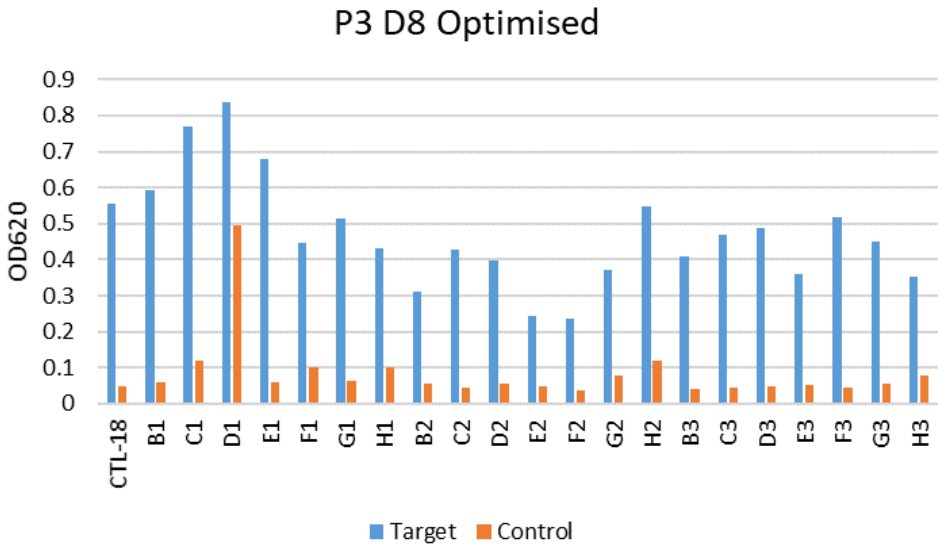
P3 D8 Optimised
OD620
0.9
0.8
0.7
0.6
0.5
0.4
0.3
0.2
0.1
0
CTL-18 B1 C1 D1 E1 F1 G1 H1 B2 C2 D2 E2 F2 G2 H2 B3 C3 D3 E3 F3 G3 H3
Target
Control

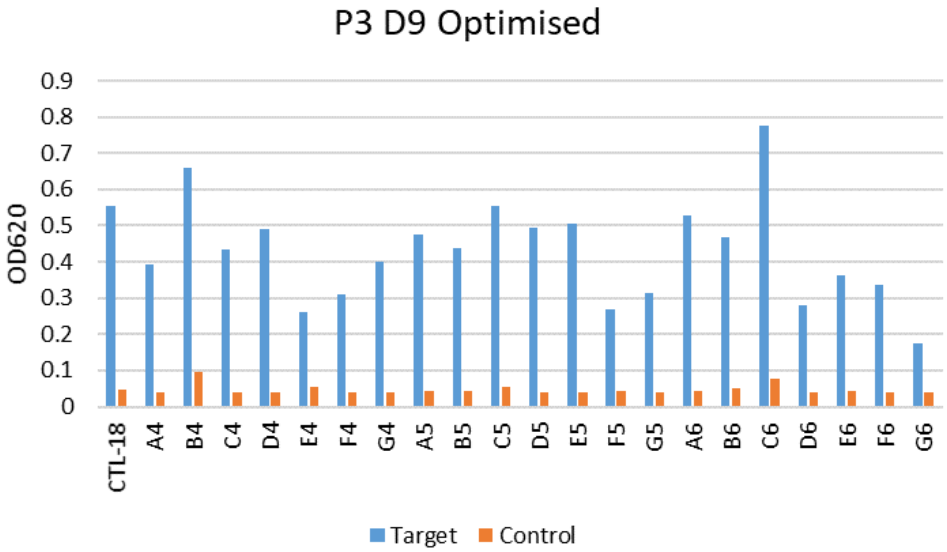
P3 D9 Optimised
OD620
0.9
0.8
0.7
0.6
0.5
0.4
0.3
0.2
0.1
0
CTL-18 A4 B4 C4 D4 E4 F4 G4 A5 B5 C5 D5 E5 F5 G5 A6 B6 C6 D6 E6 F6 G6
Target
Control

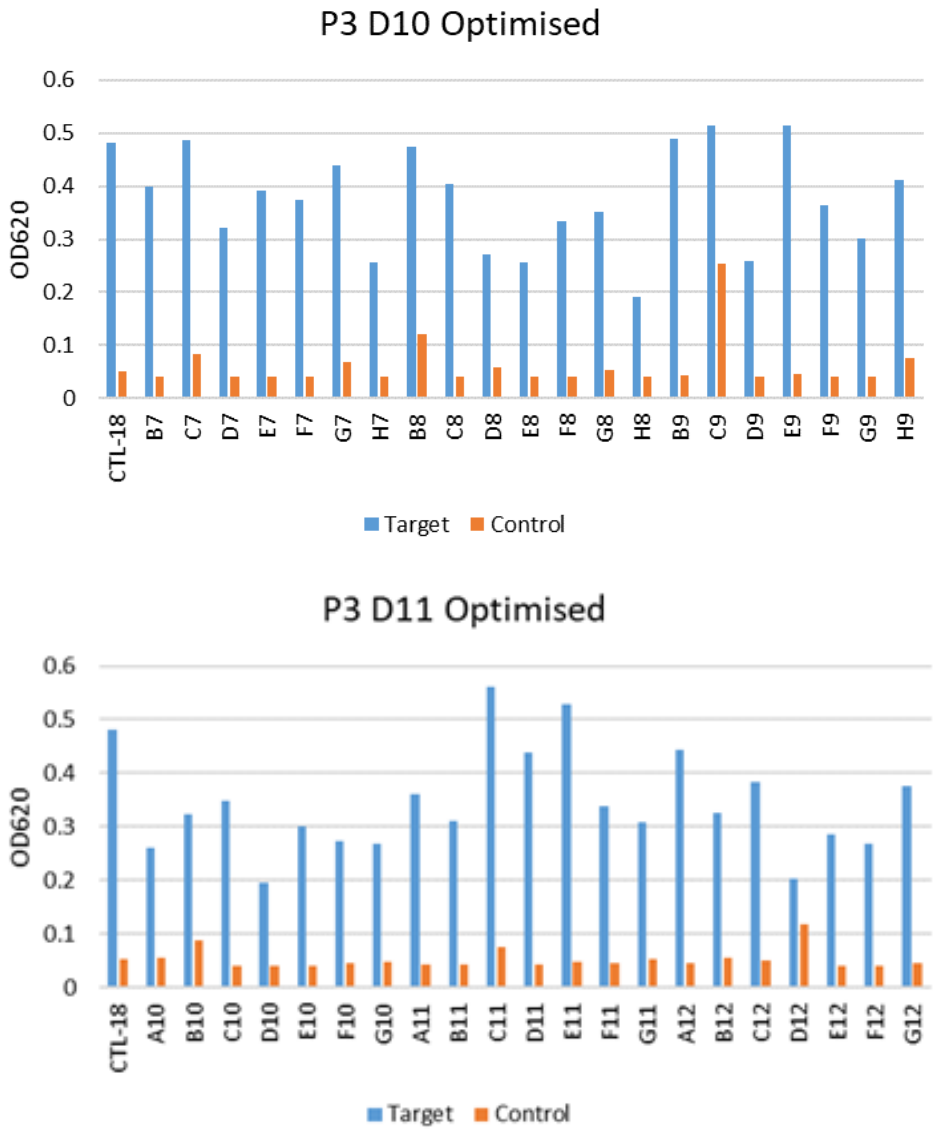

Figure 3.11.2 Phage ELISA analysis of Affimers selected from separate elutions of the enriched P2 D9 library against NDM-1. Optimised phage ELISAs (0.325µg/ml of immobilised NDM-1) were performed following each elution day. Following an overnight culture on LB (lennox) agar plates, individual colonies of infected ER2738, representing one Affimer, were selected at random. For each phage ELISA a CTL-18 control was included and empty control wells were included for negative selection. Anti-Fd bacteriophage-HRP antibody was used to identify bound phage and visualised by the addition of TMB. Following a 10 -13mins incubation, absorbance was measured at 620nm.

The phage ELISA results, shown in figure 3.11.2, identify several Affimers that bind to NDM-1 and produce an ELISA signal greater than the signal produced by CTL-18. Affimers with a high control signal, such as D1 in P3 D8 were screened out. Affimers with a higher ELISA signal than CTL-18 in each plate were selected, pDHis vectors purified (methods 2.2.2) and sequenced as shown in figure 3.11.3.

a.

	Variable Region 1									Variable Region 2								
Aff 21	G	Y	K	V	W	T	P	Y	G	T	H	W	D	N	G	G	L	R
CTL-18	**G**	**Y**	**K**	**V**	**W**	**T**	**P**	**Y**	**G**	**K**	**F**	**F**	**Q**	**G**	**G**	**K**	**I**	**Q**
CTL-B8	G	Y	K	V	W	T	P	Y	G	I	W	Q	H	T	H	N	I	M
CTL-A8	G	Y	K	V	W	T	P	Y	G	R	L	G	N	Y	G	N	F	M
CTL-E11	G	Y	K	V	W	T	P	Y	G	K	L	L	T	G	P	H	I	K
CTL-A5	G	Y	K	V	W	T	P	Y	G	K	V	F	K	A	N	M	F	H
CTL-E1	G	Y	K	V	W	T	P	Y	G	K	M	H	H	K	G	T	I	V
CTL-D3	G	Y	K	V	W	T	P	Y	G	K	S	Y	N	N	N	R	I	L
CTL-B2	G	Y	K	V	W	T	P	Y	G	L	I	M	L	D	K	N	F	I
CTL-B4	G	Y	K	V	W	T	P	Y	G	T	E	Y	K	N	L	H	Y	S
CTL-G2	G	Y	K	V	W	T	P	Y	G	T	E	L	I	Y	H	K	I	Y
CTL-D1	G	Y	K	V	W	T	P	Y	G	I	L	Q	I	H	G	T	V	R
CTL-E5	G	Y	K	V	W	T	P	Y	G	K	V	F	K	Q	G	L	M	L
CTL-C8	G	Y	K	V	W	T	P	Y	G	K	F	F	R	Q	N	M	I	R
CTL-B6	G	Y	K	V	W	T	P	Y	G	T	Y	M	R	S	G	R	I	W
CTL-F6	G	Y	K	V	W	T	P	Y	G	W	V	Q	H	M	S	L	V	R
CTL-D9	G	Y	K	V	W	T	P	Y	G	K	E	G	F	Y	G	K	F	W
CTL-C9	G	Y	K	V	W	T	P	Y	G	S	F	Y	E	S	G	Y	L	A
CTL-C12	G	Y	K	V	W	T	P	Y	G	S	L	L	K	L	G	R	V	F
CTL-D1A	G	Y	K	V	W	T	P	Y	G	V	A	L	K	R	G	Q	I	V
CTL-D3A	G	Y	K	V	W	T	P	Y	G	T	L	M	S	A	D	L	I	R
CTL-B5	G	Y	K	V	W	T	P	Y	G	R	V	G	T	R	G	V	F	Y
CTL-B6A	G	Y	K	V	W	T	P	Y	G	T	L	M	S	A	D	L	I	R
CTL-C6	G	Y	K	V	W	T	P	Y	G	V	E	L	N	R	H	Q	I	V
CTL-D7	G	Y	K	V	W	T	P	Y	G	T	I	G	S	Q	G	L	F	Y
CTL-F7	G	Y	K	V	W	T	P	Y	G	W	E	F	I	G	M	D	V	I
CTL-B10	G	Y	K	V	W	T	P	Y	G	Y	L	M	M	H	N	R	I	R
CTL-C11	G	Y	K	V	W	T	P	Y	G	K	Y	F	E	D	N	Y	I	Y
CTL-B1	G	Y	K	V	W	T	P	Y	G	W	E	L	I	G	P	N	L	W
CTL-E1A	G	Y	K	V	W	T	P	Y	G	F	E	M	W	H	N	E	L	Y
CTL-G1	G	Y	K	V	W	T	P	Y	G	R	Y	Q	E	N	F	G	I	F
CTL-B4A	G	Y	K	V	W	T	P	Y	G	V	A	N	T	F	M	G	L	R
CTL-C6A	G	Y	K	V	W	T	P	Y	G	K	I	G	I	R	G	S	F	T
CTL-C7	G	Y	K	V	W	T	P	Y	G	Y	T	N	W	G	P	I	P	L
CTL-B9	G	Y	K	V	W	T	P	Y	G	F	W	H	N	N	H	D	F	V
CTL-E9	G	Y	K	V	W	T	P	Y	G	W	E	H	Y	K	G	I	V	M
CTL-C11A	G	Y	K	V	W	T	P	Y	G	K	S	F	M	A	G	V	F	I
CTL-E11B	G	Y	K	V	W	T	P	Y	G	W	E	Y	M	Y	G	S	V	L

Basic	K H R
Acidic	D E
Polar	S T C Y N Q
Non - Polar	G A V L I M F W P

b.

		Variable Region 2								
	CTL-18	K	F	F	Q	G	G	K	I	Q
Basic	K	10	0	0	5	2	1	2	0	1
	H	0	0	3	3	2	4	2	0	1
	R	3	0	0	2	4	0	3	0	6
Acidic	D	0	0	0	0	2	2	2	0	0
	E	0	6	0	3	0	0	1	0	0
Polar	S	2	2	0	3	2	1	2	0	1
	T	6	1	0	3	1	0	2	0	1
	Y	1	3	4	1	4	0	2	1	5
	N	0	0	2	4	4	5	4	0	0
	Q	0	0	4	0	3	0	2	0	0
Non-Polar	G	0	0	5	0	4	15	2	0	0
	A	0	2	0	0	4	0	0	0	1
	V	3	4	0	0	0	0	2	6	4
	L	1	6	6	1	1	1	5	4	4
	I	2	3	0	5	0	0	2	13	3
	M	0	1	5	2	1	2	2	1	3
	F	2	2	6	1	1	1	0	9	2
	W	5	2	0	2	0	0	0	0	3
	P	0	0	0	0	0	3	0	1	0

c.

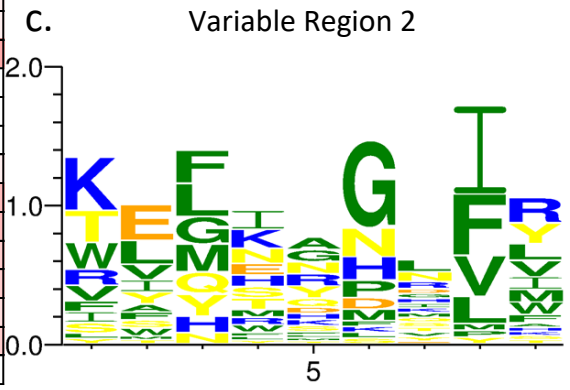

Figure 3.11.3 Amino acid sequence showing the variable regions of the Affimer hits as identified in three panning rounds of an enriched phage library against NDM-1. a) The variable loop regions of NDM-1 binding Affimers as sequenced from pDHis vectors. b) Heat map of variable region 2 showing frequency of amino acid found in each position. c) Protein logo of variable region 2 showing frequency of amino acid found in each position. Amino acid characteristics are colour-coded as indicated.

The sequencing results from the Affimer hits identified in the first three panning rounds are shown in figure 3.11.3.a. Affimers hits contain the VR 1 the same sequence as the candidate Affimers Aff21 and CTL-18. Figure 3.11.3.b shows a heat map of the second variable loop and figure 3.11.3.c shows the sequence logo and identifies common amino acids found in VR 2 of the hits. The most frequent amino acids identified in the Affimer hits following panning round three are lysine in position 2.1, glutamic acid in position 2.2, glycine in position 2.6 and isoleucine in position 2.8.

3.12 Comparison of ELISA hits

To confirm the results of the phage ELISA results from the phage display rounds, a comparison phage ELISA of all the identified hits was carried out. Phage were produced from transformed ER2738 cells (methods 2.2.1) and incubated with the optimised concentration (0.325mg/ml) on a single F96 Maxisorp Nunc-Immuno Plate (methods 2.2.10). Four biological repeats were performed and CTL-18 (show in red) was included in triplicate in each test as shown in figure 3.12.1.

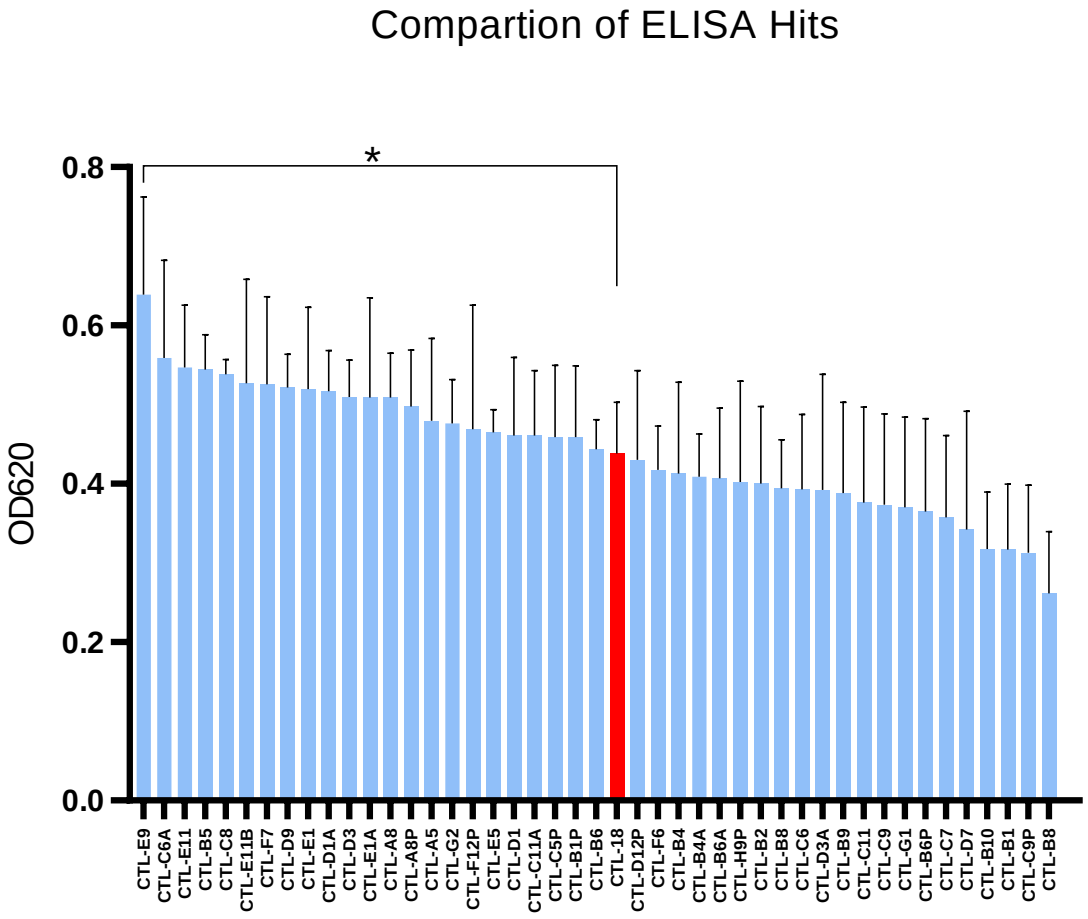

Affimer	Mean (OD620)	±SD	Mean Difference to CTL-18 (OD620)	P value
CTL-E9	0.6388	0.1236	-0.2003	0.0134
CTL-C6A	0.5593	0.1231	-0.1208	0.5869
CTL-E11	0.547	0.07888	-0.1085	0.7753
CTL-B5	0.544	0.04412	-0.1055	0.8156
CTL-C8	0.5383	0.01896	-0.09975	0.8827

	Variable Loop 2									
CTL-18	**K**	**F**	**F**	**Q**	**G**	**G**	**K**	**I**	**Q**	
CTL-E9	W	E	H	Y	K	G	I	V	M	P3D10
CTL-C6A	K	I	G	I	R	G	S	F	T	P3D9
CTL-E11	K	L	L	T	G	P	H	I	K	P1D3
CTL-B5	R	V	G	T	R	G	V	F	Y	P3D2
CTL-C8	K	F	F	R	Q	N	M	I	R	P2D10

Figure 3.12.1 Ranked average phage ELISA signal of ELISA hits identified in phage display panning rounds. Optimised phage ELISA (0.325mg/ml imobalised NDM-1) was performed `on ELISA hits identified in the phage display rounds. ER2783 cultures transformed with pDHis vectors containing Affimer inserts were infected with M13 helper phage to produce phage for phage ELISA. CTL-8 was included in triplicate for each repeated (n=4 biological repeats) and is indicated by the red bar. To detect signal, phage were incubated with anti-Fd bacteriophage-HRP antibody followed by the addition of TMB and Absorbance measured at 620nm (p=0.0115).

The ranked mean ELISA results indicates that 23 Affimers out of 44 have a higher OD_{620} signal that CTL-18 as shown in figure 3.12.1. Whereas, 21 Affimers have a lower ELISA signal. The highest mean ELISA signal was for CTL-E9 at OD_{620} 0.6388 (±SD 0.1236) and is significatly (p=0.0115) greater that the OD_{620} for CTL-18 at 0.4385 (±SD 0.06431) as indicated in figure3.12.2. The candiated Affimer, CRL-18, is indcated in the bar graph by the red bar. The next four Affimers with the highest OD_{620} are CTL-C6A (0.5593 ±SD 0.1231), CTL-E11 (0.547 ±SD 0.07888), CTL-B5 (0.544 ±SD 0.04412) and CTL-C8 (0.5383 ±SD 0.01896) . Along with CTL-E9, these Affimers

were subcloned into pET11a expression vectors (figure3.13.1) to produce Affimer protein to be tested in β-lactamase activity assays.

3.13 Affimer Subcloning, Production and Purification

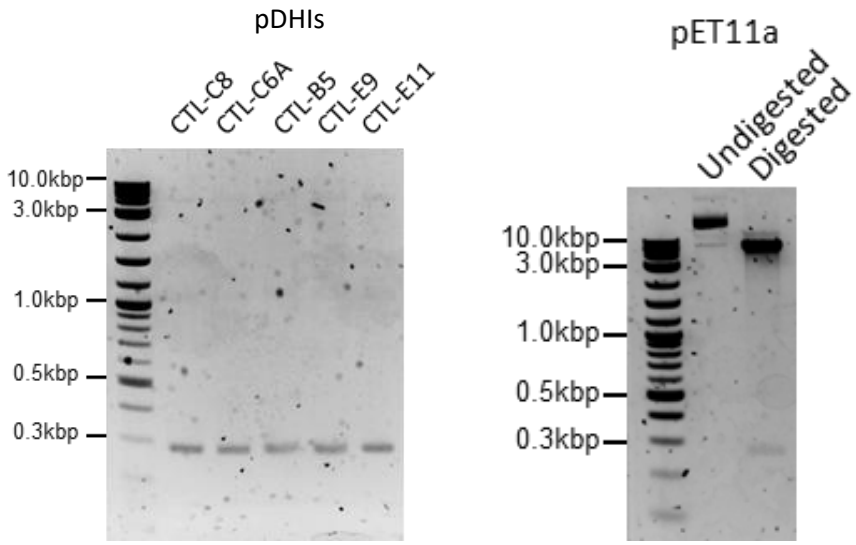

Figure 3.13.1 Agarose Gel electrophoresis analysis of Affimer subcloning. a) Amplification of Affimer insert from pDHis vector by PCR. Inserts for the 5 Affimers to be subcloned are identified by bands at 0.3kbp. b) Digested and undigested pET11a vector when undergoing a double digestion with *NotI*-HF™ and *NheI*-HF™ restriction enzymes. The band at around 7.0kbp indicates the linear digested vector with the excised insert at 0.3kbp.

BL21 star™ (DE3) cells were transformed with pET11a vectors (methods2.2.1) and Affimers were produced and purified as previously described. SDS-PAGE analysis of the production and puification process are shown in figure 3.13.1.

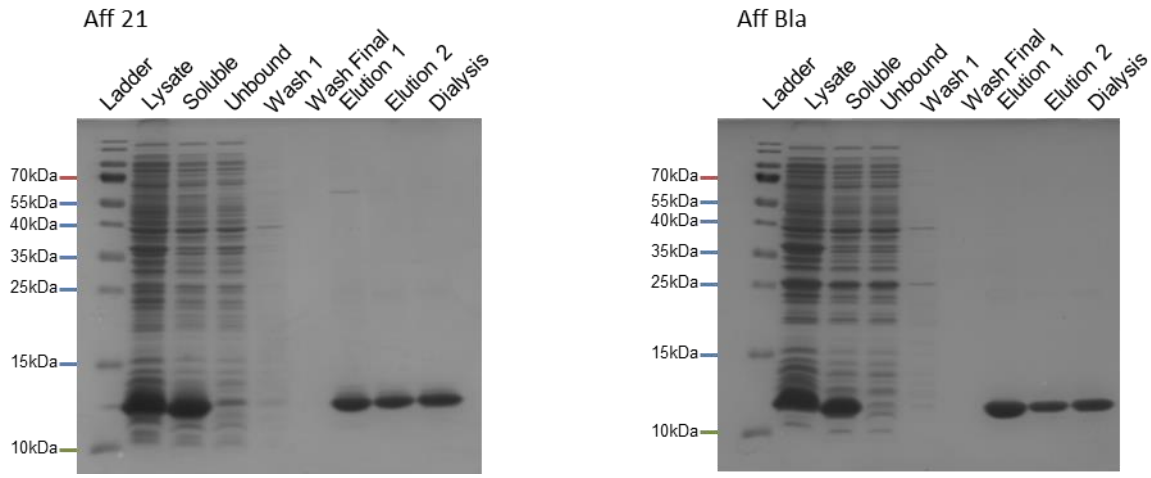

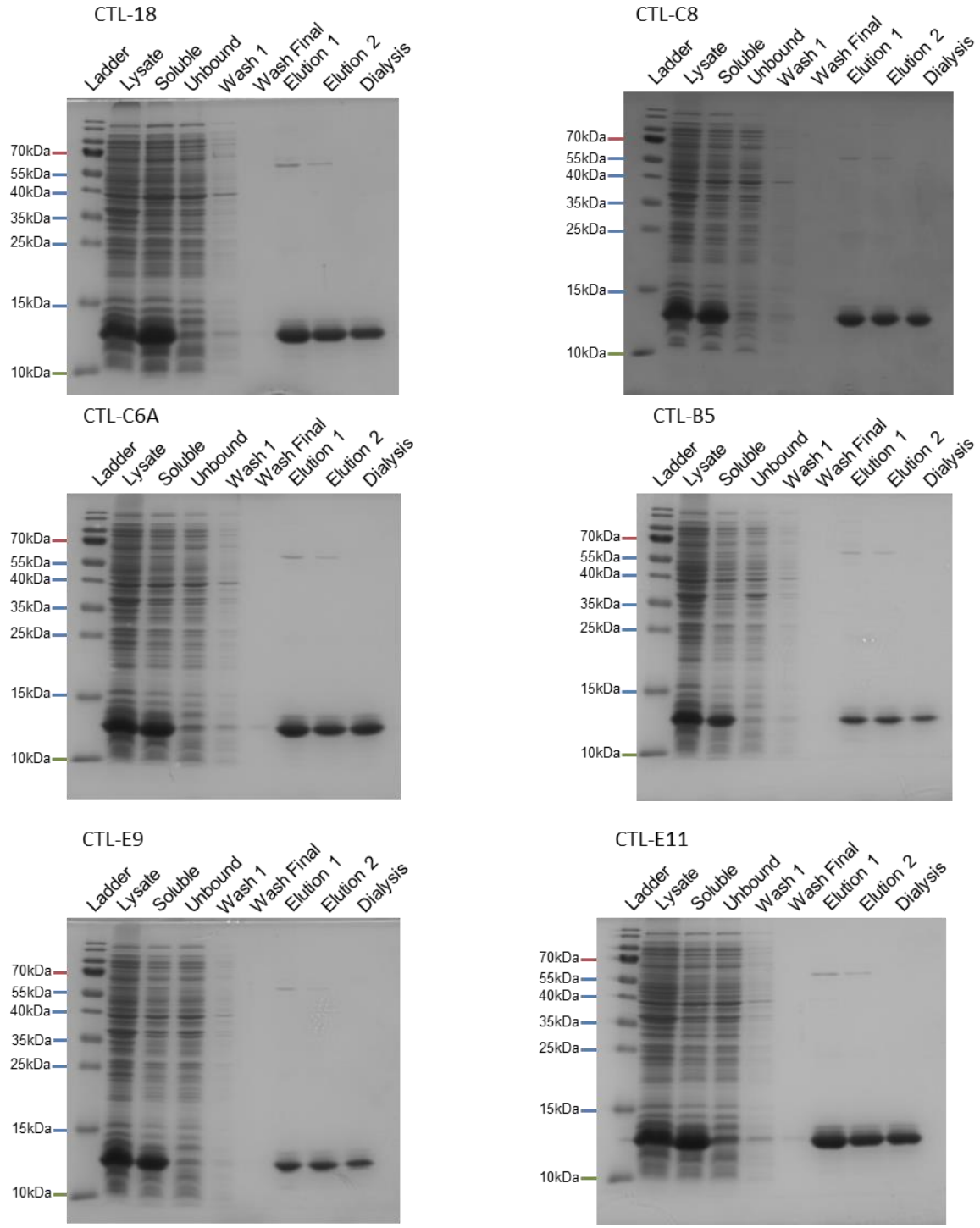

Figure 3.13.2 SDS-PAGE analysis of Affimer production and purification. 1µl samples were taken throughout the production and nickel ion affinity purification of Affimer protein. Proteins were analysed by SDS-PAGE and Coomassie staining to confirm size and purity of product. Affimer protein is indicated by the band at 12kDa.

Affimer protein was purified from 50ml cultures using NiNTA resin as per methods 2.27. SDS-PAGE anaylays of 1µl samples (methods2.2.8) idicated that purified Affimer (12kDa) was produced and present in the dialysed sampleas shown in figure 3.13.2. Nanodrop Lite readings were taken and converted to concentration as described in methods 2.2.3.

3.14 Confirmation of Affimer Concentrations

Affimer	Molecular Weight	Extinction Coefficient	Absorbance 0.1%	Theoretical pI	Dialysed Sample Concentration (mg/ml)
Aff - 21	**12335.96**	**23950**	**1.941**	**8.01**	**1.587**
CTL - 18	**12333.09**	**18450**	**1.496**	**9.05**	**2.135**
CTL - C8	15139.49	23950	1.582	9.49	1.820
CTL - C6A	14878.15	23950	1.61	9.37	2.689
CTL - B5	14954.21	25440	1.701	9.37	0.672
CTL - E9	15062.36	30940	2.054	9.00	0.890
CTL - E11	14906.25	23950	1.607	9.35	2.367

Figure 3.14.1 Physical and chemical properties of purified Affimer Reagents. Amino acid Sequence analysis was performed by ExPASy ProtParam software to determine chemical and physical properties of Affimers. 5 NDM-1 binding Affimers identified during phage display were analysed.

Affimer physical and chemical parameters, including extinction coefficients, were determined by sequence analysis using ExPASy ProtParam online software as shown in table 3.14.1. Nanodrop drop A_{280} reading were used to determine concentration. To confirm nanodrop readings, SDS-PAGE analysis was performed by loading 1ug of each Affimer and comparing intensity of resulting 12kDa band as shown in figure 3.14.2

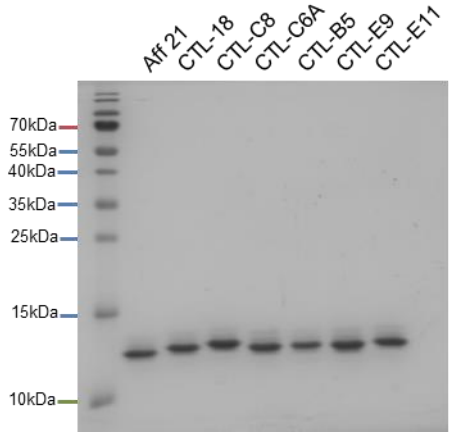

Figure 3.14.2 SDS-PAGE analysis of 1µg of Affimer sample. Nanodrop reading were used to determine the concentration of Affimer samples (CTL-18 to CTL-E11). To confirm accurate nanodrop readings, 1µg of each Affimer was analysed by SDS-PAGE gel. The intensities of the ~12kDa Affimer binds are comparable in each batch

As shown in figure 3.14.2, the comparable intensities of Affimer bands (~12kDa) on SDS-PAGE gels confirms the amount of Affimer loaded on to the gel to be approximately the same therefore, confirming the concentrations as measured by nanodrop.

3.15 β-lactamase activity assay

To analyse the affimer mediated inhibition of NDM-1 activity, β-lactamaes activity asayays were carried out as per methods 2.2.9. The inhibatory effect of Aff 21 and CTL-18 were compared to the Affimers identified in the phage display rounds (CTL-C8, CTL-C6A, CTL-B5, CTL-E9 and CTL-E11). Each condition was performed in triplicate per run and three technical repeats were performed.

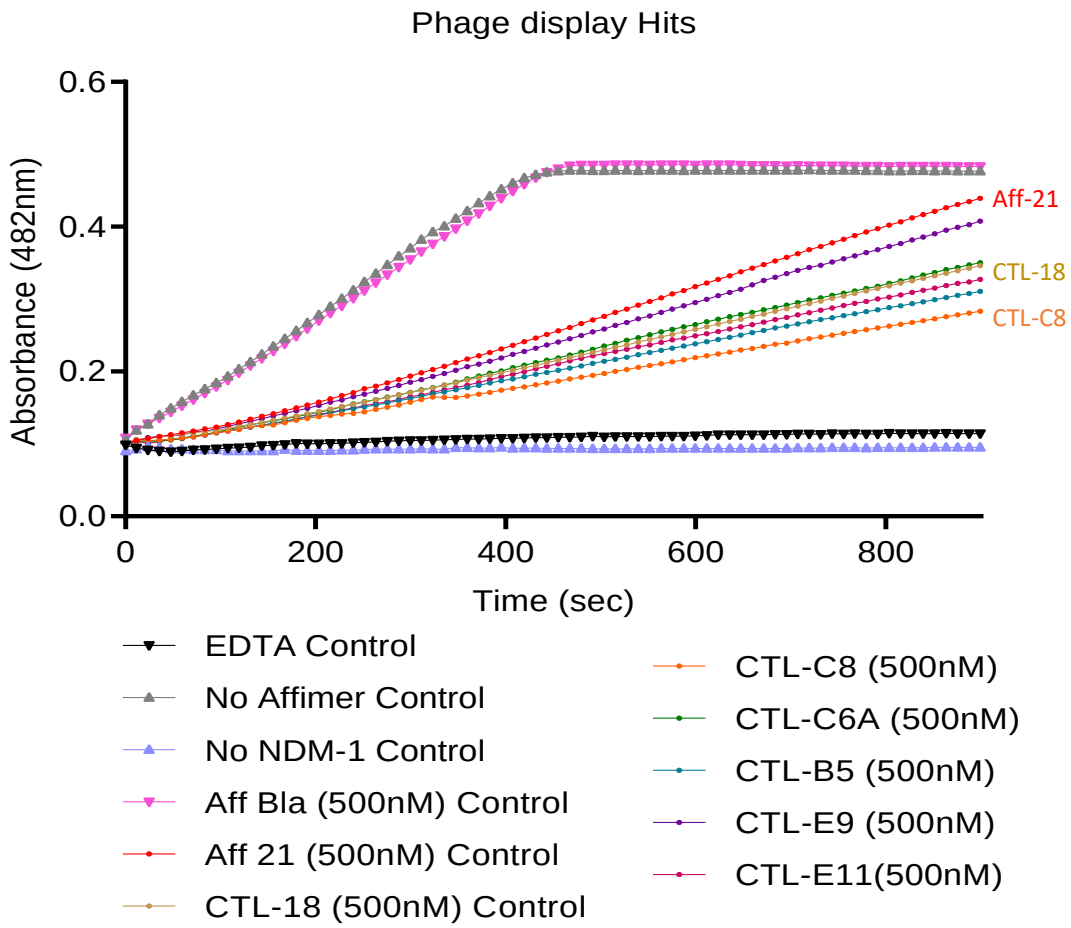

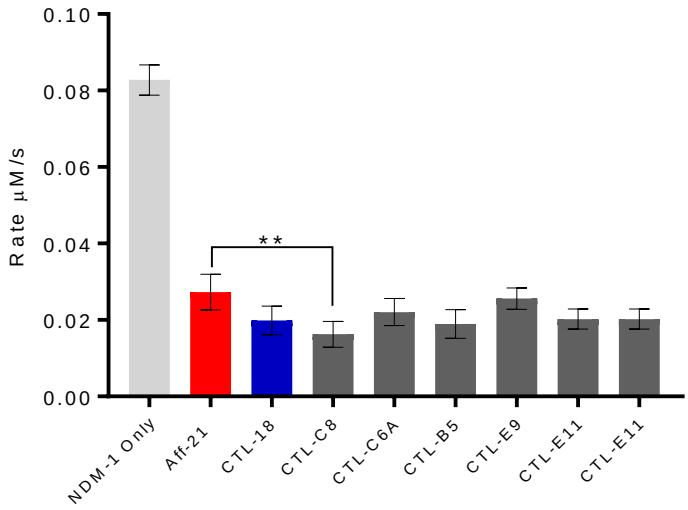

Figure 3.15.1 Affimer mediated inhibiti on **of NDM-1 activity as quantified by nitrocefin hydrolysis.** Nitrocefin (65mM) was used to quantify the activity of NDM-1 (100nM) at 25°C by measuring absorbance 482 nm every 12sec for 15mins. a) Affimer reagents (500nM) were incubated with NDM-1 to analyse the inhibitory effect. b) Rate of NDM-1 activity was determined by normalising absorbance values to EDTA control before converting to concentration (n=3 technical repeats). The initial rate was determined by linear regression for the first 250sec. (p=0.0076)

As shown in figure 3.15.1, the β-lactamase activity assay suggests that Affimers CTL-C8 to CTS-E11 inhibit NDM-1 hydrolysis activity. Hydrolysis of the β-lactam ring in nitrocefin as measured by absorbance change at 482nm and the mean initial rate of hydrolysis of NDM-1 only is 00.083 µM/s (SD±0.0040). As previously described, NDM-1 activity is inhibited by Aff 21 to 0.027µM/s (SD±0.0047) and CTL-18 to 0.020µM/s (SD±0.0037). Compared to Aff 21, the Affimer CTL-C8 appears to show significantly (p=0.0076) improved inhibition of NDM-1 activity to 0.016µM/s (SD±0.0034).

Chapter 4

Discussion

4.1 Affimer Reagent as an inhibitor of NDM-1

Bacterial resistance to antimicrobials is a threat to human health. In particular, the rapid and global dissemination of multidrug resistance, such as that conferred by NDM-1, has highlighted the need for novel therapeutics. One strategy is to re-sensitise drug resistant bacteria to widely available antibiotics by inhibiting the resistance mechanism. This project has confirmed the identification of an Affimer reagent, Aff 21, as an effective inhibitor of NDM-1 hydrolysis activity. Additionally, an affinity maturation process has identified two more Affimers, CTL-18 and CTL-C8, that inhibit NDM-1 activity to a greater extent than Aff 21. The affinity maturation process involved the development of a stringent phage display strategy to screen for binders with a high NDM-1 binding affinity. Whilst further development and characterisation is needed, the Affimer reagents identified here have the potential to be co-administered with currently available antibiotics as effective therapy against antimicrobial resistant bacteria.

4.2 Affinity maturation of Affimer 21

The use of clavulanic acid, to target serine based β-lactamase inhibitors, in conjunction with β-lactam antibiotics has proven to be clinically successful (Docquier and Mangani, 2018). However, inhibitors that are effective against metallo-β-lactamases, such as NDM-1, have yet to be approved for therapeutic use. Targeting enzymes for therapy in other fields of medicine is well-established with many approved drugs available (Robertson, 2007). One of the major challenges to developing an enzyme inhibitor is to mitigate off target effects, therefore, structural proteins may prove to be advantageous over small molecules (Sha et al., 2017). Affimer reagents have previously been shown to bind to protein targets with high specificity, being developed to bind to FcγRIIIa but not FcγRIIIb (Robinson et al., 2018). Therefore, Affimers may be ideal reagents to specifically bind to and inhibit NDM-1 as targeted therapy and mitigate off-target effects.

The work presented here builds on previous work by L De Faveri that identified an Affimer reagent, Aff 21, as an inhibitor of NDM-1 activity. β-lactamase activity assays confirmed the significant inhibition of NDM-1 activity when incubated with Aff 21.

One of the advantages of Affimer reagents is that site directed mutagenesis of the variable regions can be made (Tiede et al., 2017). Therefore, an affinity maturation process can take place in order to identify binders that have a greater inhibitory effect. To identify improved inhibitors, Affimer binders had been identified from an initial screening of three separate libraries against NDM-1 in phage display (C Tiede and L De Faveri). The 'LP' library was generated by randomising the non-essential amino acids in variable region 1 (as identified previously by alanine screening). The β-lactamase activity assays in this report suggests that sequence changes to the first variable region do not significantly improve the inhibition of NDM-1. One Affimer reagent, LP2-7, appears

to slightly improve inhibition and has an isoleucine in position 1.4 (as oppose to valine) and phenylalanine (as oppose to tyrosine) in position 1.8. This Variable Region 1 sequence, identified in LP2-7, may be useful in future work and could be combined with an optimised variable region 2 to generate an improved inhibitor.

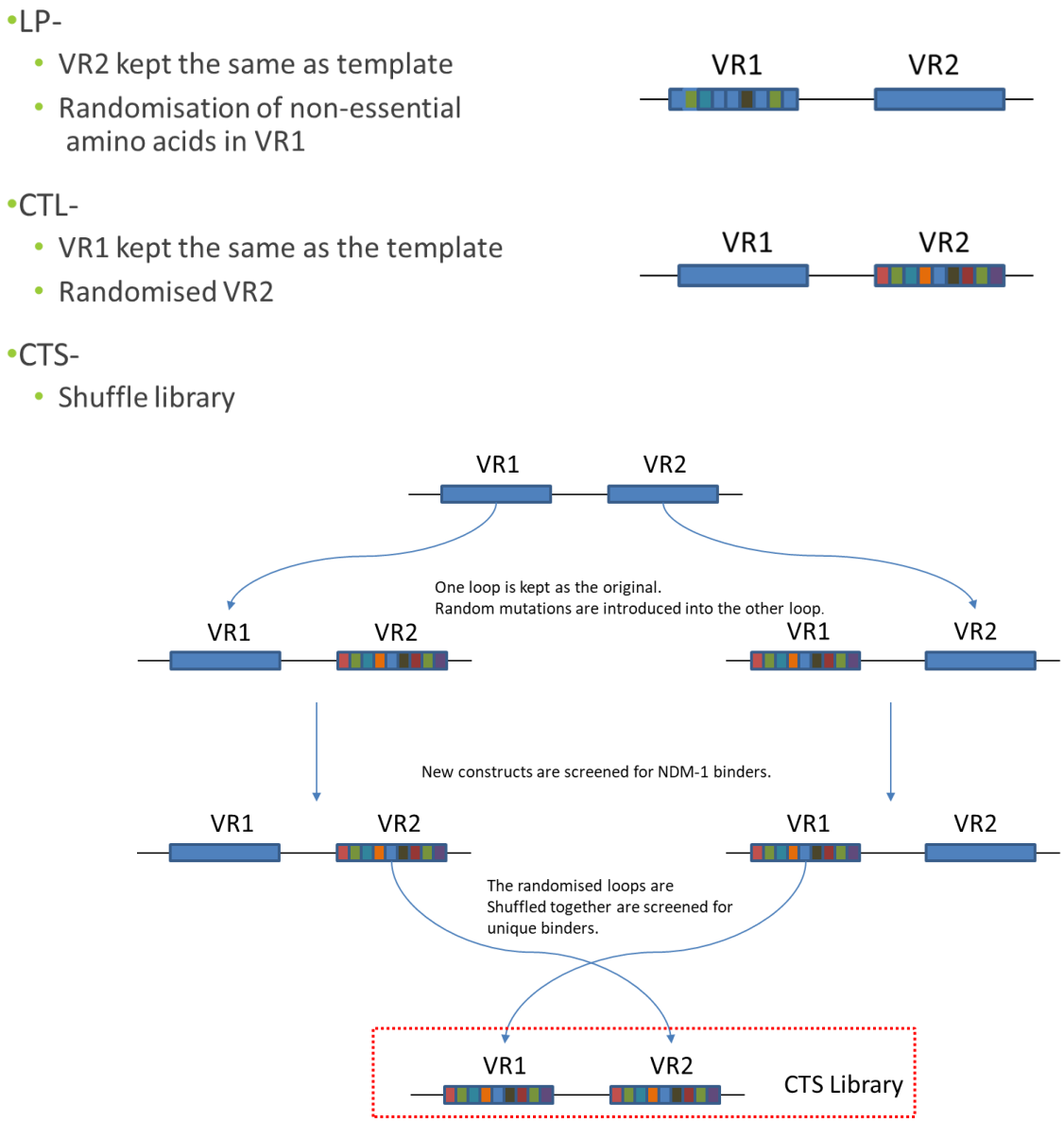

Figure 4.2.1 Schematic showing the generation of the three phage libraries. Three enriched phage libraries were generated by C Teide and L De Faveri to be used to identify NDM-1 binders in phage display.

The 'CTL' library retained the same sequence in the variable region 1 as Aff 21 and a randomised variable region 2. From the CTL library, several binders (including CTL-18) showed improved inhibition compared to Aff 21. This result is promising as it suggests that changes to the variable region 2 may result in an Affimer that has improved inhibition of NDM-1 activity.

From the CTS library, CTS-22 was identified as inhibiting NDM-1 activity. This shuffle library, as highlighted in figure 4.2.1, was generated in three steps. 1) Two separate libraries were

generated where one of the variable regions had the same sequence as the template (Aff 21), and the other variable region was randomised. 2) From these two separate libraries, NDM-1 binders were identified. 3) The randomised variable regions of the binders are then shuffled together to generate a new shuffled library. This shuffled, CTS, library is screened against NDM-1 to identify binders that are tested in this report. Interestingly, despite the random generation of the variable region, only one binder identified in this screen had a VR1 sequence that differed from Aff 21. This further suggests that the sequence of VR 1 identified in Aff 21 is likely to be the most efficient binder and inhibitor.

4.3 Phage Display Optimisation Strategy

Phage display allows the screening of a diverse library of Affimer reagents against a target molecule and allows the selection of highly specific binders and negative selection of non-specific binders (Huang et al., 2012). Following the identification of CTL-18, the CTL library was screened against biotinylated NDM-1. Since the CTL library contains a common variable region 1, it was expected that the vast majority of Affimers would bid to NDM-1. Therefore, a stringent phage display protocol was devised to select for binders with a high binding affinity. The use of phage display for affinity maturation has previously been reported (Thie et al., 2009). To select for Affimer binders with a fast association rate, the enriched CTL library was incubated with the target for a short 1 minute. To select for Affimer binders with slow disassociation rates, a washing protocol was followed over several days to remove binders that disassociate within this period. Finally, to identify binders with a higher affinity to CTL-18, the concentration of bound target to be used in the phage ELISAs was optimised in a pre-trial.

The optimised pre-trial involved immobilizing an ELISA plate with increasing concentrations of biotinylated NDM-1 from 0µg/ml to 10µg/ml. The concentration at which 50% of the maximal signal was achieved, the OD_{50}, was used as the optimal concentration at 0.325µg/ml. Therefore, when carrying out phage ELISA on binders identified during phage display, a signal that is higher than that achieved for CTL-18 may have a higher affinity to NDM-1 than CTL-18.

In all three panning rounds, competition washing reduced the number of eluted phage as shown by the reduction in cell count following the competition washes. This suggests that binders with a shorter disassociation rate are screened out. The low number of binders eluted from the control wells suggest a low level of non-specific binders and therefore an enriched library from the Day 3 elution was generated to be used in Panning round 2. Since only three binders were identified in the phage ELISA as having higher signals than CTL-18, Panning round two and three were performed with more elution days.

To determine the most appropriate NDM-1 binders to take forward to a β-lactamase activity assay, an optimised phage ELISA was performed with all the binders previously identified in the panning rounds (n=4). The absorbance signal was ranked with CTL-E9 having a significantly ($p=0.0134$) higher ELISA signal than CTL-18. The next four highest signals (CTl-C6A, CTL-E11, CTL-B5, CTL-C8) were also taken forward to be analysed by β-lactamase activity assay.

The β-lactamase activity assay revealed that the Affimer CTL-C8 inhibits NDM-1 activity to the greatest extent. The β-lactamase activity assay suggests that CTL-C8 significantly improved inhibition of NDM-1 activity compare to Aff21. This was contrary to what was expected as CTL-C8 had the lowest phage ELISA signal. The Affimer with the highest phage ELISA signal, CTL-E9, did not show an improved inhibition compared to CTL-18. This suggests that Affimers that produce a higher phage ELISA absorbance signal do not necessarily result in improved inhibition of NDM-1. This disparity may be explained by a mixed population of M13 phage generated during phage ELISA. Two factors may affect this. First, M13 phage can display up to 5 Affimer proteins and therefore an avidity effect could have influenced the ELISA signal. Secondly, whilst the generation of phage for each Affimer was carried out in unison, it is likely that there is a disparity of phage concentration between each condition. Therefore, it is likely that ELISA signal does not directly correlate to binding affinity and should only be used to confirm Affimer binding to target. To test this further, all Affimers identified as NDM-1 binding should be tested in a β-lactamase activity assay to identify Affimers with greater inhibitory effect. Furthermore, a full understanding of Affimer binding affinity to NDM-1 should be determined. Affinity of candidate Affimers could be determined by surface plasmon resonance (SPR) and compared to β-lactamase activity assay results.

The stringent phage display strategy has led to the identification of an Affimer, CTL-C8, that binds to NDM-1 and inhibits activity to a significantly greater extent than Aff 21. However, it is unlikely that ELISA signal directly predicts affinity or inhibitory effect. Further characterisation of Affimer binding to NDM-1 is required to compare the three candidate Affimers.

4.4 Characterisation of Affimer binders

The amino acid sequences of Affimer binders isolated in the panning rounds can be compared to understand the possible protein-protein interactions. Throughout the panning rounds, an increased frequency of non-polar residues in position VR 2.3, VR 2.6 and VR 2.8 may be of importance. Non-polar residues in these positions may suggest that hydrophobic interactions between Affimer and NDM-1 may be essential for forming high affinity binding. In VR1, non-polar amino acids in positions VR 1.1. VR 1.4, VR 1.5, VR 1.7 and VR 1.9 further suggest the importance of hydrophobic interactions within the binding domain. If this interaction occurs

within the active site of NDM-1, this hydrophobic nature could displace the nucleophilic water molecule (or hydroxyl group) within the active site; thereby inhibiting the enzyme activity. However, further analysis is required to determine the location of Affimer binding. Understanding this interaction, in particular the displacement of the water molecule, may help in the development of small molecule drug design (Barillari et al., 2007). Additionally, the emergence of basic residues in position VR 2.1 and VR 2.8 may play a role in interacting with the positively charged Zinc ions within the active site of NDM-1. Further characterisation of the protein-protein interaction between Affimers and NDM-1 is required to fully understand the mechanism of inhibition. This may help in the development of small molecule inhibitors (Fry, 2006).

4.5 Further work: Characterisation of Affimer binding

In order to fully understand the mechanism of Affimer inhibition of NDM-1 activity, further characterisation of Affimer binding is required. The mechanism of inhibition (competitive or allosteric) and further investigation into the binding mechanism are needed to fully understand and develop the Affimer inhibitor.

Recent attempts, by L Adams and C Tiede, to co-crystallise NDM-1 with the Affimer CTL-18 have been successful. Whilst further analysis is needed, initial results suggest that the Affimer binds in the active site. To confirm this, Michaelis–Menten enzyme kinetics should be carried out to determine the mechanism of inhibition. Furthermore, the crystal structure indicates that a conformation change is observed in the bound Affimer. This surprising finding needs further investigation to determine the amino acids involved. This may lead to modifications to residues outside of the variable regions to improve Affimer binding.

Further analysis of the binding residues in the variable regions is required. In this report, the frequencies of the amino acids in the VR2 of Affimer binders identified during phage display were analysed. This identified lysine in position 2.1, glycine in position 2.6 and isoleucine in position 2.8 as the most frequent residues. Interestingly, each of these residues are found in CTL-18 and the lysine and isoleucine are found in CTL-C8. Further investigation, such as alanine scanning mutagenesis, may help map the residues involved in binding (Cunningham and Wells, 1989). Previous alanine scanning results of Aff 21, by L De Faveri however, did not identify any residues in VR2 that are essential for NDM-1 binding. Further analysis of the CTL-18 and NDM-1 co-crystal may reveal key interactions.

4.6 Further development of Affimer inhibitors as therapeutics

Characterisation of the Affimer binding and further affinity maturation may result in an improved Affimer binder. Further development and investigations are required to assess the viability of Affimers as NDM-1 inhibiting therapies.

The use of β-lactam/β-lactamase inhibitors as effective treatment against drug resistant strains of bacteria has been shown to be clinically successful (Chaïbi et al., 1999). The effectiveness of candidate Affimers to restore sensitivity to β-lactams should be assessed in clinical isolates. Initial results by L De Faveri suggested that Aff 21 re-sensitised clinical strains of bla_{NDM-1} carrying *Klebsiella pneumoniae* to meropenem. Confirmation of these results are required and further investigations using CTL-18 and CTL-C8 should be performed.

Whilst these results are encouraging, intracellular delivery of the Affimer should be considered. NDM-1 is thought to be anchored to the outer membrane and it has been suggested that secretion of NDM-1 in outer membrane vesicles is likely (González et al., 2016; King and Strynadka, 2011b). Fluorescently labelled NDM-1 binding Affimers and microscopy may confirm the localisation of NDM-1. Additionally, strategies to improve Affimer internalisation should be explored. This may include conjugation of the Affimer to Cell-penetrating peptide to improve bacterial cell uptake (Nekhotiaeva et al., 2004). The cell membrane of bacteria remains a challenge in tackling antimicrobial resistance and the development of novel therapeutics.

4.7 Conclusion

In conclusion, this report confirms the use of Affimer reagent to inhibit the enzyme activity of NDM-1. Affinity maturation by phage display strategies was carried out to identify Affimers with improved inhibition of NDM-1 activity. Three candidate Affimers (Aff 21, CTL-18 and CTL-C8) have been identified. Further characterisation of these Affimers is required.

5. References

Abraham, E.P., and Chain, E. (1940). An enzyme from bacteria able to destroy penicillin [1]. Nature *146*, 837.

Adedeji, W.A. (2016). The Treasure Called Antibiotics. Ann. Ibadan Postgrad. Med. *14*, 56–57.

Bagge, N., Schuster, M., Hentzer, M., Ciofu, O., Givskov, M., Greenberg, E.P., and Høiby, N. (2004). Pseudomonas aeruginosa Biofilms Exposed to Imipenem Exhibit Changes in Global Gene Expression and-Lactamase and Alginate Production. Antimicrob. Agents Chemother. *48*, 1175–1187.

Bajaj, H., Scorciapino, M.A., Moynié, L., Page, M.G.P., Naismith, J.H., Ceccarelli, M., and Winterhalter, M. (2016). Molecular Basis of Filtering Carbapenems by Porins from β-Lactam-resistant Clinical Strains of *Escherichia coli*. J. Biol. Chem. *291*, 2837–2847.

Barbas, C.F., Burton, D.R., Scott, J.K., Silerman. G.j., (2001). Phage display : a laboratory manual. New York: Cold Spring Harbor Laboratory Press.

Barillari, C., Taylor, J., Viner, R., and Essex, J.W. (2007). Classification of Water Molecules in Protein Binding Sites. J. Am. Chem. Soc. 2007, 129, 9, 2577-2587

Bhullar, K., Waglechner, N., Pawlowski, A., Koteva, K., and Banks, E.D. (2012). Antibiotic Resistance Is Prevalent in an Isolated Cave Microbiome. PLoS One *7*, 34953.

Bush, K. (2013). Proliferation and significance of clinically relevant β-lactamases. Ann. N. Y. Acad. Sci. *1277*, 84–90.

Carattoli, A. (2013). Plasmids and the spread of resistance. Int. J. Med. Microbiol. *303*, 298–304.

Carfi, A., Pares, S., Duée, E., Galleni, M., Duez, C., Frère, J.M., and Dideberg, O. (1995). The 3-D structure of a zinc metallo-beta-lactamase from Bacillus cereus reveals a new type of protein fold. EMBO J. *14*, 4914–4921.

Chaïbi, E.B., Sirot, D., Paul, G., and Labia, R. (1999). Inhibitor-resistant TEM β-lactamases: Phenotypic, genetic and biochemical characteristics. J. Antimicrob. Chemother. *43*, 447–458.

Cox, G., and Wright, G.D. (2013). Intrinsic antibiotic resistance: Mechanisms, origins, challenges and solutions. Int. J. Med. Microbiol. *303*, 287–292.

Cunningham, B., and Wells, J. (1989). High-resolution epitope mapping of hGH-receptor interactions by alanine-scanning mutagenesis. Science (80-.). *244*, 1081–1085.

Dessen, A., Mouz, N., Gordon, E., Hopkins, J., and Dideberg, O. (2001). Crystal structure of PBP2x from a highly penicillin-resistant Streptococcus pneumoniae clinical isolate: a mosaic framework containing 83 mutations. J. Biol. Chem. *276*, 45106–45112.

Do, N.T.T., Ta, N.T.D., Tran, N.T.H., Than, H.M., Vu, B.T.N., Hoang, L.B., van Doorn, H.R., Vu, D.T. V, Cals, J.W.L., Chandna, A., et al. (2016). Point-of-care C-reactive protein testing to reduce inappropriate use of antibiotics for non-severe acute respiratory infections in Vietnamese primary health care: a randomised controlled trial. Lancet. Glob. Heal. *4*, e633-41.

Docquier, J.D., and Mangani, S. (2018). An update on β-lactamase inhibitor discovery and development. Drug Resist. Updat. *36*, 13–29.

European Parliament (2018). MEPs back plans to halt spread of drug resistance from animals to humans | News | European Parliament. Accessed: 01/08/2019 [Available at : http://www.europarl.europa.eu/news/en/press-room/20181018IPR16526/meps-back-plans-to-halt-spread-of-drug-resistance-from-animals-to-humans]

Evans, B.A., and Amyes, S.G.B. (2014). OXA β-lactamases. Clin. Microbiol. Rev. *27*, 241–263.

Fang, H., Ataker, F., Hedin, G., and Dornbusch, K. (2008). Molecular epidemiology of extended-spectrum beta-lactamases among Escherichia coli isolates collected in a Swedish hospital and its associated health care facilities from 2001 to 2006. J. Clin. Microbiol. *46*, 707–712.

Fleming, A. (1929). On the Antibacterial Action of Cultures of a Penicillium, with Special Reference to their Use in the Isolation of B. influenzæ. Br. J. Exp. Pathol. *10*, 226–236.

Forsberg, K.J., Reyes, A., Wang, B., Selleck, E.M., Sommer, M.O.A., and Dantas, G. (2012). The Shared Antibiotic Resistome of Soil Bacteria and Human Pathogens. Science. *337*, 1107–1111.

Foster, S.J., Smith, T.J., and Blackman, S.A. (2000). Autolysins of Bacillus subtilis: multiple enzymes with multiple functions. Microbiology *146*, 249–262.

Fry, D.C. (2006). Protein–protein interactions as targets for small molecule drug discovery. Biopolymers *84*, 535–552.

González, L.J., Bahr, G., Nakashige, T.G., Nolan, E.M., Bonomo, R.A., and Vila, A.J. (2016). Membrane anchoring stabilizes and favors secretion of New Delhi metallo-β-lactamase. Nat. Chem. Biol. *12*, 516–522.

Gorman, K., McGinnis, J., and Kay, B. (2018). Generating FN3-Based Affinity Reagents Through Phage Display. Curr. Protoc. Chem. Biol. *10*, e39.

Green, V.L., Verma, A., Owens, R.J., Phillips, S.E. V., and Carr, S.B. (2011). Structure of New

Delhi metallo-β-lactamase 1 (NDM-1). Acta Crystallogr. Sect. F Struct. Biol. Cryst. Commun. *67*, 1160–1164.

Guo, Y., Wang, J., Niu, G., Shui, W., Sun, Y., Zhou, H., Zhang, Y., Yang, C., Lou, Z., and Rao, Z. (2011). A structural view of the antibiotic degradation enzyme NDM-1 from a superbug. Protein Cell *2*, 384–394.

Gutierrez, A., Laureti, L., Crussard, S., Abida, H., Rodríguez-Rojas, A., Blázquez, J., Baharoglu, Z., Mazel, D., Darfeuille, F., Vogel, J., et al. (2013). β-lactam antibiotics promote bacterial mutagenesis via an RpoS-mediated reduction in replication fidelity. Nat. Commun. *4*, 1610.

Hall, B.G., and Barlow, M. (2003). Structure-Based Phylogenies of the Serine ?-Lactamases. J. Mol. Evol. *57*, 255–260.

Hall, B.G., and Barlow, M. (2005). Revised Ambler classification of β-lactamases. J. Antimicrob. Chemother. *55*, 1050–1051.

Hawker, J.I., Smith, S., Smith, G.E., Morbey, R., Johnson, A.P., Fleming, D.M., Shallcross, L., and Hayward, A.C. (2014). Trends in antibiotic prescribing in primary care for clinical syndromes subject to national recommendations to reduce antibiotic resistance, UK 1995-2011: analysis of a large database of primary care consultations. J. Antimicrob. Chemother. *69*, 3423–3430.

Higgins, M.K., Bokma, E., Koronakis, E., Hughes, C., and Koronakis, V. (2004). Structure of the periplasmic component of a bacterial drug efflux pump. Proc. Natl. Acad. Sci. *101*, 9994–9999.

Höltje, J. V (1998). Growth of the stress-bearing and shape-maintaining murein sacculus of Escherichia coli. Microbiol. Mol. Biol. Rev. *62*, 181–203.

Huang, J.X., Bishop-Hurley, S.L., and Cooper, M.A. (2012). Development of Anti-Infectives Using Phage Display: Biological Agents against Bacteria, Viruses, and Parasites. Antimicrob. Agents Chemother. *56*, 4569–4582.

Jacoby, G.A. (2009). AmpC β-Lactamases. Clin. Microbiol. Rev. *22*, 161–182.

Khachatourians, G.G. (1998). Agricultural use of antibiotics and the evolution and transfer of antibiotic-resistant bacteria. CMAJ.. 159 (9), 1129-1136

Kim, Y., Cunningham, M.A., Mire, J., Tesar, C., Sacchettini, J., and Joachimiak, A. (2013). NDM-1, the ultimate promiscuous enzyme: substrate recognition and catalytic mechanism. FASEB J. *27*, 1917–1927.

King, D., and Strynadka, N. (2011a). Crystal structure of New Delhi metallo-β-lactamase reveals molecular basis for antibiotic resistance. Protein Sci. *20*, 1484–1491.

King, D., and Strynadka, N. (2011b). Crystal structure of New Delhi metallo-β-lactamase reveals molecular basis for antibiotic resistance. Protein Sci. 9, 1484-91

Kmietowicz, Z. (2017). Few novel antibiotics in the pipeline, WHO warns. BMJ *358*, j4339.

Kohanski, M.A., Dwyer, D.J., and Collins, J.J. (2010). How antibiotics kill bacteria: From targets to networks. Nat. Rev. Microbiol. *8*, 423–435.

Koide, A., Bailey, C.W., Huang, X., and Koide, S. (1998). The fibronectin type III domain as a scaffold for novel binding proteins. J. Mol. Biol. *284*, 1141–1151.

Koronakis, V., Sharff, A., Koronakis, E., Luisi, B., and Hughes, C. (2000). Crystal structure of the bacterial membrane protein TolC central to multidrug efflux and protein export. Nature *405*, 914–919.

Lauwereys, M., Arbabi Ghahroudi, M., Desmyter, A., Kinne, J., Holzer, W., De Genst, E., Wyns, L., and Muyldermans, S. (1998). Potent enzyme inhibitors derived from dromedary. Eur. Mol. Biol. Organ. J. *17*, 3512–3520.

Liénard, B.M.R., Garau, G., Horsfall, L., Karsisiotis, A.I., Damblon, C., Lassaux, P., Papamicael, C., Roberts, G.C.K., Galleni, M., Dideberg, O., et al. (2008). Structural basis for the broad-spectrum inhibition of metallo-β-lactamases by thiols. Org. Biomol. Chem. *6*, 2282.

Lubell, Y., Blacksell, S.D., Dunachie, S., Tanganuchitcharnchai, A., Althaus, T., Watthanaworawit, W., Paris, D.H., Mayxay, M., Peto, T.J., Dondorp, A.M., et al. (2015). Performance of C-reactive protein and procalcitonin to distinguish viral from bacterial and malarial causes of fever in Southeast Asia. BMC Infect. Dis. *15*, 511.

Meini, M.-R., Llarrull, L.I., and Vila, A.J. (2014). Evolution of Metallo-β-lactamases: Trends Revealed by Natural Diversity and in vitro Evolution. Antibiot. (Basel, Switzerland) *3*, 285–316.

Meini, M.R., Llarrull, L.I., and Vila, A.J. (2015). Overcoming differences: The catalytic mechanism of metallo-β-lactamases. FEBS Lett. *589*, 3419–3432.

Michael, C.A., Dominey-Howes, D., and Labbate, M. (2014). The antimicrobial resistance crisis: causes, consequences, and management. Front. Public Heal. *2*, 145.

Mojica, M.F., Bonomo, R.A., and Fast, W. (2016). B1-Metallo-β-Lactamases: Where Do We Stand? B1-Metallo-β-Lactamases Where Do We Stand? Curr Drug Targets. 17, 1029–1050.

Munita, J.M., and Arias, C.A. (2016). Mechanisms of Antibiotic Resistance. Microbiol Spectr. *4*.

Munita, J.M., Arias, C.A., Unit, A.R., and Santiago, A. De (2016). HHS Public Access Mechanisms of Antibiotic Resistance. Microbiol. Spectr. *4*, 1–37.

Murakami, S., Nakashima, R., Yamashita, E., and Yamaguchi, A. (2002). Crystal structure of bacterial multidrug efflux transporter AcrB. Nature *419*, 587–593.

Muyldermans, S., Atarhouch, T., Saldanha, J., Barbosa, J.A., and Hamers, R. (1994). Sequence and structure of VH domain from naturally occurring camel heavy chain immunoglobulins lacking light chains. Protein Eng. *7*, 1129–1135.

Nature Editorial (2018). Wanted: A reward for antibiotic development. Nat. Biotechnol. 36, 555.

Nekhotiaeva, N., Elmquist, A., Rajarao, G.K., Hällbrink, M., Langel, Ü., and Good, L. (2004). Cell entry and antimicrobial properties of eukaryotic cell-penetrating peptides. FASEB J. *18*, 394–396.

NICE (2019). British National Formulary | CO-AMOXICLAV (NICE). Accessed: 28/07/2019 [Available: https://bnf.nice.org.uk/drug/co-amoxiclav.html#indicationsAndDoses]

Nikaido, H. (1994). Prevention of drug access to bacterial targets: Permeability barriers and active efflux. Science (80-.). *264*, 382–388.

Nordmann, P., and Poirel, L. (2002). Emerging carbapenemases in Gram-negative aerobes. Clin. Microbiol. Infect. *8*, 321–331.

OIE (2018). OIE Annual report on antimicrobial agents intended for use in animals (Paris). Accessed: 25/07/2019 [Available: https://www.oie.int/fileadmin/Home/eng/Our_scientific_expertise/docs/pdf/AMR/A_Third_Annual_Report_AMR.pdf]

Osano, E., Arakawa, Y., Wacharotayankun, R., Ohta, M., Horii, T., Ito, H., Yoshimura, F., and Kato, N. (1994). Molecular characterization of an enterobacterial metallo beta-lactamase found in a clinical isolate of Serratia marcescens that shows imipenem resistance. Antimicrob. Agents Chemother. *38*, 71–78.

Park, J.T., and Uehara, T. (2008). How Bacteria Consume Their Own Exoskeletons (Turnover and Recycling of Cell Wall Peptidoglycan). Microbiol. Mol. Biol. Rev. *72*, 211–227.

Paterson, D.L., and Bonomo, R.A. (2005). Extended-spectrum beta-lactamases: a clinical update. Clin. Microbiol. Rev. *18*, 657–686.

Payne, D.J., Hueso-Rodríguez, J.A., Boyd, H., Concha, N.O., Janson, C.A., Gilpin, M., Bateson, J.H., Cheever, C., Niconovich, N.L., Pearson, S., et al. (2002). Identification of a series of tricyclic natural products as potent broad-spectrum inhibitors of metallo-beta-lactamases. Antimicrob.

Agents Chemother. *46*, 1880–1886.

Piddock, L.J. V (2006a). Multidrug-resistance efflux pumps-not just for resistance. Nat Rev Microbiol. 4(8) 629-36

Piddock, L.J. V (2006b). Clinically relevant chromosomally encoded multidrug resistance efflux pumps in bacteria. Clin. Microbiol. Rev. *19*, 382–402.

Poole, K. (2004). Resistance to β-lactam antibiotics. Cell. Mol. Life Sci. *61*, 2200–2223.

Rahbarnia, L., Farajnia, S., Babaei, H., Majidi, J., Veisi, K., Ahmadzadeh, V., and Akbari, B. (2017). Evolution of phage display technology: from discovery to application. J. Drug Target. *25*, 216–224.

Reading, C., and Cole, M. (1977). Clavulanic Acid: a Beta-Lactamase-Inhibiting Beta-Lactam from Streptomyces clavuligerus. Antimicrob Agents Chemother. 11, 852-827

Robertson, J.G. (2007). Enzymes as a special class of therapeutic target: clinical drugs and modes of action. Curr. Opin. Struct. Biol. *17*, 674–679.

Robinson, J.I., Baxter, E.W., Owen, R.L., Thomsen, M., Tomlinson, D.C., Waterhouse, M.P., Win, S.J., Nettleship, J.E., Tiede, C., Foster, R.J., et al. (2018). Affimer proteins inhibit immune complex binding to FcγRIIIa with high specificity through competitive and allosteric modes of action. Proc. Natl. Acad. Sci. *115*, E72–E81.

Rotondo, C.M., and Wright, G.D. (2017). Inhibitors of metallo-β-lactamases. Curr. Opin. Microbiol. *39*, 96–105.

Salverda, M.L.M., De Visser, J.A.G.M., and Barlow, M. (2010). Natural evolution of TEM-1 β-lactamase: experimental reconstruction and clinical relevance. FEMS Microbiol. Rev. *34*, 1015–1036.

Sha, F., Salzman, G., Gupta, A., and Koide, S. (2017). Monobodies and other synthetic binding proteins for expanding protein science. Protein Sci. *26*, 910–924.

Simpkin, V.L., Renwick, M.J., Kelly, R., and Mossialos, E. (2017). Incentivising innovation in antibiotic drug discovery and development: progress, challenges and next steps. J. Antibiot. (Tokyo). *70*, 1087–1096.

Smeal, S.W., Schmitt, M.A., Pereira, R.R., Prasad, A., and Fisk, J.D. (2017). Simulation of the M13 life cycle I: Assembly of a genetically-structured deterministic chemical kinetic simulation. Virology *500*, 259–274.

Sohier, J.S., Laurent, C., Chevigné, A., Pardon, E., Srinivasan, V., Wernery, U., Lassaux, P.,

Steyaert, J., and Galleni, M. (2013). Allosteric inhibition of VIM metallo-β-lactamases by a camelid nanobody. Biochem. J. *450*, 477–486.

Spratt, B.G. (1975). Distinct penicillin binding proteins involved in the division, elongation, and shape of Escherichia coli K12. Proc. Natl. Acad. Sci. U. S. A. *72*, 2999–3003.

Sun, Q., Law, A., Crowder, M.W., and Geysen, H.M. (2006). Homo-cysteinyl peptide inhibitors of the L1 metallo-β-lactamase, and SAR as determined by combinatorial library synthesis. Bioorg. Med. Chem. Lett. *16*, 5169–5175.

Tada, T., Miyoshi-Akiyama, T., Shimada, K., Shimojima, M., and Kirikae, T. (2013). IMP-43 and IMP-44 metallo-β-lactamases with increased carbapenemase activities in multidrug-resistant Pseudomonas aeruginosa. Antimicrob. Agents Chemother. *57*, 4427–4432.

Tanaka, S.I., Takahashi, T., Koide, A., Ishihara, S., Koikeda, S., and Koide, S. (2015). Monobody-mediated alteration of enzyme specificity. Nat. Chem. Biol. *11*, 762–764.

Tang, A.A.-S., Tiede, C., Hughes, D.J., McPherson, M.J., and Tomlinson, D.C. (2017). Isolation of isoform-specific binding proteins (Affimers) by phage display using negative selection. Sci. Signal. *10*, eaan0868.

Tehrani, K.H.M.E., and Martin, N.I. (2018). β-lactam/β-lactamase inhibitor combinations: an update. Medchemcomm *9*, 1439–1456.

Thie, H., Voedisch, B., Dübel, S., Hust, M., and Schirrmann, T. (2009). Affinity Maturation by Phage Display. pp. 309–322.

Thomas, P.W., Zheng, M., Wu, S., Guo, H., Liu, D., Xu, D., and Fast, W. (2011). Characterization of Purified New Delhi Metallo-β-lactamase-1. Biochemistry *50*, 10102–10113.

Threlfall, E.J., Ward, L.R., and Rowe, B. (1999). Resistance to ciprofioxacin in non-typhoidal salmonellas from humans in England and Wales— the current situation. Clin. Microbiol. Infect. *5*, 130–134.

Tiede, C., Tang, A.A.S., Deacon, S.E., Mandal, U., Nettleship, J.E., Owen, R.L., George, S.E., Harrison, D.J., Owens, R.J., Tomlinson, D.C., et al. (2014). Adhiron: A stable and versatile peptide display scaffold for molecular recognition applications. Protein Eng. Des. Sel. *27*, 145–155.

Tiede, C., Bedford, R., Heseltine, S.J., Smith, G., Wijetunga, I., Ross, R., AlQallaf, D., Roberts, A.P., Balls, A., Curd, A., et al. (2017). Affimer proteins are versatile and renewable affinity reagents. Elife *6*, 43–48.

Tipper, D.J., and Strominger, J.L. (1965). Mechanism of action of penicillins: a proposal based on their structural similarity to acyl-D-alanyl-D-alanine. Proc. Natl. Acad. Sci. U. S. A. *54*, 1133–1141.

Tomasz, A. (1979). The Mechanism of the Irreversible Antimicrobial Effects of Penicillins: How the Beta-Lactam Antibiotics Kill and Lyse Bacteria. Annu. Rev. Microbiol. *33*, 113–137.

Toney, J.H., Hammond, G.G., Fitzgerald, P.M., Sharma, N., Balkovec, J.M., Rouen, G.P., Olson, S.H., Hammond, M.L., Greenlee, M.L., and Gao, Y.D. (2001). Succinic acids as potent inhibitors of plasmid-borne IMP-1 metallo-beta-lactamase. J. Biol. Chem. *276*, 31913–31918.

Venkatachalam, K. V, Huang, W., LaRocco, M., and Palzkill, T. (1994). Characterization of TEM-1 beta-lactamase mutants from positions 238 to 241 with increased catalytic efficiency for ceftazidime. J. Biol. Chem. *269*, 23444–23450.

Ventola, C.L. (2015). The antibiotic resistance crisis: part 1: causes and threats. P T *40*, 277–283.

Viswanathan, V.K. (2014). Off-label abuse of antibiotics by bacteria. Gut Microbes *5*, 3–4.

Voets, G.M., Fluit, A.C., Scharringa, J., Schapendonk, C., van den Munckhof, T., Leverstein-van Hall, M.A., and Stuart, J.C. (2013). Identical plasmid AmpC beta-lactamase genes and plasmid types in E. coli isolates from patients and poultry meat in the Netherlands. Int. J. Food Microbiol. *167*, 359–362.

Waxman, D.J., Yocum, R.R., and Strominger, J.L. (1980). Penicillins and cephalosporins are active site-directed acylating agents: evidence in support of the substrate analogue hypothesis. Philos. Trans. R. Soc. Lond. B. Biol. Sci. *289*, 257–271.

Wilke, M.S., Lovering, A.L., and Strynadka, N.C. (2005). β-Lactam antibiotic resistance: a current structural perspective. Curr. Opin. Microbiol. *8*, 525–533.

Wise, E.M., Park, J.T., and Park, J.T. (1965). Penicillin: its basic site of action as an inhibitor of a peptide cross-linking reaction in cell wall mucopeptide synthesis. Proc. Natl. Acad. Sci. U. S. A. *54*, 75–81.

Woodman, R., Yeh, J.T.-H., Laurenson, S., and Ferrigno, P.K. (2005). Design and Validation of a Neutral Protein Scaffold for the Presentation of Peptide Aptamers. J. Mol. Biol. *352*, 1118–1133.

World Health Organisation (2017). Fact sheet on sustainable development goals : health targets. Antimicrobial Resistance. Accessed: 16/08/2019 [Available:

http://www.euro.who.int/__data/assets/pdf_file/0005/348224/Fact-sheet-SDG-AMR-FINAL-07-09-2017.pdf?ua=1]

Yamaguchi, Y., Kuroki, T., Yasuzawa, H., Higashi, T., Jin, W., Kawanami, A., Yamagata, Y., Arakawa, Y., Goto, M., and Kurosaki, H. (2005). Probing the role of Asp-120(81) of metallo-beta-lactamase (IMP-1) by site-directed mutagenesis, kinetic studies, and X-ray crystallography. J. Biol. Chem. *280*, 20824–20832.

Yang, M., Sunderland, K., and Mao, C. (2017). Virus-Derived Peptides for Clinical Applications. Chem. Rev. *117*, 10377–10402.

Yong, D., Toleman, M.A., Giske, C.G., Cho, H.S., Sundman, K., Lee, K., and Walsh, T.R. (2009). Characterization of a new metallo-β-lactamase gene, blaNDM-1, and a novel erythromycin esterase gene carried on a unique genetic structure in Klebsiella pneumoniae sequence type 14 from India. Antimicrob. Agents Chemother. *53*, 5046–5054.

Yoshimura, F., and Nikaido, H. (1985). Diffusion of beta-lactam antibiotics through the porin channels of Escherichia coli K-12. Antimicrob. Agents Chemother. *27*, 84–92.

Zhang, H., and Hao, Q. (2011). Crystal structure of NDM-1 reveals a common β-lactam hydrolysis mechanism. FASEB J. *25*, 2574–2582.

Zhao, W.-H., and Hu, Z.-Q. (2011). IMP-type metallo-β-lactamases in Gram-negative bacilli: distribution, phylogeny, and association with integrons. Crit. Rev. Microbiol. *37*, 214–226.

Zou, D., Huang, Y., Zhao, X., Liu, W., Dong, D., Li, H., Wang, X., Huang, S., Wei, X., Yan, X., et al. (2015). A Novel New Delhi Metallo-β-Lactamase Variant, NDM-14, Isolated in a Chinese Hospital Possesses Increased Enzymatic Activity against Carbapenems. Antimicrob. Agents Chemother. *59*, 2450–2453.